

**Concepts and Models for the Characterization of the West Gedaref
Hydrogeologic System, Sudan**

Vorgelegt von
M.Sc.-Ingenieurin
Muna Mirghani
Aus Khartoum

Von der Fakultät VI
Bauingenieurwesen und Angewandte Geowissenschaften
der Technischen Universität Berlin
Zur Erlangung des akademischen Grades

Doktorin der Ingenieurwissenschaften
- Dr. Ing.-

genehmigte Dissertation

Promotionsausschuß:

Vorsitzender: Prof. Dr.-Ing. H. Wolff

Berichter: Prof. Dr. rer. nat. U. Tröger

Berichter: Prof. Dr. habil. P. Udluft

Tag der wissenschaftlichen Aussprache: 10. Dezember 2001

Berlin 2002

D83

Zusammenfassung

Das Ziel der Forschungsarbeit war es, Konzepte und Techniken anzuwenden, die mit wenigen Daten eine Beschreibung des Grundwassersystems im Gebiet West Gedaref im Sudan ermöglichen und dieses zu verstehen. Um Schätzungen der lokalen hydraulischen Eigenschaften und die hydrogeologischen Bedingungen zu Erfassen, wurden klassische quantitative Methoden der Hydrogeologie angewendet. Um den Grundwasserleiter räumlich zu beschreiben, wurden Modelle benutzt, bei denen die Konfiguration der heterogenen hydraulischen Parameter T und S, der hydraulische Grundwasserstand sowie die Grundwasserneubildungskinetik des Grundwasserleiters variiert wurden..

Nach den deterministischen und stochastischen Annäherungen wurde ein Begriffsrahmen für die Analyse definiert. Im Gegenteil zum Konzept der eindeutigen Parameter, wurden geostatistische Methoden angewandt die auf der Zufallsfunktionskonzeption basieren, das mehrfache Realisierungen erlaubt. Die Zufallsfunktionshypothese ließ die Kennzeichnung des heterogenen Transmissivitätsfeldes, als wesentlicher Eingabebestandteil zum Flussmodell zu. Mit dieser Annahme wurde ein numerischer Simulator für die finiten Elemente benutzt, um die quasi dreidimensionalen Fließparameter zu kalibrieren. die aus stationären und instationären Messungen für eine vorläufige wasserwirtschaftliche Planung gewonnen wurden. Die Resultate der invertierten und der direkten Lösung des Fließmodells zeigen, dass geostatistische Methoden, die Heterogenität des Grundwasserleiters innerhalb des gerichteten Bereiches darstellen können. Die Transmissivitätsverteilung zeigt die beträchtliche räumliche Heterogenität an, die vermutlich durch die komplizierten tektonische Strukturen verursacht werden. Die mittlere Transmissivität erstreckt sich von 2.8×10^{-4} bis $2 \times 10^{-3} m^2/s$, mit einem regionalen Mittelwert von $4.29 \times 10^{-4} m^2/s$. Der durchschnittliche Speicherkoeffizient wird auf 2.0×10^{-3} geschätzt.

Die Ergebnisse zeigen, dass die Grundwasserneubildung des Sandsteingrundwasserleiters Azaza-Abu Naga die vertikale Zusickerung und der Zufluss vom östlichen Basaltgrundwasserleiter ist. Das angenommene Fließmodell führt zu einem maximal sicheren Ergebnis von $10 \times 10^3 m^3/d$ (bei geschätzten 18% Grundwasserneubildung für das Gedaref-Becken) aus dem mittleren Sandsteingrundwasserleiter von Azaza-Abu Naga. Diese Menge wird teils durch vertikales Zusickern (ungefähr $4 \times 10^3 m^3/d$) und teils von den Grenzzuflüssen gebildet. Bei weiterer Nutzung des Grundwassers aus dem limitierten System wird erwartet, dass ein freier Grundwasserleiter entsteht.

Die Forschungsergebnisse zeigen, dass die vorteilhaftesten Bereiche für die Entwicklung der Grundwasserentnahme im West Gedaref das Azaza, Abu Naga und der Bereich um die Senke des Allaya-Wadisystems sind.

Abstract

The purpose of this research was to apply concepts and techniques, which with limited data lead to a better understanding of the west Gedaref groundwater system.

Classical quantitative hydrogeology has been used to provide local estimates of hydraulic properties and averages of hydrogeologic conditions. Then conceptual models are used to allow spatial characterization of aquifer properties, namely: the aquifer configuration, the heterogeneous hydraulic parameters T and S, the hydraulic head as well as the recharge rate.

Following deterministic and stochastic approaches a conceptual framework for analysis was defined. Contrary to the concept of unique model parameters, geostatistical methods are based on the random function concept where multiple realizations exist. The random function hypothesis allowed for the characterization of the heterogeneous transmissivity field, an important input to the flow model. Based on the adopted assumptions a finite element numerical simulator was used to calibrate quasi three dimensional flow parameters conditioned against steady and transient head measurements and a tentative water budget estimate. The results of the inverse solution and the forward solution of the flow model showed the ability of geostatistics to identify aquifer heterogeneity within the targeted range.

The transmissivity distribution indicates considerable spatial heterogeneity probably caused by the complex tectonic structural pattern in the area. The mean transmissivity ranges between 2.8×10^{-4} to $2 \times 10^{-3} \text{ m}^2/\text{s}$, with a regional average of $4.29 \times 10^{-4} \text{ m}^2/\text{s}$. The average storativity is estimated at 2.0×10^{-3} .

The study results showed that the main source of recharge to the Azaza-Abu Naga sandstone aquifer is the vertical leakage and underflow from eastern basalt aquifer. The adopted flow model lead to a maximum safe yield of $10 \times 10^3 \text{ m}^3/\text{d}$ (around 18% of the potential recharge estimated for the Gedaref basin) from the Azaza –Abu Naga middle sandstone aquifer. This amount is partly drawn from vertical leakage (about $4 \times 10^3 \text{ m}^3/\text{d}$), and partly from boundary inflows. Additional development is expected to jeopardize the limited aquifer storage and convert the flow into unconfined conditions.

The study indicated that the most favorable areas for the development of groundwater in the west Gedaref are the Azaza, Abu Naga and the area around the valley of Al-Laya wadi system.

Acknowledgments

First, I am most grateful to Prof. Dr. Uwe Tröger for giving me the opportunity to write my Ph.D. thesis at his prestigious institute. The trust and freedom he gave me in the organization of the work created comfortable and fruitful atmosphere for the work. Beside the regular seminar discussions, his door was always open to me, even when he had piles of work. We worked together with ease and enjoyment.

My special thanks go to Dr. habil. Traugott Scheytt for the careful review of the draft and the meaningful suggestions he made. Dr. Scheytt readiness to solve all kinds of problems I faced is highly appreciated.

I wish to Thank Prof. Dr. Udluft and Dr. habil Thorweihe for accepting to be members of the Ph.D. committee.

Many thanks go to Dr. habil. Barbara Theilen-Willige, Dr. Heinz Burger and the geologist Kai Hahne for their kind cooperation. I benefited from their help and discussions on image processing and GSLIB software.

My thanks go to Prof. Badr-Eldin Khalil, Dr. Omer Kheir, Dr. Idris Mohamed and Dr. Osman Abdel-Latif for their great support during the data collection and the field visit in Sudan, on which this work was based.

I would like to express my gratitude to the family of Gaffar El-Rashid for their hospitality during my stay in Gedaref.

I am grateful to all my ministry colleges at the groundwater research authority in Khartoum and in Gedaref for their valuable support and help.

My thanks go to Dr. Susanna Grams who could not have been nicer or more supportive and helpful to me in many occasions.

I would like to thank all members of the hydrogeology group for their cooperation and help, especially mentioning Elli, Mrs. Steinbock, Ilka, Daniela, Petra and Winfried.

I am grateful to the "KAAD program for talented foreign academics" for their continuous contributing to my living expenses throughout my study period. Special thanks go to Mr. Merkl of Tübingen KSG-office, Mr. Romünda of Berlin KSG-office and Ms Saure of Africa section in Bonn.

To my unique family no words can express my deep feeling of appreciation for their invaluable support throughout this challenging course.

Table of Contents:

Zusammenfassung.....	I
Abstract.....	II
Acknowledgment.....	III
Table of contents.....	IV
List of figures.....	VII
List of tables.....	IX
1. Introduction:.....	1
1.1. Problem statement.....	1
1.2. Previous research.....	3
1.3. Study objectives.....	4
1.4. General approach.....	4
2. Concepts and models in hydrogeology:.....	6
2.1. Introduction.....	6
2.2. Model conceptualization.....	6
2.3. The deterministic approach.....	7
2.3.1. Zoned heterogeneity model.....	8
2.4. The geostatistical approach.....	8
2.4.1. Geostatistical concepts and tools.....	9
2.4.2. Models of continuous heterogeneity.....	10
2.4.3. Geostatistical estimation methods.....	12
2.5. Numerical modeling.....	14
2.5.1. The Mathematical model and the solution method.....	14
2.5.2. The numerical simulator.....	17
2.5.3. Calibration approaches.....	17
2.6. Reliability measures.....	19
3. A Regional view:.....	22
3.1. Climate.....	22
3.2. Topography and landuse.....	24
3.3. Drainage.....	25

3.4.	Geologic history of the Gedaref region.....	27
3.5.	Groundwater occurrence.....	32
3.6.	Groundwater development.....	33
4.	Hydrogeologic characterization of west Gedaref aquifer system.....	35
4.1.	Introduction.....	35
4.2.	The aquifer system.....	35
4.2.1.	Lateral extension of the Nubian sandstone.....	36
4.2.2.	Stratigraphy of the Nubian formation.....	37
4.2.3.	Structural pattern from lineament map.....	45
4.2.4.	The aquifer sub-systems.....	47
4.3.	The Hydrologic conditions.....	51
4.3.1.	Static water level.....	51
4.3.2.	Sources of Recharge.....	52
4.3.3.	Abstraction rates.....	54
4.4.	Hydraulic characteristics.....	58
4.4.1.	Transmissivity.....	58
4.4.2.	Aquifer yield and specific capacity.....	60
4.5.	Aquifer reserves.....	61
4.6.	Water type.....	62
4.7.	Conclusion.....	64
5.	A conceptual framework for quantitative analysis and model design	68
5.1.	Introduction.....	68
5.2.	The geohydrological framework.....	68
5.2.1.	Model area confines.....	68
5.2.2.	Defining the hydrogeologic units.....	70
5.2.3.	The flow system conceptualization.....	72
5.3.	Parameterization and uncertainty analysis.....	73
5.3.1.	Head distribution.....	73
5.3.2.	Transmissivity distribution.....	76
5.3.3.	Hydrologic stresses.....	82
5.4.	The water budget.....	83
5.5.	Conclusion.....	85

6.	Numerical simulation.....	86
6.1.	Introduction.....	86
6.2.	Horizontal and vertical discretization.....	86
6.3.	Boundary conditions.....	88
6.4.	Calibration targets	89
6.5.	Calibration assessment.....	90
6.5.1.	Steady conditions.....	91
6.5.2.	Transient conditions.....	92
6.6.	Model predictions and aquifer potential.....	96
6.7.	Sensitivity analysis.....	101
6.8.	Conclusion.....	101
7.	Discussion of results.....	103
8.	General conclusion.....	107
9.	References	110

List of Figures:

Fig. 1.1:	Location of the Study area.....	2
Fig. 2.1:	Steps in developing a conceptual model.....	7
Fig. 2.2:	Illustration of flow boundary conditions.....	16
Fig. 3.1:	Monthly average temperature in Gedaref.....	22
Fig. 3.2:	Average annual rainfall at four meteorological station in Gedaref.....	23
Fig. 3.3:	Monthly average rainfall at Gedaref station.....	24
Fig. 3.4:	Monthly average rainfall and evaporation at Gedaref station.....	25
Fig. 3.5:	The topography of the Gedaref region.....	26
Fig. 3.6:	Annual fluctuations of Al-Laya discharge.....	28
Fig. 3.7:	Geological features of Gedaref region.....	29
Fig. 3.8:	The structure of the greater Gedaref basin.....	30
Fig. 3.9:	Geophysical profiles showing the subsurface geology.....	31
Fig. 3.10:	Regional piezometric surface in the Gedaref.....	33
Fig. 4.1:	Borehole location map.....	36
Fig. 4.2:	Basalt thickness map.....	37
Fig. 4.3:	Profile1.....	40
Fig. 4.4:	Profile2.....	40
Fig 4.5:	Profile 3-3'.....	41
Fig. 4.6:	Profile 4-4'.....	41
Fig 4.7a:	Profile 5.....	42
Fig 4.7b:	Profile 5-5'.....	43
Fig. 4.8:	Lithological correlation across Azaza and Abu-Naga.....	44
Fig 4.9:	Gedaref Imagery.....	48
Fig. 4.10:	Lineament pattern in the Basaltic body.....	49
Fig. 4.11:	Lineaments across the Nubian formation.....	50
Fig. 4.12:	Static water level contour in the Nubian formation.....	53
Fig. 4.13:	Groundwater hydrographs of some monitored boreholes in 1996.....	56
Fig. 4.14:	Groundwater hydrographs during 2000.....	57
Fig. 4.15:	Sampled borehole locations.....	65
Fig 4.16:	Piper diagram showing hydrofacies in the study area.....	65
Fig. 4.17:	Water facies at sampled boreholes.....	66

Fig. 4.18:	EC and Chloride distribution maps.....	66
Fig 5.1:	Location of the model area.....	69
Fig. 5.2:	Scheme of the hydrostratigraphic units of the model.....	71
Fig. 5.3:	Schematic diagram showing horizontal and vertical flow components.....	72
Fig. 5.4a:	Variogram model of hydraulic head.....	74
Fig 5.4b-d:	Spatial distribution and standard deviation of hydraulic head in 1992.....	75
Fig. 5.5:	Head distribution in 1999.....	77
Fig. 5.6:	Regression of ln T on ln SC.....	78
Fig. 5.7:	Histogram of ln T.....	78
Fig. 5.8:	Mean variogram models of lnT.....	79
Fig. 5.9a,b:	Kriging map of ln T, and associated standard deviation.....	80
Fig. 5.9c:	Standard deviation of lnT Kriging estimates.....	81
Fig. 5.10:	Random T fields resulting from stochastic simulation.....	83
Fig. 6.1:	Finite element grid used for the numerical approximation of the flow equations.....	87
Fig. 6.2:	Scatterplot of the steady state model results.....	93
Fig. 6.3:	Water budget of the steady state model.....	93
Fig. 6.4:	Modelled leakage zones.....	94
Fig. 6.5:	Transmissivity sub-units in zoned-heterogeneity model.....	95
Fig. 6.6:	Head distribution of the calibrated steady flow model.....	95
Fig. 6.7:	The water-balance and scattergram of the transient simulation	97
Fig. 6.8:	Simulated transient groundwater flow pattern.....	98
Fig. 6.9:	Water-budget and piezometric surface after 20 years simulation with additional pumpage 3000 m ³ /d	99
Fig. 6.10:	Water-budget and piezometric surface after 20 years with additional Pumpage of 5000 m ³ /d.....	100

List of Tables:

Tab. 1.1:	Projection of Water demand in Gedaref.....	2
Tab. 3.1:	Total rainfall in three meteorological stations in Gedaref.....	23
Tab. 3.2:	Monthly average evaporation in Gedaref station.....	24
Tab. 3.3:	Flood records of Al-Laya wadi.....	27
Tab. 4.1:	Borehole inventory.....	118
Tab. 4.2:	Monthly monitoring of groundwater depth during 1996/97.....	55
Tab. 4.3:	Monthly monitoring of groundwater depth during 2000.....	55
Tab. 4.4:	Transmissivity estimates from pumping tests.....	61
Tab. 4-5:	Aquifer yield estimated from pumping tests.....	63
Tab. 4-6:	Composition of groundwater from selected samples.....	123
Tab. 5.1:	Prior estimate of average zonal transmissivity values.....	82

1. Introduction

Groundwater exploration has always demanded costly data collection. As an alternative, the use of models have proved to be a cost effective approach, that allows understanding the behaviour of complex hydrogeologic systems. In the same time models serve to check the available data against possible errors. The inter relationship governing various elements of hydrogeologic models are described in mathematical terms to enable the quantification of these elements.

Numerical simulators on the other hand has emerged as an important modelling tool for estimating the hydrologic and hydraulic parameters embedded in the models representing real hydrogeologic systems. It enabled accurate calibration of complex heterogeneous hydrogeologic models, and hence reliable predictions. This has saved large effort and reduced risks of failure in the planning of water resources development projects..

1.1. Problem statement

The study area lies in east central Sudan, at the border with Ethiopia. It covers an area of about 2250 km² west of Gedaref city between longitude 35.0° and 35.5°, and latitudes 13.5° and 14.5°. The Main city of Gedaref has a population of about 267000 (projected from SAGHAYRON et al.,1996) including seasonal agricultural labour and refugees from neighbouring Ethiopia. The Gedaref enjoys highly fertile soils and relatively high rain intensities all over the region. The region is important for the economy of Sudan. It hosts the largest mechanised rain-fed farming in Sudan, which greatly contributes to food crop production, as well as to cash crops.

The city of Gedaref and its surrounding villages have long suffered from severe drinking water shortages. With the increasing population (4.7% growth rate), the problem has worsened and the supply of drinking water has dropped to only 48% of the total demand (WATER AUTHORITY REPORT,1996). The Water demand of Gedaref city is estimated by SAGHAYRON et al., 1996, taking into account the industry, services, agricultural schemes and animal demands. Table 2.1 shows the demand projection till year 2015 according to SAGHAYRON.

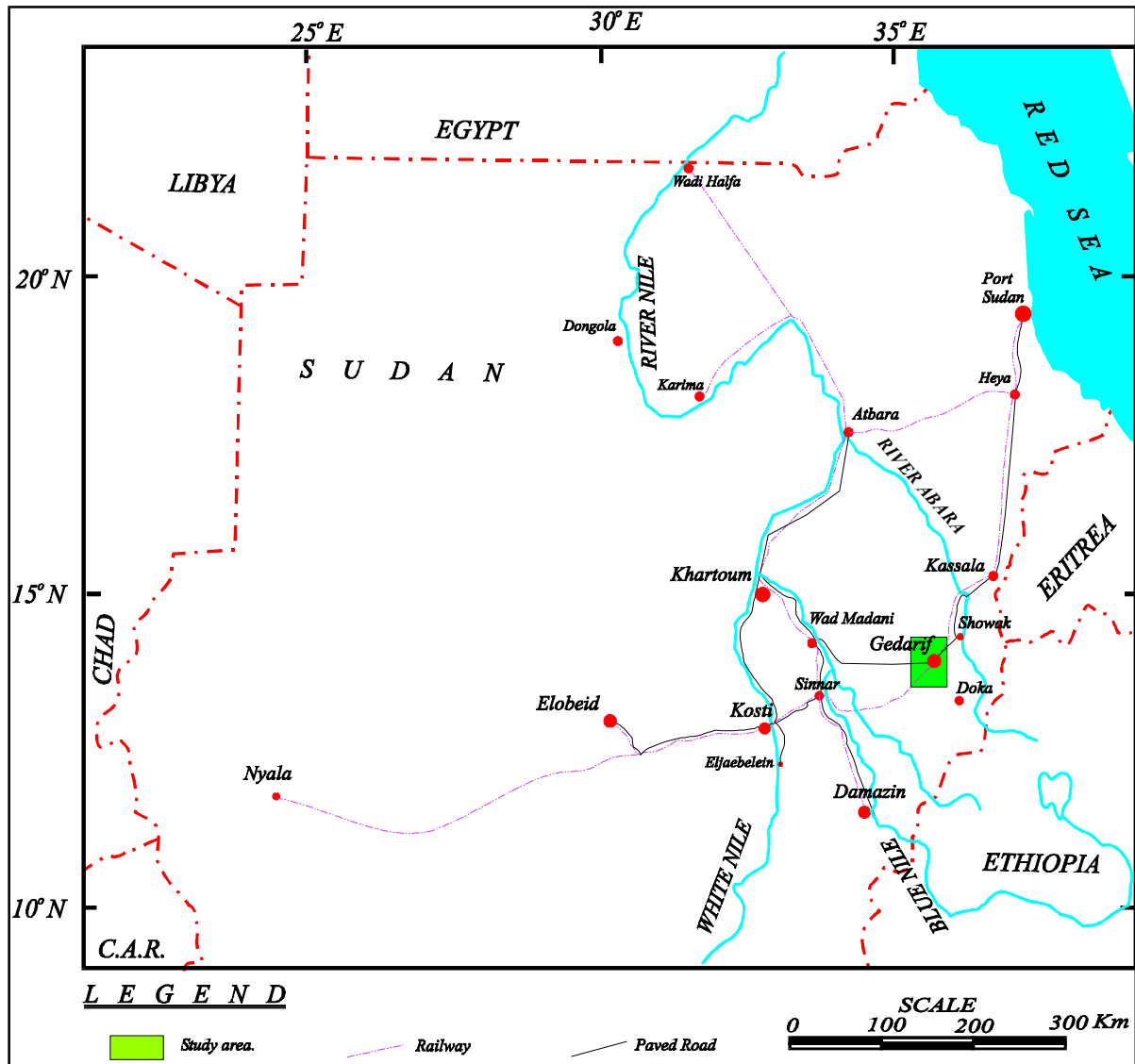


Fig. 1.1: The location of the study area in the east of central Sudan.

Table 1.1 Water Demand projection after SAGHYRON et al., 1996

Year	1997	2003	2009	2015
Demand (m ³ /d)	25,693	52,088	125,376	148,561

Currently, the city of Gedaref alone demands 25,000 m³/d. The current supply is about 6000 m³/d from the wellfields west of Gedaref, and 10,000 m³/d from river Atbara 70 km east of the city, available only during the flood season, July - October. This indicates a wide gap in Water supply during the dry summer period, March to June. Due to the seasonal nature and high cost of the surface water source, attention is directed towards groundwater development.

The search for cost effective and on the same time sustainable sources for drinking water supply in the vicinity of the Gedaref city has been a challenging task for the Water Corporation. Extensive groundwater development in Gedaref region started in the mid sixties. In the late sixties the first well field was constructed at Abu-Naga for supplying Gedaref city with drinking water in the summer season when the surface water resources from River Atbara dries up. The success of this wellfield has encouraged the development of groundwater as a better alternative compared to the heavy loaded seasonal river Atbara. A second wellfield is constructed in 1984 at El-Showak in the flood plains of Atbara river in the hope that it catches the aquifer replenished yearly from the river discharge. However, this wellfield was buried with the heavily silted floods of the river. A third wellfield is constructed in 1992 in the hope that it covers the demand shortages in the dry summer period turned out to produce brackish water with TDS reaching more than 1000 mg/l.

The above developments indicated the need for a proper planning for groundwater abstraction. This should be based on accurate characterisation of the aquifer system in the area to identify future promising drilling locations.

1.2. Previous research

Previous work on Gedaref hydrogeology is carried out by SULIEMAN, 1968, KHEIR, 1986, ADAM, 1987, VAN, 1989, HUSSEIN, 1992, IBRAHIM, 1985. They mainly concentrated on large scale studies of the available water resources in the region. In 1986, a Dutch-Sudanese cooperation project, implemented by the Rural Water Corporation (RWC), carried limited geoelectric and hydrologic investigation in the southern boundary of the study area. Some other studies such as MOUNIER, 1985 and the SUDAN PETROLEUM, 1984 concentrated on the investigation of hydrocarbon, and included regional gravity surveys that defined the extension of the greater Gedaref basin. Detailed geological studies covering the whole region are missing. Some early studies by ROXTON, 1956, WHITEMAN, 1971, JIAVLO, 1975, MULA, 1983, have concentrated on the description of the Gedaref formation and the geologic history of the region. However, they were far from any detailed geological characterisation of the basin.

Most of the above studies have confirmed that there is a good potential of ground water in the Gedaref region. According to a review by SKAP, 1990, the inflow to the Gedaref basin estimated by previous studies ranges between 7 to 29×10^6 m³/year. These studies also

indicated a high replenishment capacity as a result of the high intensity rains in the region. However, it is concluded that there is a need to investigate the actual contribution of the estimated resources potential to the exploitable groundwater storage.

1.3. Study Objectives

The main objective of the current Ph.D. research is to characterise the hydrogeology, and assess favourable areas for groundwater development in the west Gedaref region. In the scope of groundwater management, the problems of this work could be divided into two problems. The first problem concerns with fundamental analysis which has the objective to understand the physical processes. The second task is a problem oriented, carefully directed to the management decisions to be made. Close to the above problems, are the following specific objectives, which make-up the major parts of this work. These include:

1. define the physical set-up of the Gedaref region which helps to establish a broad framework for the study area.
2. characterise the surface and subsurface hydrology of the west-Gedaref Nubian sandstone basin.
3. establish a conceptual framework to model the real hydrogeologic system. This includes different assumption which lead to the estimation or quantification of several components of the aquifer system, including, hydraulic properties, recharge, etc..
4. calibrate a flow model against predefined criteria using numerical simulation techniques.
5. derive conclusions on the suitable methodologies applied for modelling the study aquifer.
6. predict the potential of new developments in the area.

To achieve this goal the study was set to develop a numerical simulator for the major sandstone aquifer in the west of the Gedaref region.

1.4. General study approach.

Towards these objectives the study of the Gedaref region has inevitably proceeded through different activities as a typical hydrogeological characterisation scheme. In chapter 2 the concepts and computation methodology are described. Chapter 3 presents a regional overview of important physical settings controlling the area hydrogeology. Having set the study objective, a reconnaissance visit is paid to the region in order to develop appropriate assumptions for a model concept. This has enabled a detailed view of the problem as provided

in chapter 4. The model concept (chapter 5) has triggered a close field investigation to obtain additional data for the model set up. Model construction (chapter 6) was based on the previous analysis and conceptualisation. It concentrates on quantifying the elements of the proposed model/s using available information on the Gedaref basin. A general discussion of the study results is given in chapter 7. I end with a summary of conclusions in chapter 8.

2. Concepts and Models in hydrogeology

2.1. Introduction

Groundwater management is mainly based on proper characterization of hydrogeological parameters. In this respect a major problem comes up, namely, the identification of various hydrogeologic parameters and their spatial-variability. The latter is actually all that what the use of numerical modeling in this study is about.

In this chapter, the methods and concepts in hydrogeological modeling are reviewed. The modeling approach and the underlying concepts applied for the flow modeling of the Azaza-Naga aquifer is introduced. Further assumptions particular to the Gedaref case are introduced occasionally as required.

A starting step in any quantification process is to develop a conceptual model of the real system under consideration. Based on the conceptual model, the appropriate methods are selected and described. This process is discussed in Section 2.2.

Generally, two approaches are common when applying numerical modeling in hydrogeology. The first, a deterministic approach, considers the hydrogeological parameters (HP) as unique and can be calculated by solving the governing equations in an inverse mode. The second approach, which is more recent, assumes that HP are random and hence is better evaluated in a geostatistical framework. The deterministic approach and the associated methods are discussed in section 2.3. Section 2.4 describes the geostatistical methods applied within the second approach. The software selected for the numerical simulation, and the mathematical formulation used in it are presented in section 2.5.

2.2 Model Conceptualization

A model concept is a set of assumptions and hypothesis that facilitate the quantification process. Several assumptions are considered in this study to describe the real aquifer system based on the available data. The adopted model concept subsequently lead to the selection of the estimation techniques required to provide the different model parameters.

A typical flow of activities for developing a model concept for the Gedaref aquifer is shown in fig. 2.1 below. Steps 3 to 5 in the flow chart are far from certain. The decision on each of these model components is governed by the quantity and quality of the available data. In the

absence of enough information, a range of assumptions and scenarios are considered to ultimately reach the optimum results against a pre-established criteria. Starting with simple assumptions and gradually increasing the model complication is recommended in modeling practice (ANDERSON and WOSSNER, 1992, HILL, 1998).

Development of a Model Concept

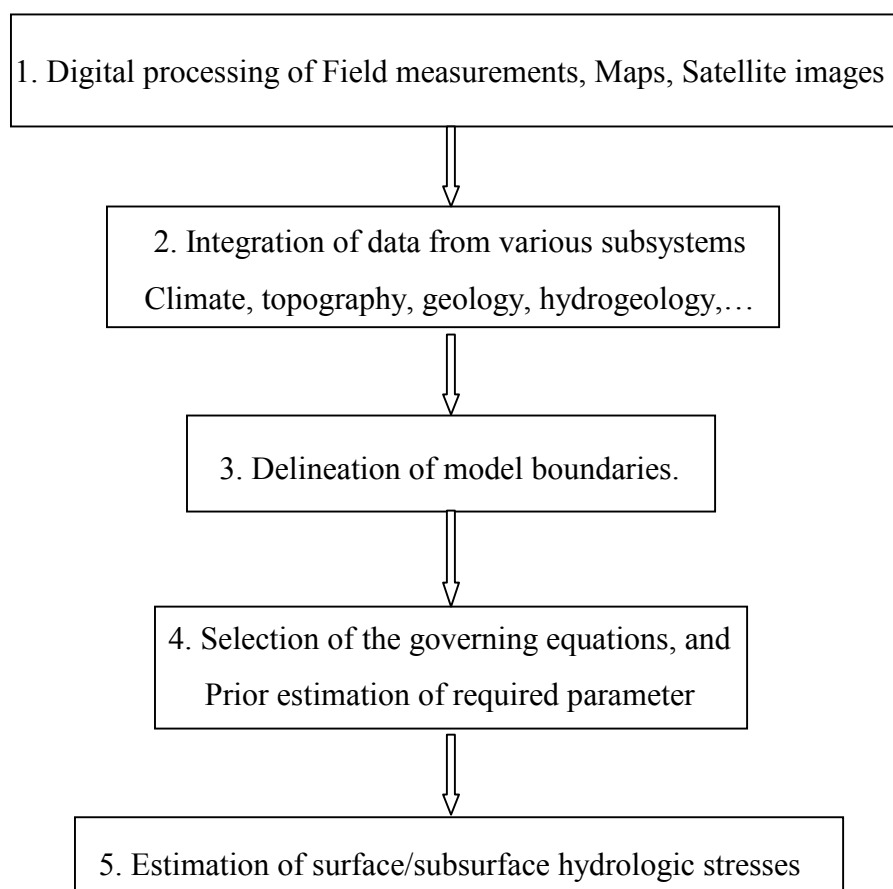


Fig. 2.1: Typical steps in developing a conceptual model.

2.3. The deterministic approach

As mentioned above, parameter identification is a basic task in hydrogeological modeling. In a deterministic approach it is required to solve the governing equation in an inverse mode to estimate a unique parameter distribution. The number of unknown parameters (called parameter dimension) in a heterogeneous aquifer is theoretically infinite (YEH, 1986). Thus

the reduction of the parameter dimension is a necessary step in the inverse solution. The parameter dimension should be compatible with the available head measurements (the independent variable). The optimum number of parameter depends on the quantity and quality of data (observations).

The homogenous zones method is the only way to model distributed systems within a deterministic framework.

2.3.1. Zoned heterogeneity

Applying the zonation method the model area is divided into a number of zones, each is characterized by a constant parameter value (e.g. transmissivity). Here the structure (the number and the shape) of the zones is defined according to the available information from aquifer pumping tests, hydraulic gradient and geologic mapping. Subsequent adjustment is made through the calibration process, and then using the resulting parameter values and sensitivity analysis.

The zonation method is considered superior to other approaches in case of limited and poor quality data (KEIDSER and ROSBJERG, 1991, YEH, 1986). It enables the modeler interference and personal judgment. Therefore, zonation result will be considered as a control for judging other parameterization schemes.

2.4. The Geostatistical approach

It has long been known that strictly deterministic description of the environment does not seem feasible. It has been argued that, in reality, information about the hydrogeologic environment is incomplete and subject to measurement as well as interpretative error. Geostatistical methods are developed mainly to account for or quantify spatial uncertainty. Geostatistics is defined as the application of probabilistic methods to regionalized variables (CHILES and DLFINER, 1999, MYERS, 1997).

In this work, geostatistics is conducted to grid scattered T and h data, and to assess uncertainty associated with their estimated values. Before describing the geostatistical models and methods, some basic concepts essential for their application are reviewed below.

2.4.1. Geostatistical Concepts and tools

The Stochastic process

In the geostatistical approach it is assumed that the regionalized variable is one of many possible realization of a random function (or a stochastic process). Stochastic models are recognized as useful analytical tools in hydrogeology (FREEZE, 1975, DELHOMME, 1979, GELHAR, 1997, ANDERSON, 1997, NEUMAN, 1997). KINZELBACH, VASSOLO and LI (1996) concluded that stochastic assessment is the only possible way to make meaningful decisions if the data are sparse. However, in reality there is no repetition/replicates; and only one set of a variable represents an observed property in space. It was hence necessary to introduce two concepts to be able to use the stochastic models to describe regionalized variables. These concepts are stationarity and ergodicity. CHILES and DELFINER (1999) justified this confusion by pointing out that “models must be distinguished from the reality it attempts to capture”.

Stationarity

According to DAVIS (1986), in contrast to a deterministic sequence whose state can be predicted exactly from its coefficient, a sequence is stochastic if it can be characterized only by its statistical properties. Stationarity (MYERS, 1989, DAGAN, 1997) is a geostatistical concept that makes possible identification of the ensemble statistics from one record. It assumes that the statistical properties of a geologic formation is the same at any point x . Physically, it means that a property is homogenous in space (DAVIS, 1986). MYERS (1989), described stationarity as too strong in all circumstance, and most statistics is based on a weak form of stationarity. One important form is the second order stationarity of the increments $Z(x) - Z(x+h)$, also called the intrinsic hypothesis. An intrinsic random function $Z(x)$ is characterized by:

- a linear drift: $m(h) = E[Z(x+h) - Z(x)] = \langle a, h \rangle$, and

- a variogram: $\gamma(h) = 0.5 \text{ var}[Z(x+h) - Z(x)]$ (see definition below)

If the linear drift is zero (i.e. the mean is constant) we have the usual form of the intrinsic model with

$$E[Z(x+h) - Z(x)] = 0$$

The intrinsic hypothesis is applicable in the presence of non-constant mean. Non-zero drift is usually treated using the model of the universal Kriging (sec. 2.4.2)

Ergodicity

The ergodicity concept assumes that one realisation (e.g. a set of Transmissivity data) is sufficient to determine the statistical properties of the ensemble of possible realizations. In this case the spatial average of the property taken to represent the expected value

Considering the fact that only one realization of the conceptually random aquifer or formation is available from the measurements of each property, stationarity and ergodicity concepts indicate that the aquifer is assumed to be statistically homogeneous.

The Variogram

As it is always the case, the important hydrogeological properties and parameters such as piezometric head, transmissivity or hydraulic conductivity, storage coefficient, yield, thickness of aquifer, hydrochemical parameters, etc. are all functions of space. According to DEMARSILY (1986) these variables (known as the regionalized variables) are not purely random, and there is some kind of correlation in the spatial distribution of their magnitudes. The spatial correlation of such variables is called the structure, and is normally defined by the variogram.

The experimental variogram measures the average dissimilarity between data separated by a vector h (GOOVAERTS, 1997). It is calculated according to the following formula.

$$\gamma(h) = \frac{1}{2N(h)} \sum_{i=1}^{N(h)} [Z(x+h) - Z(x)]^2$$

h = separation distance between two points, also called the lag distance.

In this study the experimental variogram is computed where applicable, then a theoretical model is fitted to it. The variogram model is the principal input for both interpolation and simulation schemes (sec. 2.4.3). However, modeling the variogram is not a unique process. Various studies (DAGAN and NEUMAN, 1997, CUSHMAN, 1990) tried to correlate the mathematical expressions normally used to describe variogram models to the physical characteristics of the parameters

2.4.2. Models of continuous heterogeneity

In contrast to a homogeneous aquifer whose properties do not vary in space, a heterogeneous aquifer exhibits spatial variability in its properties. Heterogeneity is modeled in the

deterministic approach using the concept of zoned heterogeneity combined with the concept of the (lumped) effective parameter estimate. In the following, the so called continuous heterogeneity models implemented in this work are discussed. Where the word continuous refers to the spatial correlation indicated by the variogram.

Transmissivity models

According to JOURNEL and HUIJBREGTS (1978), large scale fluctuations in $\log T$ are included in the analysis through the use of nested structures. However, several studies have been trying to establish a universal structural model that is justified by the physical nature of the property under consideration. In a series of articles, NEUMAN (1997, 1995, 1991) showed that a power law model is observed at a number of sites on distance scales ranging from few meters to 100 km. He concluded that, Log transmissivities exhibit self-similarity in a global or average sense. The power semivariogram takes the form

$$\gamma(h) = c h^{2\omega}$$

where h is the lag distance, c is a constant and ω ranges between $0 > \omega < 1$. NEUMAN (1995) suggested a generalized model of ω equals approximately 0.25.

A power law semivariogram assumes that the T field possesses homogeneous spatial increments, a property called intrinsic (stationary in the increments) in the traditional language of geostatistics (sec. 2.4.1). The physical basis of the above model is discussed by ANDERSON, (1991& 1997). She stated that, “the scale of analysis is critical when addressing the problem of stationarity. While it is likely that geological media are statistically homogenous at some scales, stationarity certainly will not apply at all scales. At large regional scales, geological systems are certainly non stationary”. Such systems show nested hierarchical stationary structures.

The Power law behavior implies that $\log T$ is a random fractal (ADLER, 1991, JOURNEL and HUIJBREGTS, 1978). According to WHEATCRAFT (1990), fractal models do allow consideration of nested scale of heterogeneity. ANDERSON (1997) supported fractal concept by arguing that, “Continuous heterogeneity that is characterized by nested scales of heterogeneity is called evolving heterogeneity and can be represented by a fractal model”.

From the above, it can be concluded that both a fractal or a nested hierarchical model would be physically justifiable for describing regional transmissivity structures. However, the choice of the appropriate model is judged by the end results of the estimation method (Kriging or conditional simulation).

Two variogram models are considered to describe the heterogeneous transmissivity field in Gedaref aquifer. The first model is a nested variogram model which assumes that the geologic media is composed of homogeneous zones at different scales. The second model is based on Neuman's universal scale model.

Groundwater levels variability

It is clear that groundwater levels are not stationary, as they show global trend (non-constant mean) in the direction of flow. Head distribution is computed using the universal Kriging model with a drift. The basic model of Universal Kriging is (CHILES and DELFINER, 1999).

$$Z(x) = Y(x) + m(x)$$

Where, $Z(x)$ is the variable under consideration (the head), $m(x)$ is a linear function called the drift, $Y(x)$ is the fluctuation or residual about this drift. The drift function is approximated by trial and error, to achieve minimum Kriging variance.

2.4.3. Geostatistical estimation methods

Two schemes are used to estimate the transmissivity field. One scheme is based on the Kriging interpolation (KECKLER, 1995). The second applies conditional simulation (DEUTSCH and JOURNAL, 1998) to produce conditional transmissivity fields. The latter is expected to provide better reproduction of the modeled variability in areas with large gaps in the data.

SCHAFMEISTER (1993) concluded that smooth estimates of T produced by Kriging are adequate for groundwater flow modeling. However, I believe this statement is meant in the case of even distribution of data point. In the case under study, Kriging will produce a constant mean value in areas lacking data. On the other hand, being independent of the data values, Kriging variances are not measures of local estimate accuracy (DE CESARE and POSA, 1995). Kriging error variances only provide a comparison of alternative geometric data configurations.

Stochastic simulation techniques based on proper structural analysis of the transmissivity are believed to be more appropriate to produce the spatial variability of T at the minimum data spacing. The resulting simulations are not meant to represent reality. However, if the simulation can be conditioned on available measurements, it will reflect the actual uncertainty. The use of Conditional simulation (CS) of transmissivity in this study was intended to reproduce the spatial variability, and to additionally allow for uncertainty quantification. Generally, multiple transmissivity fields are generated, and then the head distribution can be computed from the simulated transmissivity by solving the forward problem deterministically. This makes it possible to compute multiple head distributions and hence estimate the variability as a measure of uncertainty. In this work, the full potential of this method is not used due to software and time constraints. Only few transmissivity realizations are generated to check the effect of the conceptual continuous heterogeneous transmissivity models on the flow simulation results.

Estimates of Transmissivity fields are generated using both ordinary Kriging interpolation method, and the method of simulated annealing. While groundwater levels, showing trend component in the flow direction, are produced using universal Kriging.

Simulated annealing (a CS method)

The Simulated Annealing (SA) is one of several methods available for conditional simulation. In general, SA technique is expected to provide the best images of any probability distribution, given that the data reflects that distribution. With limited data set one cannot claim that a random function can be inferred from the data. However, it is generally believed that transmissivity is log-normally distributed. Then a pre-simulation run with the Sequential Indicator Simulation routine, which provides a good reflection of non-(log-) normally distributed variables is recommended by SCHAFMEISTER (1999).

SA is defined by CHILES and DELFINER (1999) as an optimization method rather than a simulation method. It starts from a pre-simulated image and iteratively exchanges two points in the grid until it reaches a minimum objective function.

SA is meant to develop analogy with the annealing process by trying to minimize an energy function (the objective function) associated with the image configuration s . This objective function is defined as follows

$$U(s) = w_1 \sum_{p=1}^{n_1} [\gamma^*(h_p; s) - \gamma(h_p)]^2 + w_2 \sum_{q=1}^{n_2} [\mu_q^*(s) - \mu_q]^2 \quad (\text{after CHILES and DELFINER, 1999})$$

The above function constrains the simulated image to reproduce a target variogram model γ , for n_1 values with a lag of h_p , while honoring data values at their location. The second part of the objective function above is used to express any other constraints against a desired value μ_q . w_1 and w_2 are weights assigned to the two parts of the objective function.

Additionally, SA can incorporate external data in the constraint function, which makes it more suitable to limited data set.

2.5. Numerical modeling

Numerical modeling is one of the important tools used in characterizing the hydrogeological regime in the Gedaref area. With the help of a numerical simulation software, a groundwater flow model is calibrated.

The main objectives of the numerical modeling of the Gedaref groundwater system is the identification of parameters used in deriving the governing equations, as well as the prediction of future development consequences.

Additionally, flow simulation in the Nubian sandstone aquifer is expected to assess conceptual errors imposed by assumptions associated with alternative flow models.

2.5.1. The mathematical model and the solution method (Finite element method)

Inhomogenous aquifer systems, in which aquifer parameters vary with space, is governed by partial differential equation. Borrowing FEFLOW convention (DIERSCH, 1998), the essentially or approximately horizontal confined flow conditions, is governed by the vertically averaged balance equation below.

$$S \frac{\partial h}{\partial t} + \frac{\partial \bar{q}_i}{\partial x_i} = \bar{Q}_p$$

$$\bar{q}_i = -T_{ij} \frac{\partial h}{\partial x_j}$$

Where:

S	= storativity,
h	= hydraulic head,
q_i	= Darcy velocity vector,
Q_ρ	= source/sink term,
T_{ij}	= transmissivity tensor,
t	= time,
x_i	= spatial coordinates.

A set of initial, boundary, and constraint conditions is required to achieve the solution of the above governing equations. Those include:

■ Initial condition:

$$h(x_i, 0) = h_I(x_i) \quad \text{in the domain } \Omega$$

Where h_I is a known spatially varying initial head distribution.

■ Flow Boundary conditions assigned to the boundary Γ bordering the domain Ω (see fig 2.2 for illustration):

- 1st kind boundary condition: specified head (Dirichlet type)

$$h(x_i, t) = h_1^R(t) \quad \text{on } \Gamma_1 \times t[0, \infty]$$

- 2nd kind boundary condition: specified flow (Neumann type)

$$\bar{q}_m(x_i, t) = \bar{q}_h^R(t) = -T_{ij} \frac{\partial h}{\partial x_j} n_i \quad \text{for 2D horizontal confined} \quad \text{on } \Gamma_2 \times t[0, \infty]$$

- 3rd kind boundary condition: flow transfer or reference hydraulic head (Cauchy type)

$$q_m(x_i, t) = -\bar{\Phi}_h(h_2^R - h) \quad \text{for 2D horizontal confined} \quad \text{on } \Gamma_3 \times t[0, \infty]$$

Here the transfer coefficient $\bar{\Phi}_h$ represents two directional functions of the form of:

$$\begin{aligned} \bar{\Phi}_h &= \bar{\Phi}_h^{in} & \text{for } h_2^R > h \\ &= \bar{\Phi}_h^{out} & \text{for } h_2^R \leq h \end{aligned}$$

- 4th kind boundary condition, single well type/ point source:

$$Q_\rho^w(x_i, t) = \sum_m Q_m^w \prod_i \{ \delta(x_i - x_i^m) \} \quad \text{for } \forall(x_i, x_i^m)$$

Where:

- h_1^R, h_2^R = known boundary hydraulic head,
- \bar{q}_{n_h} = vertically averaged normal Darcy flux (positive outward),
- \bar{q}_h^R = prescribed normal boundary flux 2D (horizontal) respectively,
- $\bar{\Phi}_h$ = fluid transfer coefficient (leakage parameter) 2D (horizontal) respectively,
- $\bar{\Phi}_h^{in}, \bar{\Phi}_h^{out}$ = directional coefficient of in-transfer and out-transfer respectively for 2D horizontal,
- Q_ρ^w = well function,
- Q_m^w = pumping injection rate of a single well m,
- x_i^m = coordinate of single well m,
- n_i = normal unit vector.

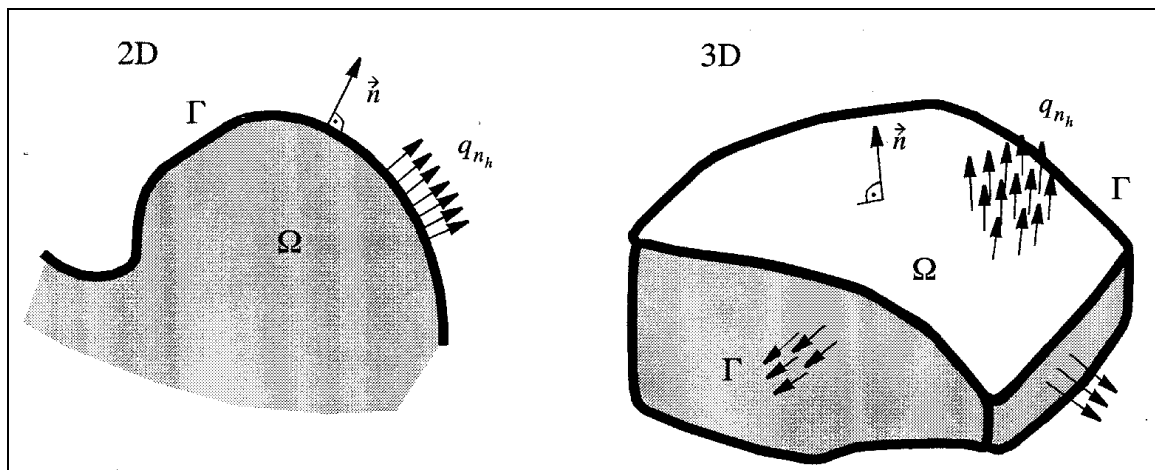


Fig. 2.2: Illustration of flow boundary conditions as formulated in the equations above (source: FEFLOW Manual, 1998)

The finite element (FE) (approximate) solution to the above governing equations leads to a set of algebraic equations, in which the unknowns are the heads at the grid nodes. The head within each element is defined in terms of the nodal values by using interpolation functions (also called basis functions). Conceptually, the FE solution is connected with Galerkin's method, which lies on a weighted residual principle expressed directly in terms of the governing partial differential equation. Taking Poisson's governing equation as an example, and assuming a trial solution $\hat{h}(x, y)$, the residual of the governing equation weighted by the

nodal basis function must be zero when integrated over the problem domain D . Galerkin's residuals are expressed mathematically as below (WANG & ANDERSON, 1995).

$$\iint_D \left(\frac{\partial^2 \hat{h}}{\partial x^2} + \frac{\partial^2 \hat{h}}{\partial y^2} + \frac{Q_p}{T} \right) N_L(x, y) dx dy = 0$$

Where N_L is the nodal basis function.

The above equation leads to a system of linear equations to solve the Poisson's equation approximately. The solution of the linear equations is normally achieved by iteration, only feasible with computer packages. The finite element solution routine imbedded in FEFLOW software is applied to solve the flow equations adopted for the Gedaref aquifer system.

2.5.2 The Numerical simulator

The numerical solution is implemented using the interactive simulation system FEFLOW (DIERISCH, 1998). "The simulation system FEFLOW is based on the physical conservation principles for mass, chemical species, linear momentum and energy in a transient and three-dimensional (if necessary two-dimensional) numerical analysis", DIERISCH, 1998.

FEFLOW is quite flexible with respect to boundary conditions through the use of constraints. For example, head boundaries (Dirichlet type) can be turned off and on during the simulation using flux constraints, and flux boundaries (Neuman type) can be limited by head. Both boundary conditions and associated constraints can be time-dependent, which adds additional flexibility. The water budget module of the program provides an important calibration tool, and allows check of the contribution of the assigned boundary conditions. FEFLOW has a built in pre- and post-processing, whereas MODFLOW (MC DONALD and HARBAUGH, 1988) and its companion codes require third-party software to set-up the model.

Other FEFLOW features that are not used in the Gedaref flow simulation are deforming mesh (to accurately represent water table). Yet, the advantages of finite element mesh used in FEFLOW, clearly show up for applications that involve complex hydrostratigraphy or areal configuration.

2.5.3. Calibration approaches

Calibration of a groundwater flow model is achieved when simulated head distribution agrees with observed one. In other words, calibration is the process of parameter estimation

conditioned on head measurements. However, more than one parameter is usually unknown. In the Gedaref case, the unknown parameters include the hydraulic properties T and S , the boundary conditions, the pumping rates, the areal recharge or vertical leakage entering or leaving the aquifer through boundary aquitards.

Generally, calibration or solving the inverse problem is approached using one of two techniques: either the direct or the indirect. The direct (also called equation error criterion) method considers the model parameters as dependent variables in a formal inverse boundary value problem (YEH, 1986). The indirect (also called the output error criterion) approach is based upon an output error criterion to be fulfilled through iterative improvement of parameters under calibration.

The indirect method proves to be more practical as it is applicable to limited observations distributed arbitrary in the flow region. The criterion used in this approach is the minimization of the mean of the difference between the observed and the calculated heads at specified observation points. Most available commercial software are based on this method. However, some of them use various optimization algorithms to perform the minimization automatically instead of the tedious trial and error way to improve the parameter estimates.

The structured approach presented by YEH and MOCK (1995) is used to calibrate the boundary flux, the vertical leakage as well as the transmissivity values in the zonation method. The approach benefited from an important conclusion of the stochastic theory, namely: “the behavior of the heterogeneous aquifer could be approximated by a homogeneous one using the geometric mean of the log normal transmissivity distribution” (GOMEZ, 1989, GELHAR, 1993). According to the adopted approach, the following steps are to be followed.

1. determination of the effective transmissivity value as equivalent to the geometric mean,
2. adjusting boundary conditions and recharge rates to minimize the bias in the simulated head,
3. after selecting the correct boundary conditions and recharge rates, the next step focused on reducing the variability around the mean by modifying the transmissivity distribution (shape of T -zones). Having the parameter structure established, an automatic calibration could also be used to get optimized parameter values at different zones.

4. finally, numerical simulations are conducted using more detailed transmissivity distribution as constructed from interpolation/ simulation of available transmissivity data.

The Optimization program (PEST)

PEST (DOHERTY, 1994) searches for a parameter set for which the sum of squared deviations between model-calculated and measurement values at the observation boreholes is reduced to minimum. The resulting values are said to be optimized.

The optimization package is used in this work only to estimate fracture transmissivity along lineament identified from the satellite imagery. However, optimization criteria turn out to be insensitive to T values of fractures far from measurement locations as indicated by the high confidence limit and variable results of T obtained in different runs.

2.6. Reliability measures

Measures to quantify the quality of calibration, data shortcomings, and confidence in parameter estimates and predictions are important to communicate the results of modeling studies to decision makers as well to the modeler (HILL, 1998). Such measures as applied in the current model study include estimates of the variance and the coefficient of variation (standard error).

Confidence in the calibration results is assessed by specifying the range of plausible simulation results, called the calibration targets. Calibration targets are assigned for both the head measurements as well as the estimated water budget components.

The error expected in head values could be attributed to various sources, such as measurement errors, the accuracy of the topographic levels, the well design and the source of the data. Additionally, discrepancies between measured and simulated head arise from unmodeled small scale heterogeneity, discretization and interpolation errors. Errors typically coming from different sources are considered random and normally distributed (SUN, 1994, CHILES, 1999, CHRISTENSEN and COOLY, 1999, MEYERS, 1997); and are hence accounted for by the head variance. An estimate of the head variance for 2D steady state is provided by MINZEL (1982) as:

$$\sigma_h^2 = \frac{8}{\pi^2} J^2 \lambda^2 \sigma_{\ln T}^2$$

where σ_h^2 is the head variance, J is the mean gradient, λ is the correlation scale, and $\sigma_{\ln T}^2$ is the variance of $\ln T$.

The above variance value provides a measure of the accuracy or the closeness of measurements to the true unknown value. The square root of the calculated variance is used to indicate the range of plausible/target head.

Directly related to the above measure/target is the mean square error criteria generally used to assess the calibration. Formulated in a mathematical form the mean square error (RMS) is:

$$E\left[(\hat{h}-h)^2\right]$$

Where E is the expected value, \hat{h} is the simulated hydraulic head, and h is the observed hydraulic head.

The RMS is divided by PRIESTLY (1981) into two terms as follows.

$$\begin{aligned} E\left[(\hat{h}-h)^2\right] &= \text{var}[\hat{h}] + B^2 \\ &= E\left[(\hat{h}-E[\hat{h}])^2\right] + (E[\hat{h}]-h)^2 \end{aligned}$$

Where, $\text{var}[\hat{h}]$ is the variance of the simulated head resulting from spatial variability of T and possible random measurement error; and B^2 is a bias term representing the deviation from the mean observed head.

The bias B^2 is minimized when the simulated \hat{h} reproduces the mean trend of the observed heads in the aquifer. According to YEH and MOCK (1995) this is achieved when the scatter plot of \hat{h} vs. h points lie along a 45° line. The remaining variance term ($\text{var}[\hat{h}]$) should lie within the above target as an indication of the model fit.

Due to the lack of measured flux data, 10-15% accuracy in the estimated water budget is considered a suitable target for the Gedaref model.

To reduce the uncertainty in the model estimated parameter, prior information should be incorporated (YEH, 1986, ANDERSON and WOSSNER, 1992, GOMEZ, 1989). The coefficient of variation ($\frac{\textit{standard deviation}}{\textit{mean}}$) is recommended by ANDERSON and WOSSNER (1992) to quantify the uncertainty associated with the prior information. This will lead to the estimation of the plausible range of parameter values and hydrologic stresses prior to calibration.

3. Description of the study area: A regional review

This chapter gives a broad overview of the large scale physical setting and the environmental conditions surrounding the investigated/study area. It provides a baseline study for the smaller scale characterization of the main area of interest: the west Gedaref groundwater sub-basin. In section 3.2 the climate prevailing in the region is discussed. This is followed by a description of the salient topographic and landuse features in section 3.3, and the drainage system in section 3.4. An extensive overview of the regional geologic history is provided in section 3.5. This includes a critic review of the available studies on Gedaref Geology.. The last section 3.6 describes the groundwater resources of the region and the state of groundwater development.

3.1. Climate

The Climate in the Gedaref region is semiarid with mean annual temperature of 28.5°C (fig. 3.2). The mean annual precipitation recorded at four meteorological stations in the Gedaref region is shown in Fig 3.1. In the south, at Doka, average rainfall reaches 676 mm/y. Further to the North the average rainfall decreases to 588 mm/y at Gedaref in the middle of the region; and even more decreasing to 463 mm/y at El Showak at the northeastern border.

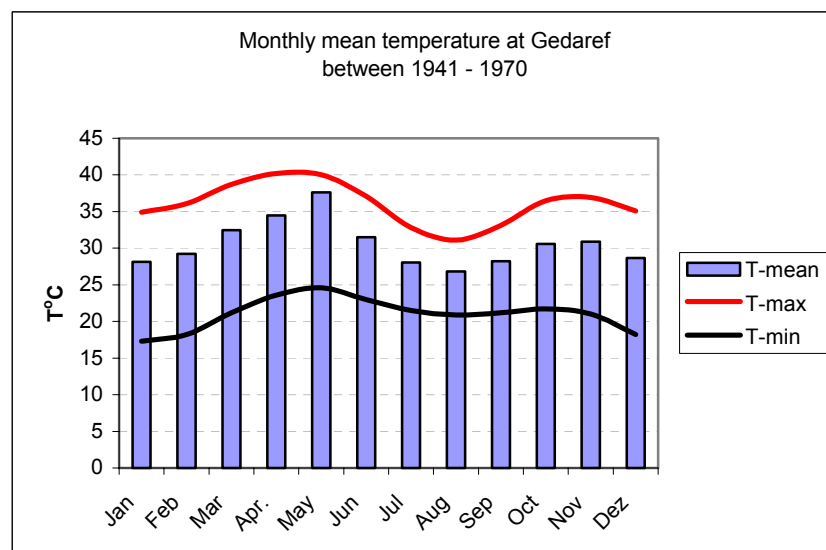


Fig. 3.1: Monthly average temperature at Gedaref. (source: Climatological Normals 1941-1970, Sudan Meteorological department).

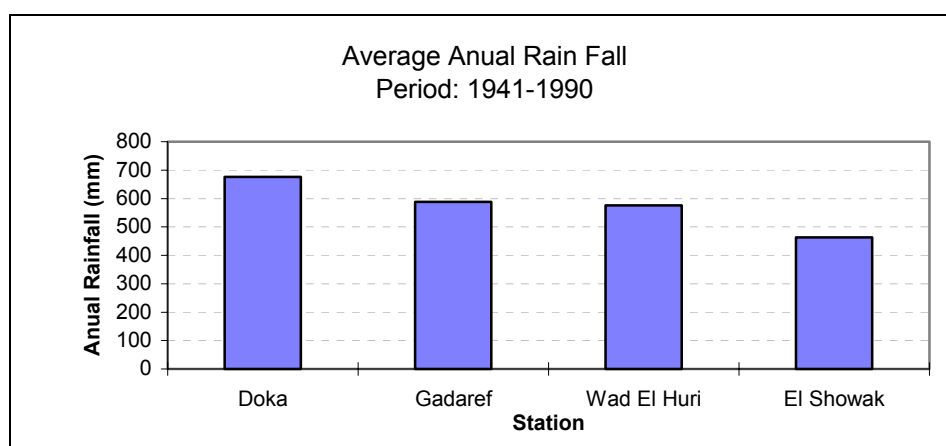


Fig. 3.2 : Average annual rainfall at four meteorological station in Gedaref Region. (sources: Sudan Meteorological Department)

The monthly rainfall records (table 3.1, fig. 3.3), show that the bulk of the rain falls in the period from mid June to September, and reaches its peak in August.

Table 3.1: Rainfall totals (mm).

Month	Gedaref 1941 - 70	Wad El Huri 1941 - 70	Doka 1941 - 70	El Showak 1951 - 80
Jan	TR	0	0	0
Feb	TR	0	0	0
March	1	TR	1	TR
Apr.	4	5	6	1
May	27	13	31	17
June	86	98	121	70
July	154	157	136	170
Aug.	188	208	196	179
Sep.	92	78	108	58
Oct.	24	16	27	9
Nov.	3	1	4	2
Dec.	0	0	0	0
Year	579	576	630	506

TR indicate rainfall below 1 mm.

(Source: climatological normals, Sudan Meteorological Department).

The maximum intensity of rain is in the range of 100 -150mm/h (AKOD, 1996, unpublished) usually in the form of convective showers and thunderstorms of short duration, small Aerial extent, and high intensity.

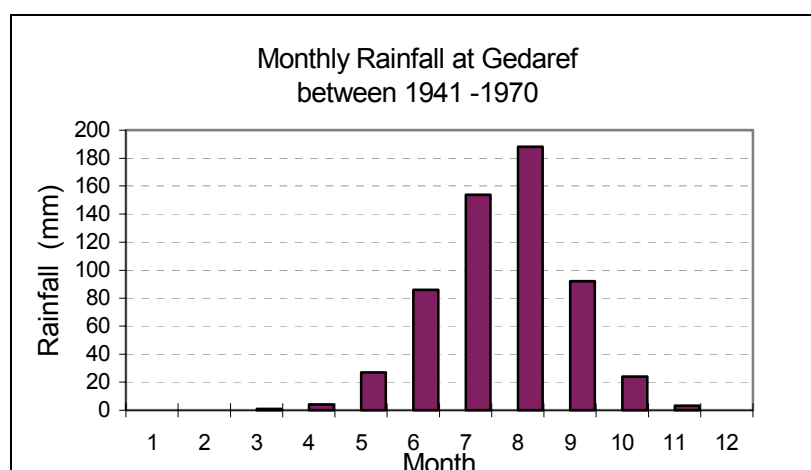


Fig. 3.3: Monthly average rainfall at the Gedaref station.

Annual potential evapotranspiration greatly exceeds annual precipitation in the Gedaref. Looking at the evaporation records (table 3.2, fig. 3.4), rainfall exceeds evapotranspiration only in August and September. 12% of the total rainfall is estimated by SKAP (1992) as excess water available for runoff and infiltration during the two months of the year.

Table 3.2: Monthly average evaporation at the Gedaref station.

Month	Evaporation Piche (mm)	Eo (mm/d)	P (total) (mm)	Eo (total) (mm)	P-Eo
Jan	13.6	6.8	TR	211	
Feb	15.6	7.8	TR	218	
Mar	19.0	9.5	1	295	
Apr	19.5	9.8	4	293	
May	16.0	8.0	27	248	
Jun	11.8	5.9	86	177	
Jul	7.3	3.7	154	113	41
Aug	4.7	2.4	188	73	115
Sep	5.6	2.8	92	84	8
Oct	9.2	4.6	24	143	
Nov	13.8	6.9	2	207	
Dec	13.6	6.8	0	211	
year	12.5	6.3	579		164

(Source: Climatological Normals, 1941 - 1970)

3.2. Topography and landuse

The topographic data of the Gedaref region (fig 3.5) is compiled from the sheets number 453, 454, 483 484, produced at a scale of 1:100,000 with 5 and 10 meters contour spacing (the Sudan Survey Department, 1989). As visible from the contour lines pattern on the topographic maps, the region is mainly characterized by a low relief between 580 - 450 m, interrupted by

isolated Quarzite and sandstone ridges and Granitic and Basic rock outcrops (Jebels). An elevated hilly basaltic ridge of up to 760 m above mean sea level, extends in the middle of the region from Gedaref to Gallabat in a northwest southeast direction.

The Gedaref region lies between the Southern Butana Shrub Savannah and the Southern Gedaref Wood Savannah land regions, (SKAP/DHV,1989). This regional boundary coincides with the 550mm annual rainfall isohyet. Most of the natural vegetation has long been cleared and replaced by mechanized farming. Farming of millet, sorghum and sesame covers much of the gently sloping land.

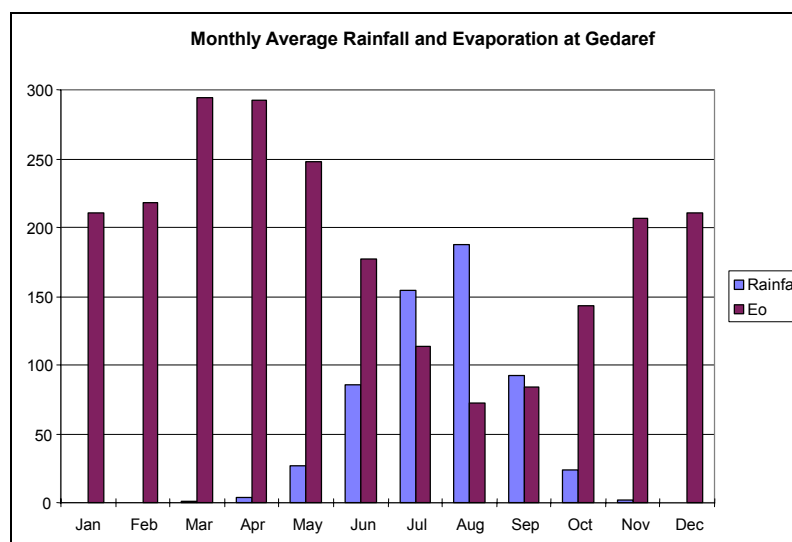


Fig. 3.4 : Monthly average rainfall and evaporation at Gedaref station

3.3. Drainage

All the area west of the Gedaref - Gallabat ridge drains to the Rahad River by way of two major wadi (khor) systems, Abu-Fargha khor in the North, and Samsam in the south (SKAP, 1992). All the land east of the ridge drains to the Atbara river. The study area lies in the middle reach of Abu Fargha catchment. The major drainage system crossing the study area is the east flowing khor Al-Laya, a major tributary of Abu-Fargha ephemeral stream (see figure 3.5).

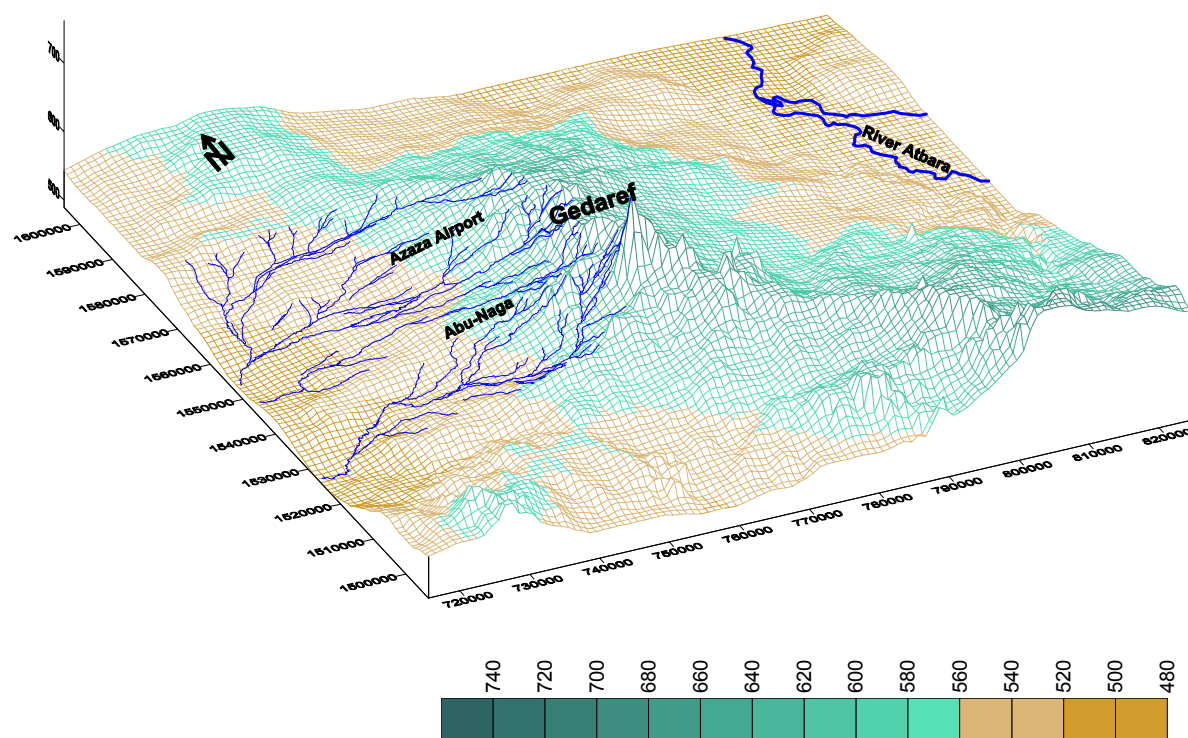


Fig. 3.5: The Topography of the Gedaref Region, levels are in m above mean sea level.

The catchment area of khor Al-Laya was estimated by AKOD (1996) at 60 km². Stream discharges are affected by the type of storms occurring in the area. Summer thunderstorms result in flash floods along the khor lines that quickly rise to a peak rate of discharge and then recede rapidly to their original state. The flows of khor Al-Laya was monitored between 1960 and 1992 by the rural water administration at the coordinates 14.02° 35.22°. There is no record of the duration of separate flood events. Table 3.3 below indicates an average of 15 flood events during the four rainy months. According to the flood records (table 3.3, fig. 3.6), the average annual discharge is about 4 Mm³ (about 6% of the total rain). However, the amount of discharge varies according to the rainfall amount and intensity. A maximum value of 12.07 Mm³ is recorded in 1973, and no single flood event occurred in 1994. According to AKOD (1996), the maximum discharge rate occurred in 1973 continued for 17.5 hours, in which a total of 4.73 Mm³ is discharged. From the tabulated records, on the average, each flood event is expected to last for a minimum duration of 0.5 hours under maximum discharge/head. However, due to its very gentle slope water-logging occurs during and after the rainy period (SKAP, 92).

Table 3.3: Flood records at Al-Laya stream.

Season	Max Head (m)	Mean Velocity (m/sec)	No. of Floods	Max. Disch. (m3/sec)	Annual Disch. m3	Observation Period	
						from	to
1960	2.45	2.593	9	143.30	2372305	28.06	30.08
1961	1.80	1.892	19	62.98	2138400	03.07	17.09
1962	3.40	4.667	17	82.00	3056282	04.07	08.10
1963	3.80	1.273	28	263.35	4353768	07.06	05.10
1964	2.05	3.684	16	151.88	3186660	19.06	29.08
1965	3.10	1.400	17	140.88	9150987	24.06	03.08
1966	2.73	2.258	16	175.17	3997199	10.06	18.09
1967	3.00	1.795	21	158.78	5453253	25.06	28.09
1968	2.95	2.333	12	200.90	2173131	27.06	18.09
1969	2.04	2.333	15	122.27	2066103	01.07	30.08
1970	2.30	1.944	20	68.89	1390239	09.07	06.10
1971	2.30	1.167	14	70.03	2120589	22.07	30.08
1972	3.50	2.000	16	127.24	8365320	01.07	04.09
1973	3.90	5.385	16	871.50	12068352	15.07	10.10
1974	2.07	1.750	16	21.20	4937508	02.07	06.09
1975	3.00	1.400	24	175.88	7420428	16.06	25.09
1976	2.20	2.917	19	161.60	5368439	30.06	26.09
1977	2.40	1.750	13	126.00	4020070	17.06	10.10
1978	2.80	1.795	20	135.25	7231207	29.06	10.10
1979	3.20	2.333	12	305.81	7070423	02.07	17.09
1980	3.42	1.944	9	256.55	5805072	21.06	24.08
1981	3.37	3.182	10	337.61	4959601	11.07	05.09
1982	3.95	3.500	13	791.00	10388250	19.07	26.09
1983	2.55	1.429	14	110.57	1322649	16.06	02.10
1984	2.68	1.667	15	265.30	4386672	19.07	30.09
1985	1.20	0.636	9	11.72	119061	27.08	15.10
1986	3.13	1.556	18	160.48	2947085	06.07	31.10
1987	2.19	1.061	8	84.78	4135671	01.07	31.10
1988	3.03	1.167	15	128.38	1433106	02.07	23.09
1989	3.81	1.250	15	204.88	6391539	17.07	26.09
1990	2.81	1.167	8	106.34	2919915	14.07	25.09
1991	3.10	1.750	9	314.35	3125637	14.07	21.08
1992	2.63	1.522	12	144.79	2407491	17.07	13.10
1993	0.59	0.598	1	6.41	94887	07.09	31.10
1994	0.00	0.000	0	0.00	0	-	-
1995	1.31	1.250	11	37.75	1063476	-	-
1996	3.60	1.750	21	281.40	4904001	01.07	31.10
Median	2.80	1.75	15	143.3	3997199		

3.4. Geological History of the Gedaref Region

The area under consideration belongs to the west Gedaref subbasins which occupy an area of 2250 km² in the western portion of the Greater Gedaref sedimentary Basin. The latter is generally flat lying to gently sloping (EL SEED, 1989) sandstone formation covering an area of 28000 km² (GIBB, 1987) in the east of central Sudan, and continues into Ethiopia (fig. 3.7).

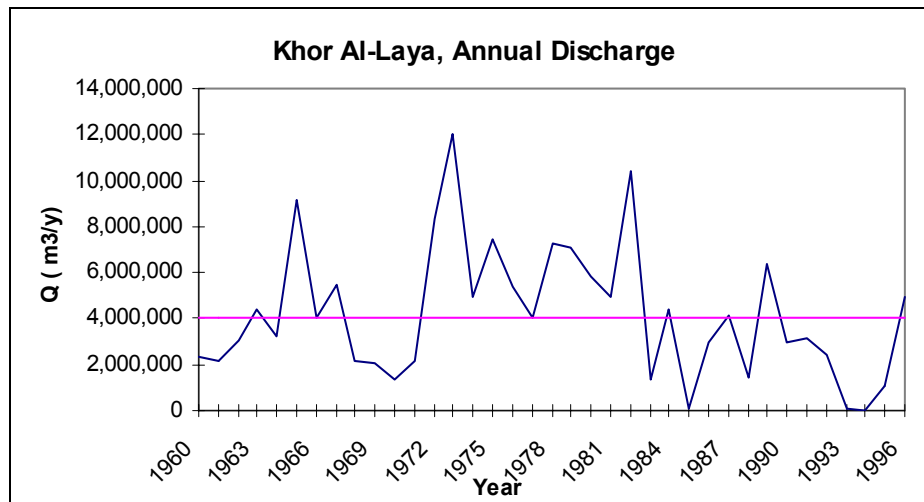
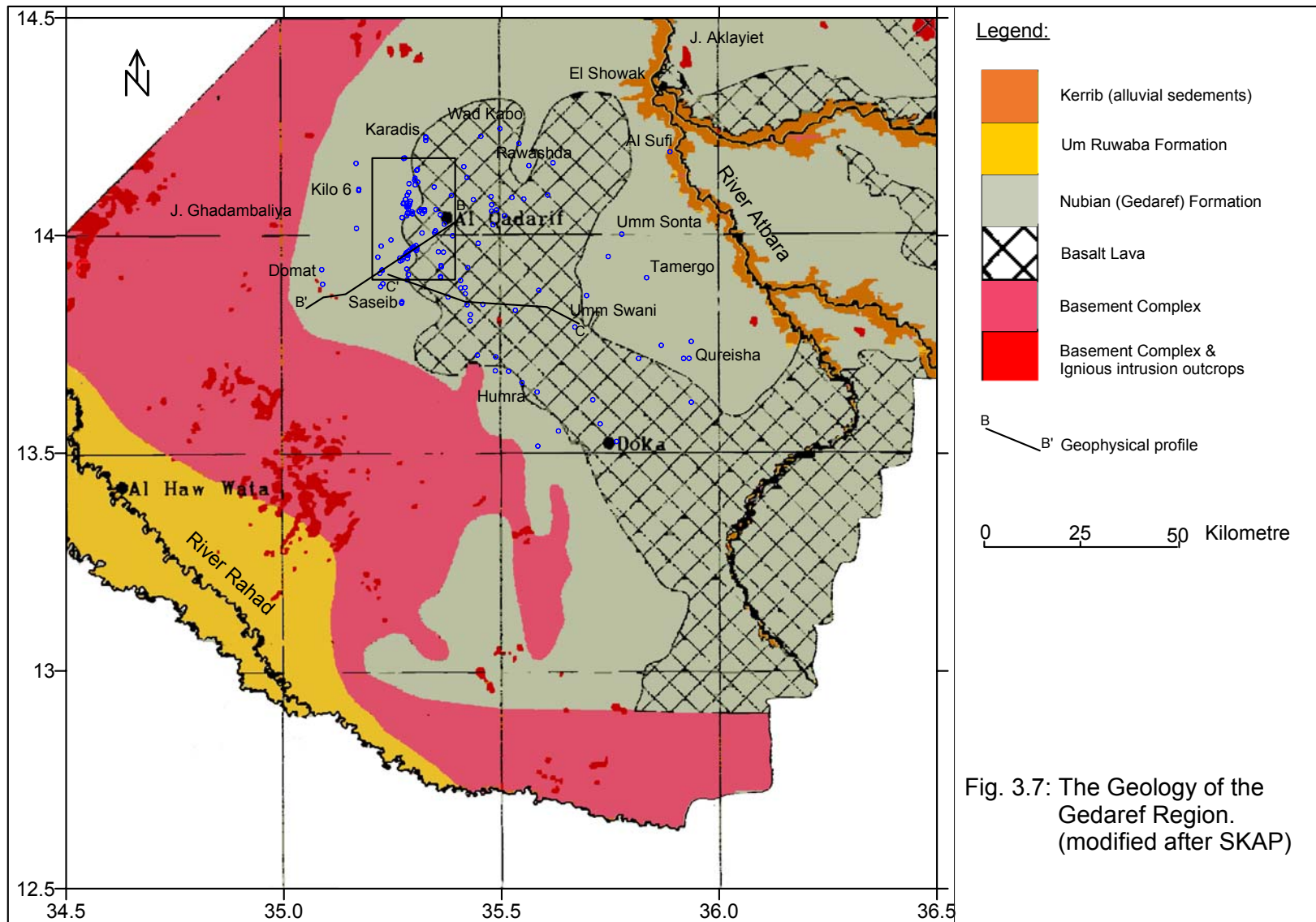
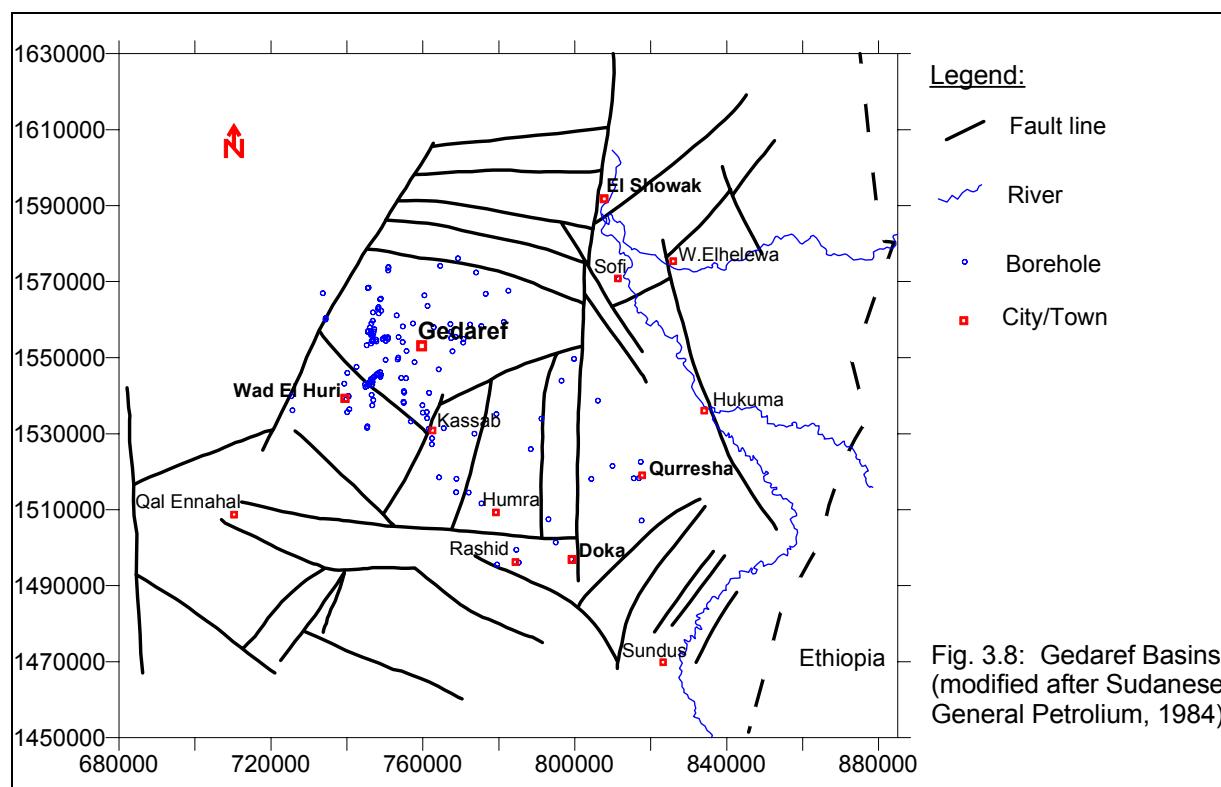


Fig. 3.6: Annual fluctuations of Al-Laya discharge.

The origin of the Gedaref region basins seems to have a complex nature. GIDDO, (1985) suggested that they have the same history of development and age as those of central Sudan and western Sudan Basins. A geological and geophysical study by MULA and OMER (1983) concluded that the Nubian sedimentation is probably initiated by pre-cretaceous and cretaceous movements, which uplifted the Butana crystalline massif to the west of Gedaref, and created a vast subsiding structural basin (graben) passing by Gedaref in a roughly north-south direction. They also suggested that this major basin is limited by two major faults to its eastern and western borders, but movements generated step faulting intra-minor subbasins. A more detailed gravity study (Gravity map, 1984) conducted later in 1984 by the Sudanese General Petroleum corporation has confirmed the above interpretations of MULA and OMER (1983). The result of the latter study shown in fig 3.8, indicated the presence of a structurally controlled major sedimentary Basin at Gedaref with a maximum depth of more than 3 km, and a number of minor subbasins probably caused by step faulting.

It is believed that the structural Gedaref Basin consists of a gently undulating peneplain with depressions and Basins created by a long period of erosion of the Pre-Cambrian Basement Complex igneous and metamorphic granites, schists, gabbros and serpentines (SKAP, 1992). The resulting depression was filled with the Gedaref Formation since the Mesozoic period. These sediments were gradually transformed through subsidence and increasing pressure into conglomerates, sandstones and mudstones.





BUSSERT (1998) concluded that “in the Gedaref basin, sedimentation was purely continental. Sandy braided rivers streamed dominantly towards the northwest. They changed basin-wards into anastomosing rivers accompanied by extensive, long lived flood plains and lakes“. He added that those rivers had no connection to the sedimentary basins in central northern Sudan. It is believed that the climate during deposition of the Gedaref Formation was arid with enough rain or flooding to flush soils and prevent formation of saline lakes.

According to RUXTON (1956) “the beds now included in the Gedaref Formation consist of conglomerate, sandstones, sandy mudstones and mudstones, and exhibit many of the characteristic features of the Nubian Formation that crops out further west“. CHIALVO (1975) and OMER (1983) confirmed the latter findings by concluding that the sandstones in the Gedaref are believed to be cretaceous sediments having the same characteristics of the Nubian sandstone in other parts of Sudan. In many places the sandstones are silicified to such an extent that they are almost quartzites, for example Jebel Matna area. Outcrops are rare, and throughout much of the region the Gedaref sandstones are overlain by basaltic intrusive and extrusive rocks. At greater depths the Sandstone becomes highly silicified.

The basin was subjected to a series of normal faults striking parallel to the axis of the basin (ALMOND et al., 1984). Cross sections B-B' and C-C' below which were produced from a geophysical survey by the RURAL WATER CORPORATION in 1989 give some examples of the high throw faults.

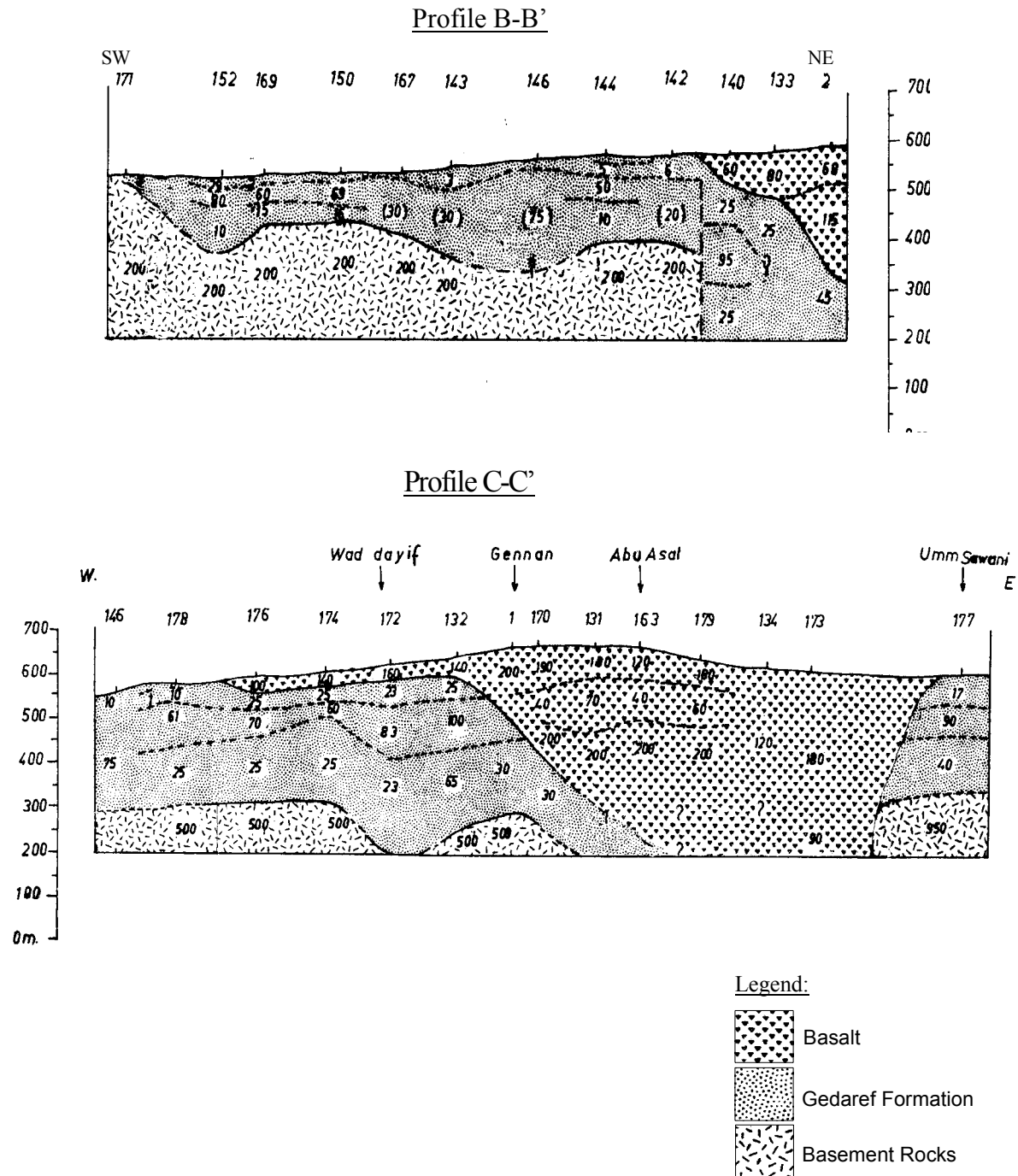


Fig. 3.9: Geophysical Profiles showing the extension of the west Gedaref sandstone formation, and the Basalt intrusion, (Source: RWC/ TNO, 1979). For the location of the profiles and the horizontal scale refer to fig. 3.7; The vertical scale is in m above sea level.

The re-development of the Gedaref basin began already in the early Tertiary period and was probably connected with a reactivation of fault zones already created (ALMOND et al., 1984). It is believed that, already at this time volcanic activities within the area of the disturbances have prevailed. WIPKI (1995) showed that, one of the main disturbance in the Gedaref area in the direction 70° corresponds to the extension of the Central African fault zone. The second direction with $135^\circ - 150^\circ$ runs approximately parallel to the rift axle of the Red Sea (135°). In the course of the further development, NW-SE running fault zones thrust upon along the oligocene basalts, Trachyte and Rhyolithe (ALMOND et al., 1984).

The volcanic activities extruded large sheets of Basalts onto the Gedaref Formation (fig. 3.9), and into cracks and fissures between the base of the Gedaref Formation and the underlying Basement Complex rocks. During the late Tertiary and Pleistocene periods dark cracking clays (Vertisols) were deposited which now blanket most of the study area.

3.5. Groundwater occurrence

The main aquifer in the region is the Nubian sandstone. A secondary aquifer of low productivity is the weathered and fractured Basalt cutting through the Nubian formation. The latter extends westward for about 30 km to the Basement boundary. It extends to the east beyond the Ethiopian Sudanese border.

Groundwater level data in the investigated area are available at 127 boreholes out of 148 wells tapping the Nubian sandstone and the Basalt aquifers. The first figure includes both 15 boreholes in the northern wellfield (named Azaza), and 17 boreholes in the southern one (named Abu-Naga). This data set is obtained from the archive of the Gedaref water administration, and it comprises the water depth measurements conducted upon the construction or rehabilitation of the boreholes in the period between 1989 and 1992. The drilling logs showing the aquifer horizons, as well as the well design are included in the archive data, too. As some of the wells are constructed since the late sixties and early seventies, the natural groundwater depth might have varied in the considered measurement period. However, the archive data is considered to represent the natural state of the aquifer. Also, assuming that most drilling operations took place during the dry summer season, large seasonal variations expected in groundwater levels are ignored.

The piezometric surface in the sandstone generally lies at 14.63 (Rashid) to 123.7 m (Sharafa) below the ground surface.

Plotting the groundwater contour reference to the sea level (fig. 3.10) indicates that, the regional flow direction is generally towards the East and the West forming a water divide along the basaltic ridge. This piezometric map was plotted assuming that both the basalt and the sandstone aquifers are hydraulically connected.

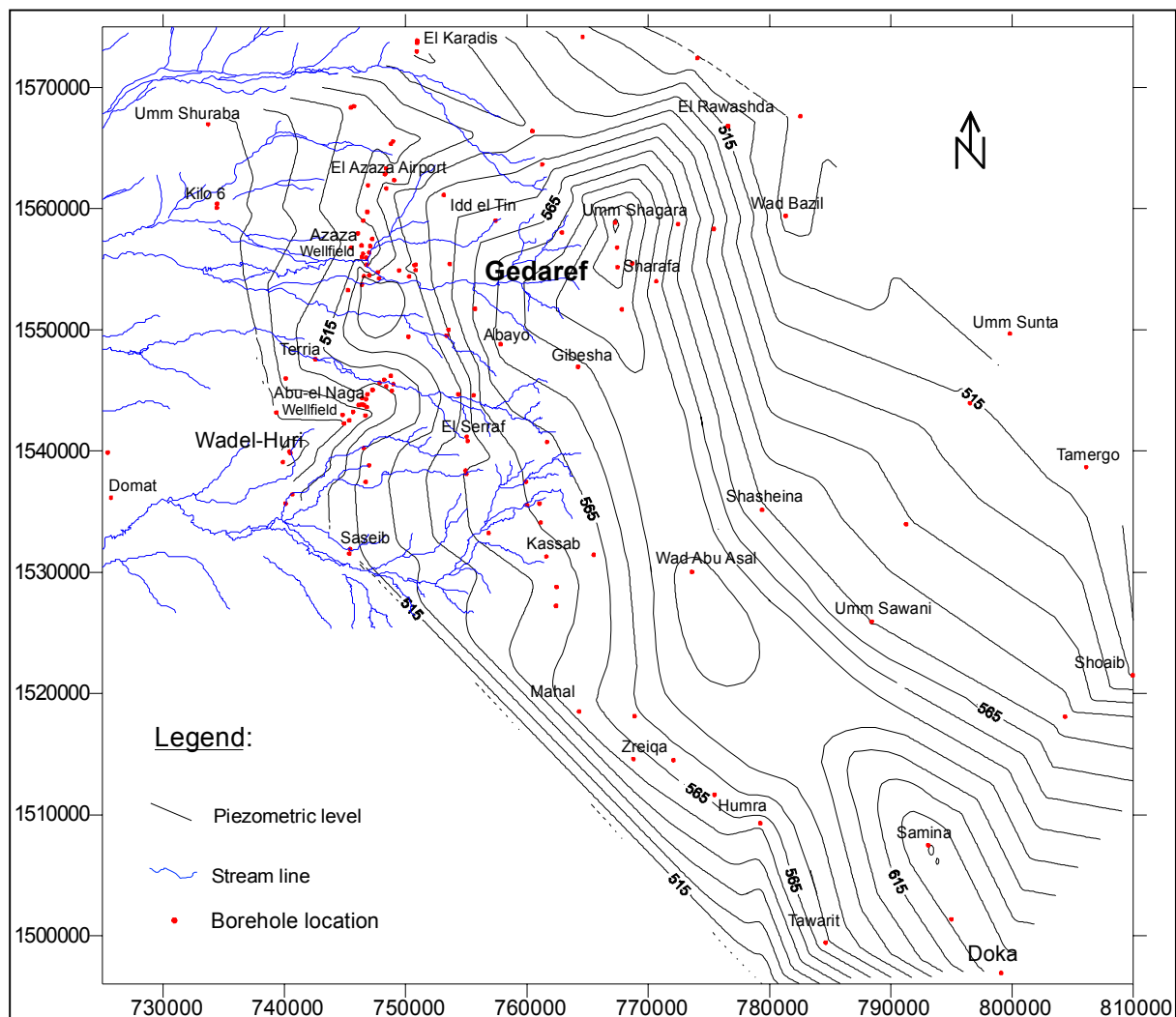


Fig 3.10: Piezometric map of Gedaref region.

3.6. Groundwater Development

Groundwater in the region is used almost only for domestic and livestock water supplies. Apart from the scattered village-owned wells, two wellfields are constructed to supply the

main city of Gedaref with its need for drinking water. These are the Azaza and Abu-Naga wellfields.

Azaza wellfield

Azaza wellfield (fig. 3.10) lies about 10 km northwest of the Gedaref city. It extends along a north-northeast south-southwest axis between latitudes $14^{\circ} 02'$ - $14^{\circ} 08.5'$ N and longitudes $35^{\circ} 18'$ - $35^{\circ} 23'$ E. The aquifer system in Azaza basin is developed mainly in the Gedaref sandstone Formation. Azaza well field is constructed in 1992 and started working in the end of 1992. It supplies Gedaref by 20% (up to 50% in the dry season when river Atbara dries out) of its total supply (SAGHAYRON et al., 1996). A total of 16 wells (127 - 194 m deep below ground surface) were drilled, one borehole is dry (Azaza 5). Only five boreholes are currently working with a pumping rate of $3000 \text{ m}^3/\text{d}$ (Gedaref Water Corporation report).

Abu-Naga wellfield

Abu-Naga Basin lies near Abu-Naga village 14 km south-west of the Gedaref, and extends about 10 km further in this direction to the sandstone margin at Wad-el-Huri. A high ridge caused by a fault trending in north-south direction acts as an eastern boundary to the Basin (SULEIMAN, 1968).

Abu-Naga well field is partly constructed in 1971 and expanded later in the eighties and nineties. It consists of 20 wells (135 - 296 m deep), 4 abandoned, 16 existing, and only 8 are currently working. The total abstraction from the 8 working wells is $3000 \text{ m}^3/\text{d}$.

4. Hydrogeological characterization of the West Gedaref Aquifers

4.1 Introduction

In the previous chapter the regional characteristics of the Gedaref Basin was described. This chapter concentrates on the west Gedaref sandstone aquifer which is the main source of drinking water for the city of Gedaref. Archive data and data collected during the field visit are analyzed and correlated to obtain an understanding of the hydrogeologic system in the Nubian formation.

Hydrogeological characterization of the subbasin is considered as a first step towards further chapters in the thesis. It includes different methods to quantify the hydrogeological parameter in the study area. Data processing, analysis, correlation, as well as digital image processing are used for the interpretation of available data.

This chapter is divided into three parts. Part one focuses on the geologic features of the Nubian formation, and presented in sections 4.2. Part two (section 4.3 and 4.4) studies the hydrologic and hydraulic characteristics of the sub-basin.

4.2. The aquifer system

The focus here is to define the extension and the boundaries of the sandstone aquifer system which will represent the geometric framework for the flow modeling in the next chapters.

In the previous chapter, it appeared that the west Gedaref sandstone formation is bounded to the east by thick basalt flows. To the north, west and south, basement rocks are cropping out or coming close to the surface. Data on the subsurface geology in the study area are derived from drilling logs of 94 boreholes available at the archive of the Groundwater Administration in Khartoum and in the archive of its regional office in Gedaref. Figure 4.1 shows the location of the investigated borehole logs.

This section consists of three parts, namely: (a) delineation of the Nubian limits west of Gedaref; (b) identification and correlation of the stratigraphic layers; and (c) identification of the structural setting; (d) combining stratigraphic and structural elements to define geometry of the different hydrogeologic units.

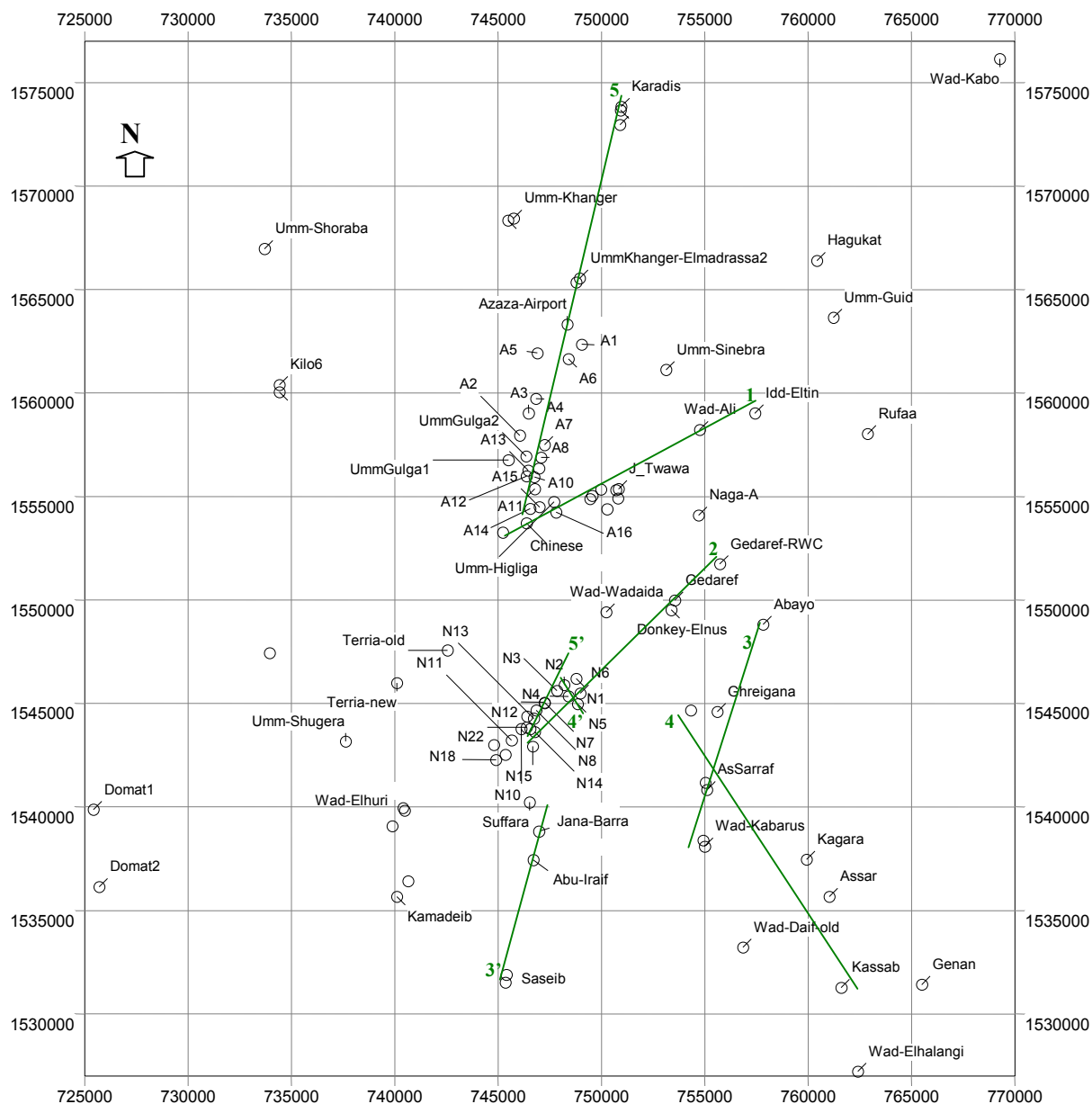


Fig 4.1: Well location map showing boreholes tapping the Nubian Aquifer. Lines indicate profiles presented below in figures 4.3 to 4.7.

4.2.1. Lateral extension of the Nubian sandstone

As mentioned earlier volcanic eruptions in the deepest center of the Gedaref Basin left behind extensive basaltic flows, dikes and sills. In the search for a basalt-free Nubian formation, the distribution of the Basalt thickness is investigated from borehole logs. Information from 53 boreholes drilled through the Basalt body are used to define the thickness and the extent of the volcanic flows. Figure 4.2 represents an isopach of the Basalt thickness more than 80m.

As it is clear from figure 4.2 and from the subsurface log descriptions presented in figures 4.3 to 4.6, the eastern limit of the sandstone aquifer is found along a line roughly passing from Umm-Sinebra through Wad-Ali, Jebel Twawa, Wad-Wadida and continues further to the south southeast. Basalt of more than 100 m thick is found east of this border underlain by thick Mudstone. The Nubian Formation thins out towards the northern, western and southern directions, to reach a depth of less than 100 m beyond El-Karadis, Umm-Shoraba, Kilo6, Umm-Raad, Umm-Shugerat, Wad el Huri down to the south of Saseib.

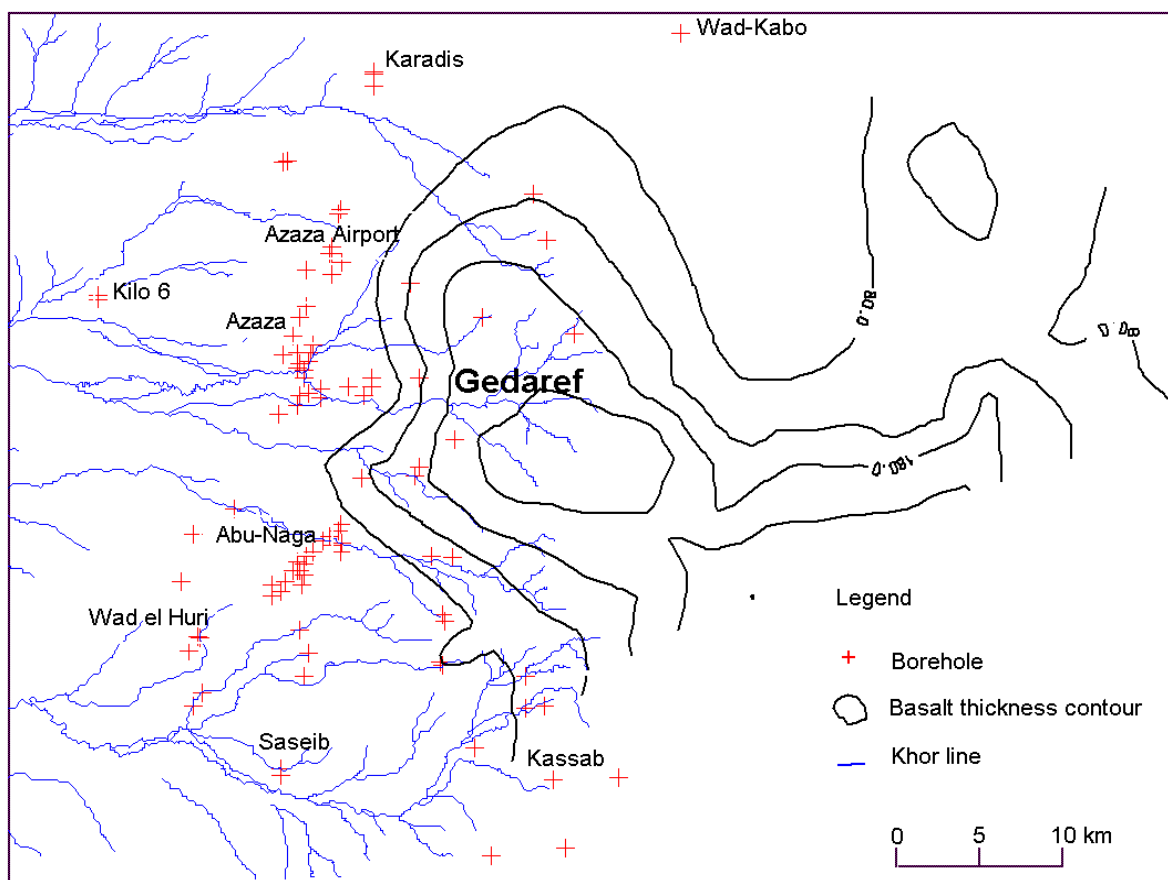


Fig. 4.2: Basalt thickness contour drawn from borehole logs.

4.2.2. Stratigraphy of the Nubian formation

The stratigraphy of the west Gedaref formation seems to be rather complicated and probably fractured with various structures. Tentative correlation of borehole logs along several profiles (see figure 4.1) has led to the description of the subsurface geological units and their extensions.

Borehole logs in the area indicate that the geology consists of interbedded sandstone and Mudstone underlain by the basement complex. The depth to Basement generally increases in a south-southeast direction (ranging from 131 m at Wad-Kabo to 273 m at N17).

The Basement level varies within few kilometers in the area. These variations could be attributed either to faulting or to undulations in the topography of the Basement. North of Azaza Airport (fig. 4.7a) the depth to Basement increases in a south-southwest direction from 135.9 m at Wad-Kabo to 198 m at Azaza Airport (An1) and 190 m at A1. About 750 meters south of borehole A1 the Basement level rises more than 40 meters at borehole A6 (155.5 m), and then continues again to fall down slowly to reach 190 at borehole A2 (see figures 4.7). Surprisingly, a geophysical survey carried out in the area (GRAS, 1990) showed that the depth to Basement at Umm-Gulga, (around one kilometer southeast from borehole A2) is found to be at 133.0 m below the ground, almost 60.0 m higher than at A2.

Immediately overlying the Basement Complex is a thin, hard Mudstone layer. This unit is in turn overlain by Sandstone of 50-120 m thick, which is divided into three major layers separated by mudstone beds of varying texture and thickness.

The total thickness of the Sandstone layers north of A6 is relatively thin representing only about 30% of the Nubian formation thickness. Southward between A6 and A14 (Azaza wellfield) sandstone thickness reaches more than 70% close to Al-Laya Khor.

The area between boreholes A1 to A3 is injected by highly weathered basalt sills of 25 m average thickness at a depth of 30-40 meters below the ground surface. About 420 m south of A1 (330 m north of A6) hard basalt is encountered at a shallow depth and drilling could not penetrate further than 72 m at the location of A5.

At the Azaza wellfield, the sandstone highly overweight the mudstone. Compared to Abu-Naga (see fig. 4.7b), there is no clear layering pattern in the Nubian Formation encountered in drilling logs of the Azaza wellfield. Thin mudstone and clayey lenses (7 -9 m thick) divide the aquifer into three layers.

Further to the South at the Abu-Naga wellfield thick continuous layers of Mudstone and Sandstone are distinguished (fig. 4.7b). The total thickness of the formation in the Abu-Naga area has been proved in borehole N17 at 272.9 m above the Basement complex.. Borehole N9 reached a depth of 250 m in Nubian formation.

Referring to the Geophysical survey carried by the Rural Water Corporation around Abu-Naga area (chapter 3, profiles B & C), the total depth of the Nubian formation hardly varies within this wellfield. The stratigraphy at the wellfield areas identified from drilling logs is correlated as shown in figure 4.8.

At Abu-Naga the Gadaref formation is covered by weathered to hard Basalt thinning out towards the west. Basalt thickness ranges from 56.39 m (at N5) to 16.76 m at N16. Hard mudstone exists directly below the Basalt at the top of the Nubian formation and persists to a depth of 50 m. About 10-15 m sandstone layer then followed. Relatively soft mudstone bed 30 m thick is underlain by coarse grained sandstone layer of 36 m average thickness. Then, loosely consolidated, mainly coarse grained Sandstone are found interbedded with the mudstone at the bottom of the formation.

In general, the subsurface geology in the west Gedaref is dominated by Nubian formation of a thickness reaching more than 270 meters overlying the Basement Complex. It is generally characterized by alternating beds of sandstone and mudstone. The formation is partly covered by basaltic flows 17 to 56 meters thick. The uppermost layer consists of superficial deposits of sandy clays and black cotton soil of maximum 10 m.

It is shown from the description above, that the stratigraphy of the Nubian Formation in the study area is divided into three Sandstone layers separated by mudstone beds. The uppermost sandstone layer (about 15 m thick) is fine-grained with mudstone intercalations, occasionally hard, ferrogenous and contains different impurities. The middle (40-50m thick) and the bottom (10-40 m) sandstone consist of whitish, well sorted, rounded to sub-rounded, coarse-grained sandstone and coarse sand, sometimes gravely. According to the log description, both layers are productive aquifers. The mudstone beds vary in thickness within a range of 7-30m.

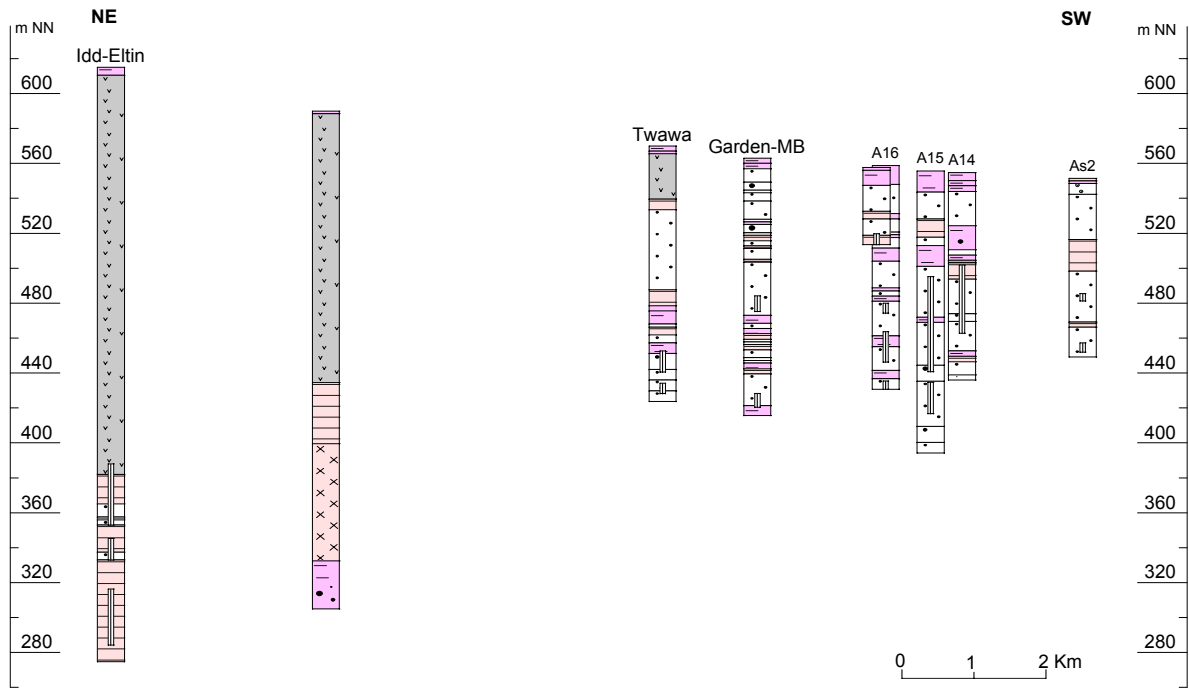
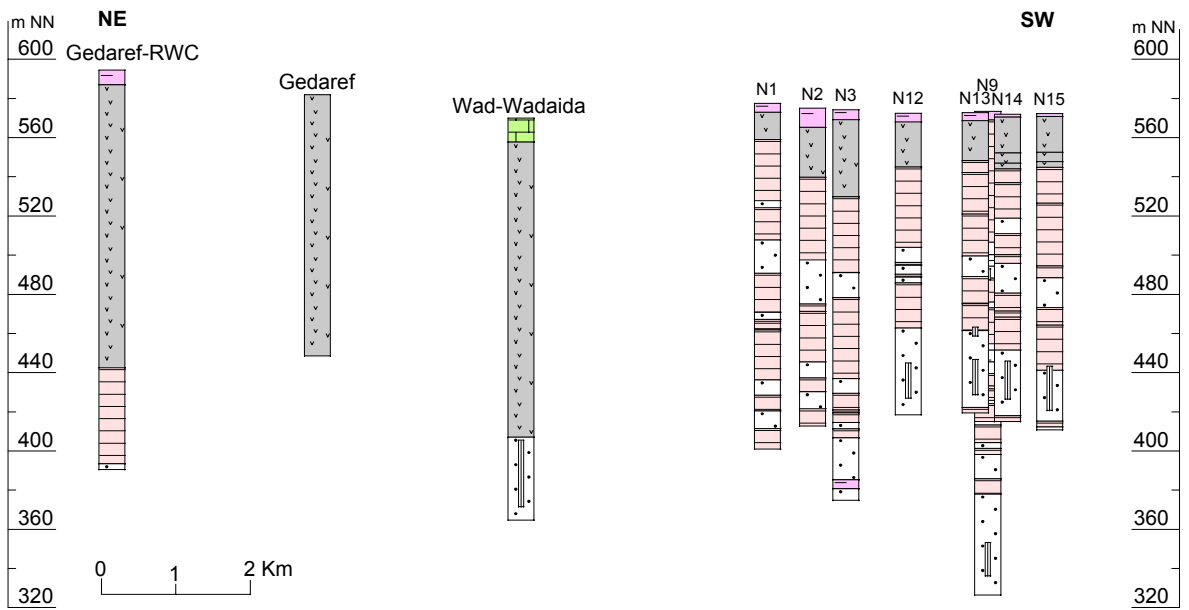


Fig. 4.3: Profile 1 showing the eastern Basalt boundary at Twawa area. For the location of the profiles see fig. 4.1.



Legend



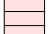

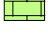
-  Clay
-  Basalt
-  Mudstone
-  Sandston
-  Limestone

Fig. 4.4: Profile 2 showing Basalt Nubian border At Abu-Naga area.

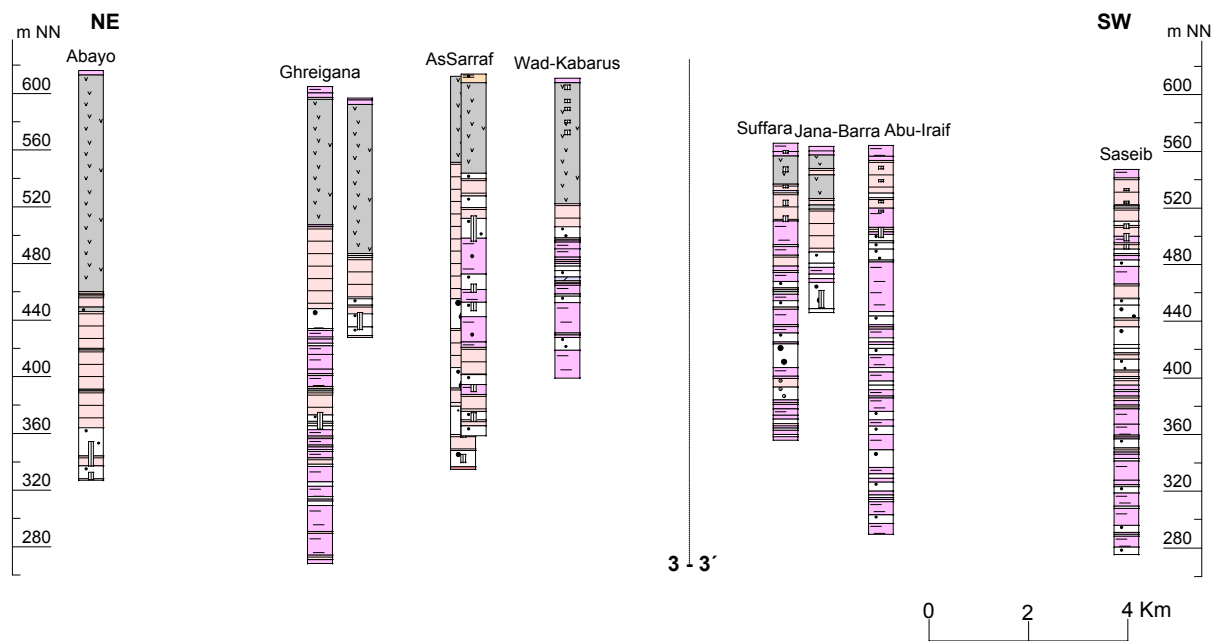


Fig. 4.5: Profile 3-3' showing the changing lithology of the Nubian formation towards the southwest.

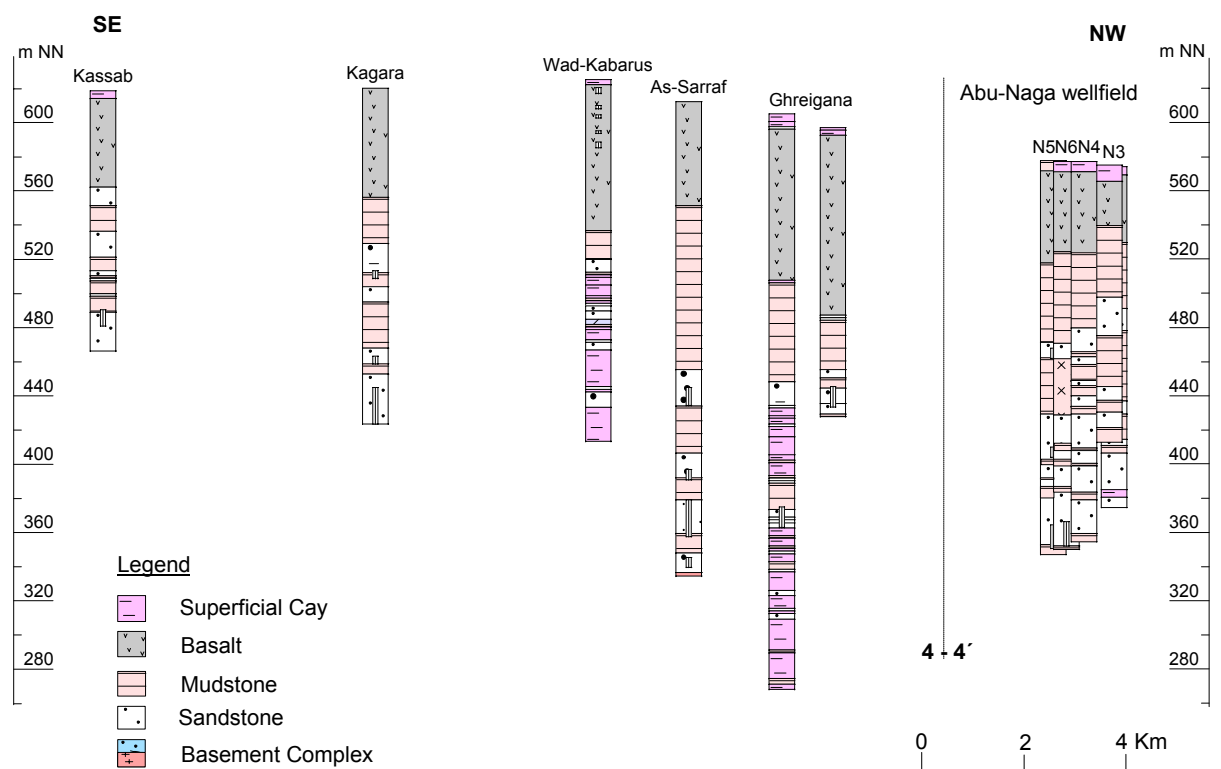


Fig. 4.6: Profile 4-4' showing the lithology of the Nubian formation east of Abu-Naga wellfield.

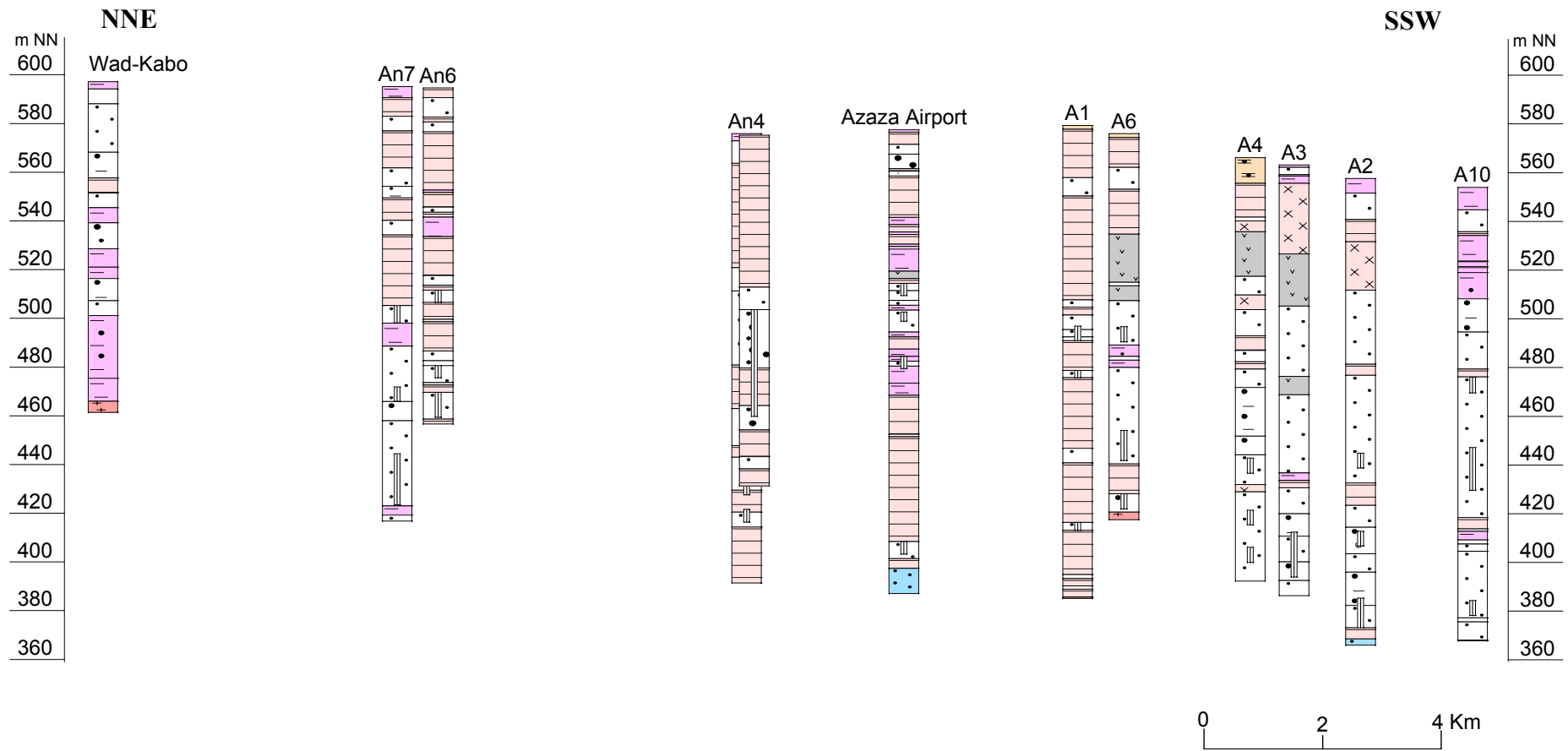


Fig. 4.7a: profiles 5 showing the variation in the Basement level from north to south.

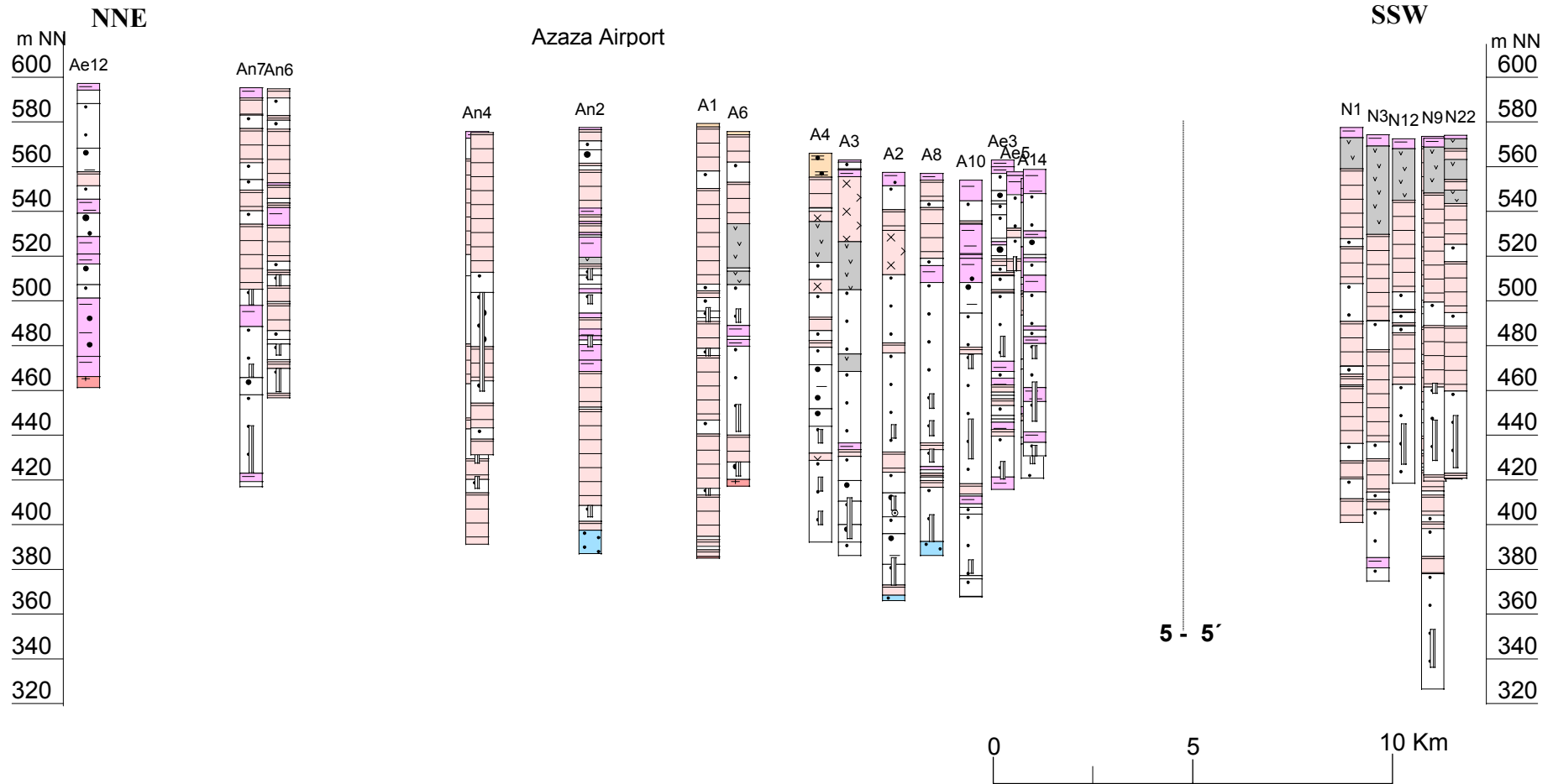


Fig.4.7b: Profile 5-5' showing the lithological characteristics south of profile 5.

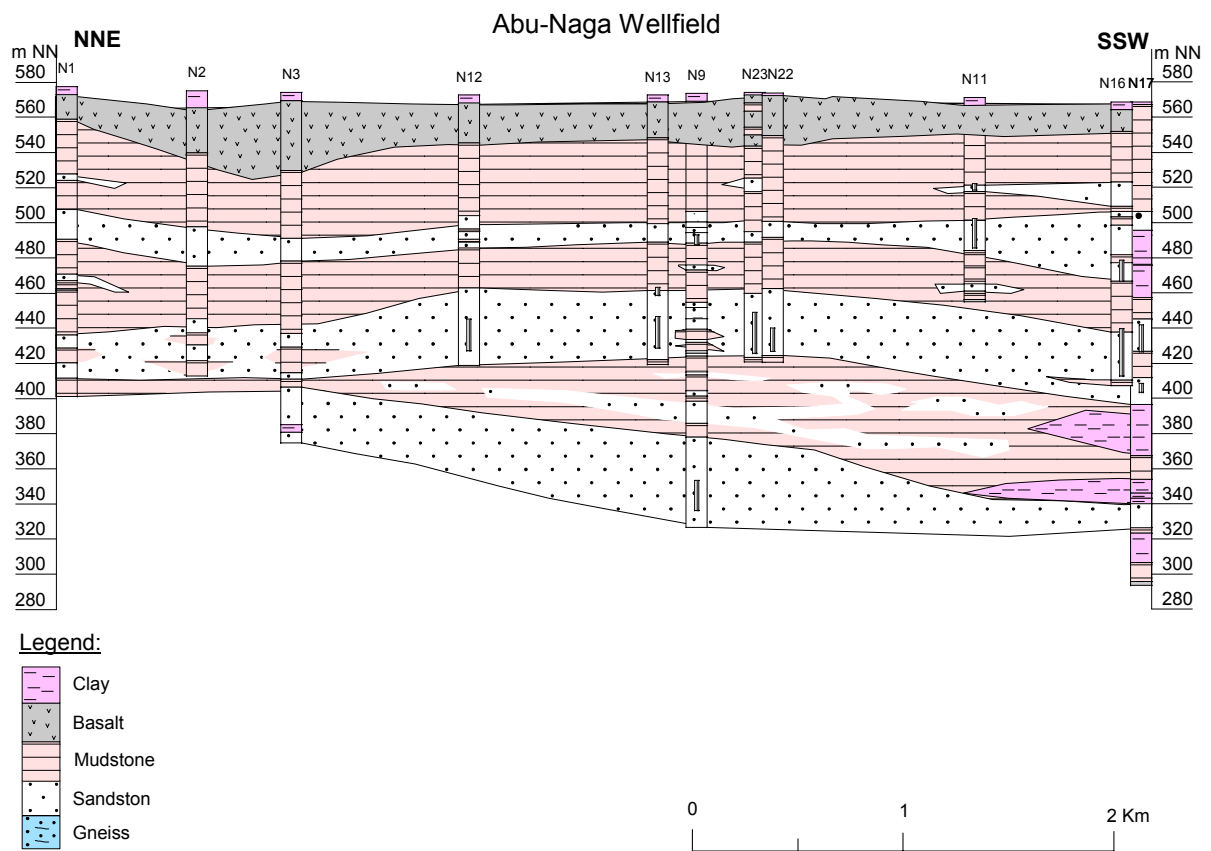
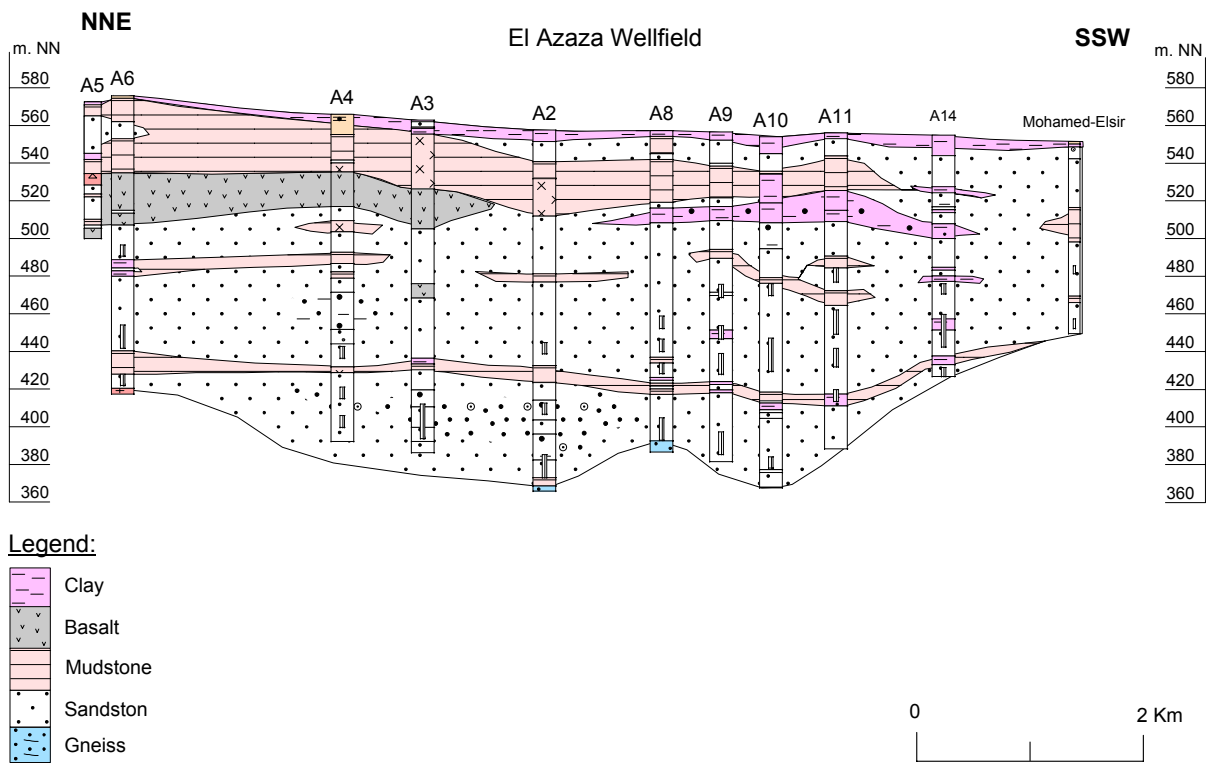


Fig. 4.8: showing the correlation of different lithological layers across Azaza and Abu-Naga wellfields.

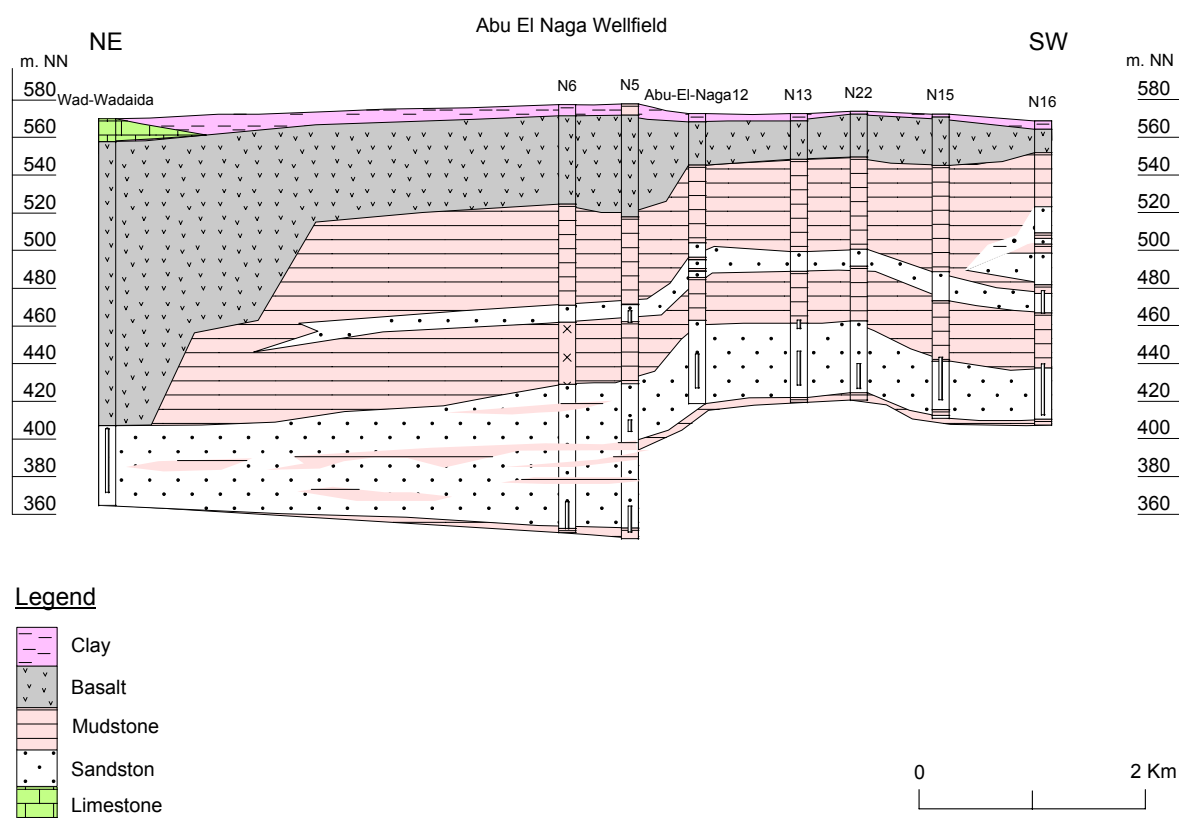


Fig. 4.8: continued.

4.2.3. Structural pattern from Lineament map (satellite image)

As indicated earlier, the Gedaref region was subject to complex tectonic activities, which greatly shaped the hydrogeology of the study area.

With the absence of detailed geological mapping in the study area, the use of remote sensing data in this study was necessary to support the hydrogeologic interpretation. Specific attention is paid to the lineament pattern, which represents traces of structural activities. The main concern of this analysis is to eventually relate the groundwater flow regime to the structural effect.

Description of the multi-spectral scanner (MSS) Scene

A Landsat 3 MSS scene from the archive of the SFB 69 project is used for the purpose of this analysis. The original MSS image covers $185 \times 185 \text{ km}$ strip with a resolution (pixel size) of $79 \times 58 \text{ m}$. The pixel size indicates the low spatial resolution provided by the Landsat 3 MSS. Linear features are expected to appear wider than the original linear features on the ground.

The MSS image is also characterised by low spectral resolution. Landsat 3 is a four channel multi-spectral scanner, recording wavelength between $0.5 \mu m$ and $1.1 \mu m$ within the VIS and NIR (visible and near infra-red) spectrum. The width of each of the four spectral bands are: $0.5 - 0.6 \mu m$, $0.6 - 0.7 \mu m$, $0.7 - 0.8 \mu m$ and $0.8 - 1.1 \mu m$.

Data of three bands are combined with bands 4, 2 and 1 as red, green and blue respectively. The image processing started with the geo-referencing of the scene with the help of a digital processing software and GIS system. The image is referenced to UTM zone 36 north according to six topographic map scale 1:100000. The output pixel size is set at $50 \times 50 m$. Further digital image filtering and improvements are carried out to eliminate system errors and signal noise, and to improve the contrast/visibility of different features. The area of interest is then cut-out and enlarged for subsequent interpretation (see figure 4.9).

Lineament analysis

Based on the below visible Landsat MSS image of Gedaref (fig 4.9), an image analysis has been carried out. Some linear elements and features of probable tectonic origin are investigated.

Using visual interpretation, the quality of the analysis largely depends on the image quality. However inclusion of regional knowledge was helpful to support the interpretation. Considering the geologic history, the topography and the drainage pattern, the lineament both in the basaltic body (fig 4.10) as well as in the Nubian formation (fig. 4.11) are drawn.

As traced in figure 4.11, in the center of the Gedaref basin lineaments striking NW-SE to NNW-SSE (130° to $152^\circ N$) dominate, and show up as high ridge dividing the basin topographically into two parts. Crossing the latter are NE-SW to ENE-WSW (40° to $71^\circ N$) lineaments, also leaving its trace on the topography and as Khor lines across the Nubian sediments. The foremost lineament pattern in the sandstone west of the central Gedaref ridge is the NE-SW to ENE-WSW set. Additionally, E-W ($\sim 100^\circ N$) oriented lineaments are observed along far persisting parallel khor system flowing towards the west. Between Al-Laya and Al-Toria Khors dense lineament net of all the direction identified above is observed. In the western margin of the Gedaref basin as well as in the bordering basement rocks the NE-

SW to ENE-WSW striking lineaments are dominant, accompanied with khor lines as landscape features.

The prevailing lineament directions identified in the Gedaref match up those directions known from previous studies (MULA, 1983, MUNIEUR, 1985, RWC STUDY, 1989, TOTAL SOUDAN, 1985). The NW-SE trending lineament are associated with the tertiary basalt eruptions along extensional structures parallel to the plate margin developing along the red sea depression (TOTAL SOUDAN, 1985). Some of the NE-SW and the NW-SE lineaments observed in the Nubian formation run parallel to the underlying bedrock structure (refer to fig. 3.8) revealed by the gravity study of TOTAL SOUDAN (1985). The ENE-WSW oriented lineaments are probably connected to the famous central Africa shear zone, as it is the case in other know basins in Sudan.

The above identified patterns suffer from the absence of field control, which makes the verification of the lineament difficult. However, some lineaments are supported by clear physical/landscape settings, mainly the topography, and the drainage pattern. Well logs have also helped as control at few locations.

4.2.4. The aquifer sub-systems

From the stratigraphic information and the lineaments identified from the image analysis, the west Gedaref aquifer system could be divided horizontally into three sub-systems of similar stratigraphic characteristics. One aquifer covers the area north of the Azaza airport. The latter is connected southward to a second sub-system extending over the area of the two wellfields from A6 to N17. The third aquifer extends from south Abu-Naga to Saseib. Beside the stratigraphic differences, some structures are believed to mark the boundaries between the sub-aquifers.

Further analysis will concentrate on the multi-layered aquifer developed in Azaza and Abu Naga area. The Azaza-Abu Naga aquifer system covers about 300 km² west of Gedaref city, and occupies the horizons between 380 - 420m, 430 - 480m and 490- 505m above mean sea level.

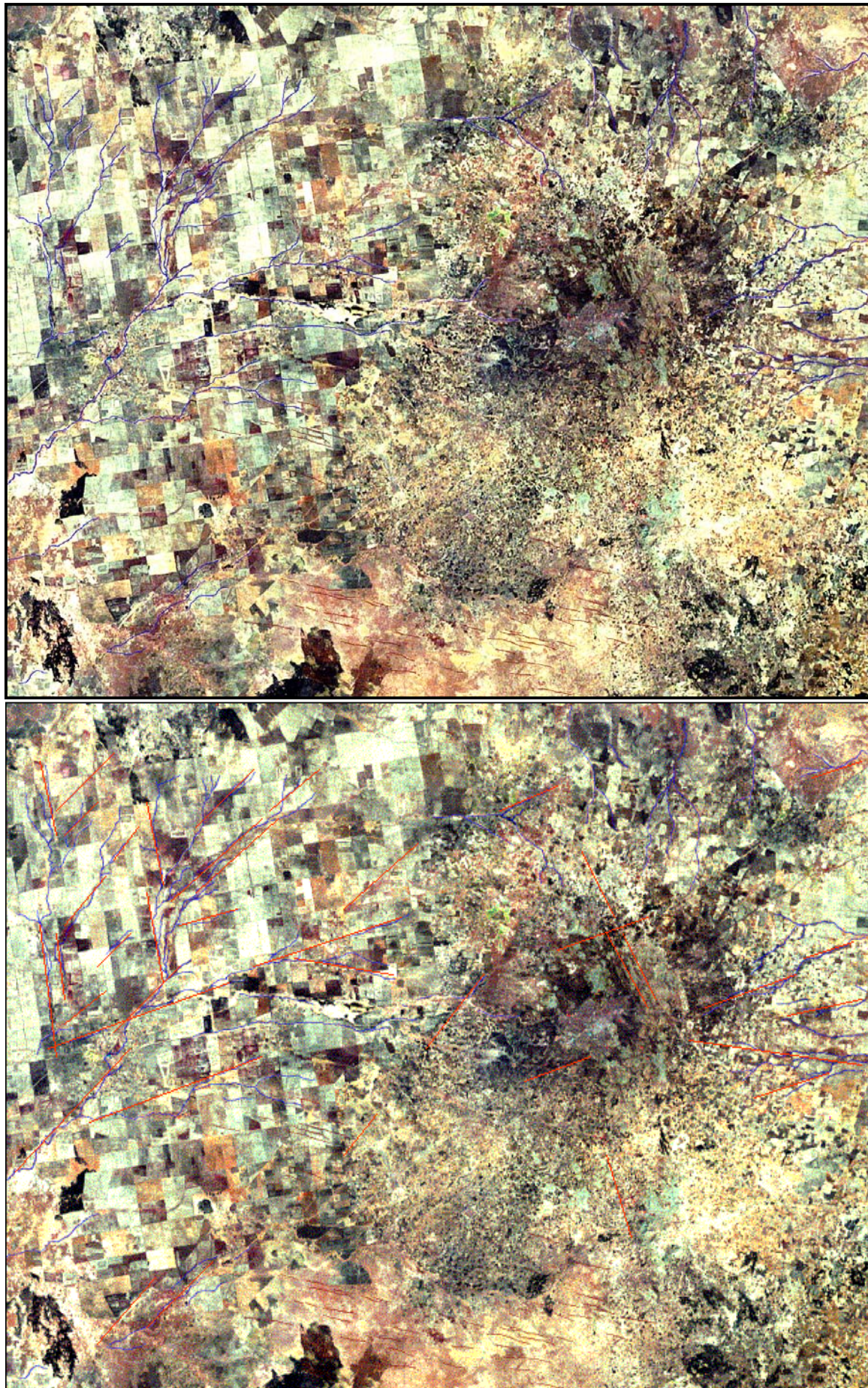


Fig 4.9: Landsat MSS image of the Gedaref showing drainage pattern as an indicator for subsurface zones of weakness.

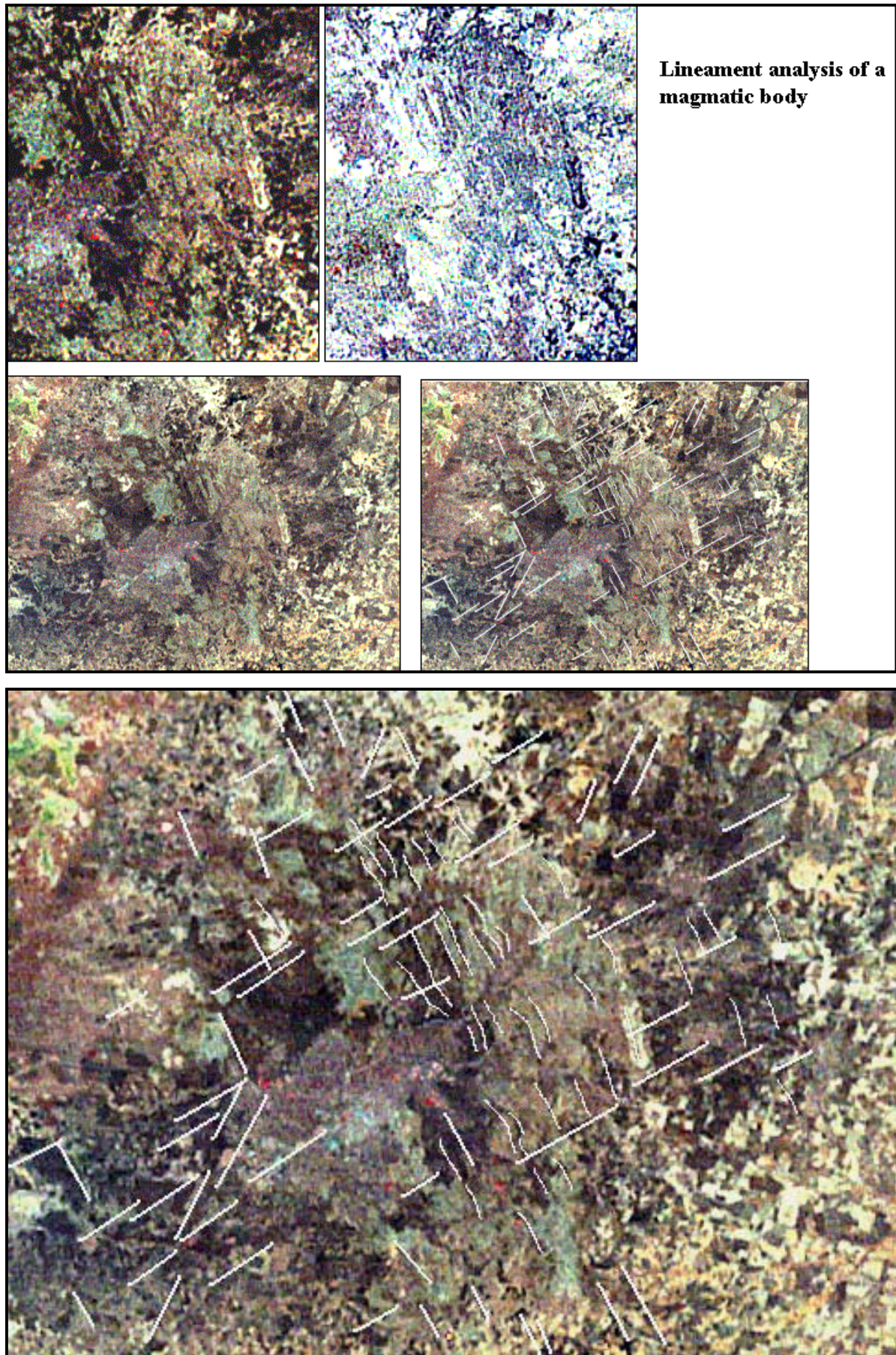


Fig 4.10: Lineament pattern in the basaltic body.

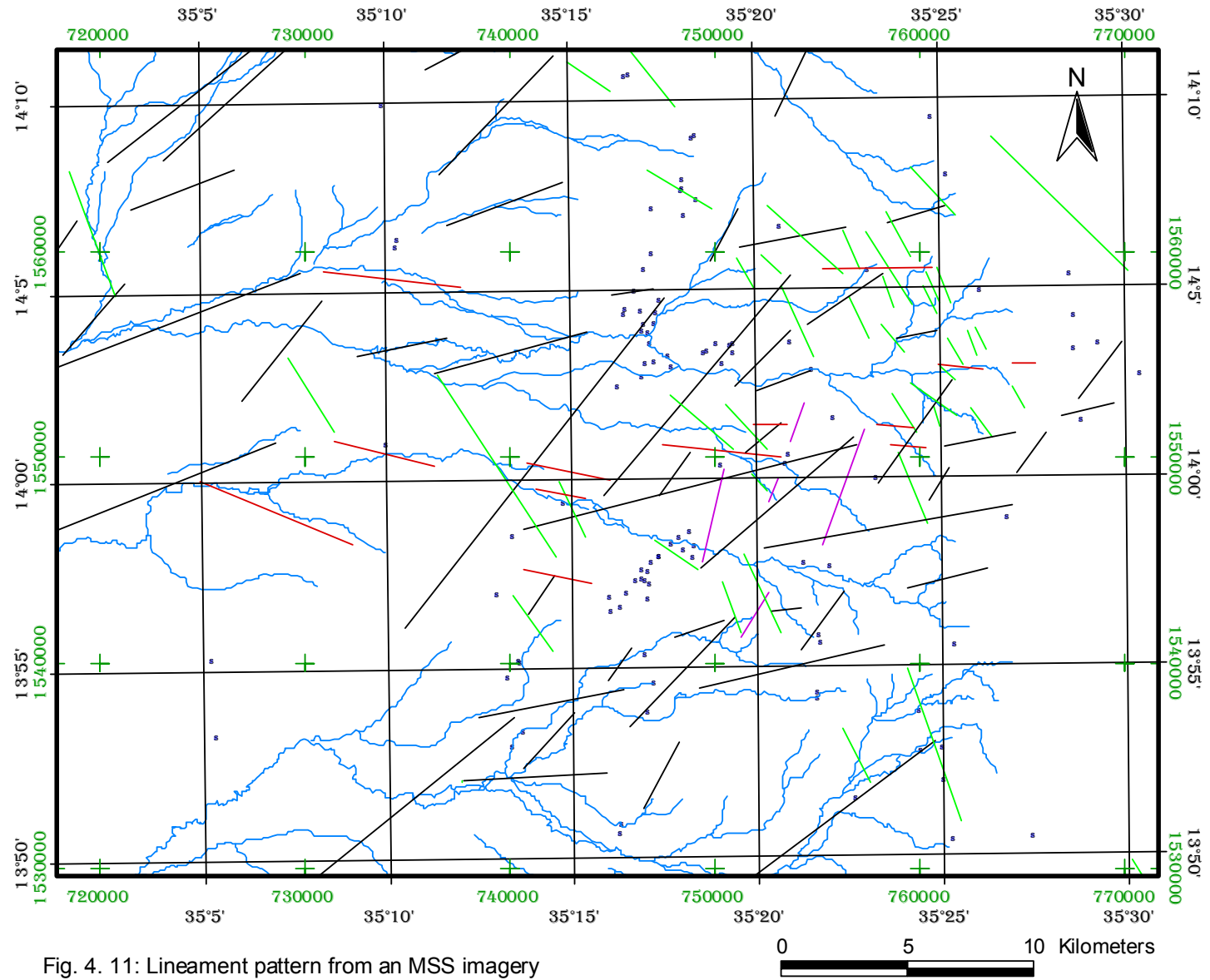


Fig. 4. 11: Lineament pattern from an MSS imagery

4.3. The Hydrologic conditions

Here the natural and anthropogenic mechanisms controlling how water enters, flows through and exits the Gedaref hydrogeologic system are discussed. These include (in separate subsections) the distribution of groundwater level and the expected flow pattern, the natural recharge as well as the abstraction rates across the region.

4.3.1. Static water level

Water level measurements are analyzed to work out the general direction of groundwater flow, the location of recharge and discharge areas, and the connection between aquifers and surface water systems in the region. For this purpose, the following sets of data are used:

- the archive record at 148 boreholes (table 4.1, Appendix) measured upon the construction or rehabilitation of the boreholes between 1989 to 1991;
- head measurements conducted in 1999 during the field investigation within the framework of the current study, which included 34 locations. Regular monitoring of groundwater depth is continued along year 2000 at non-operating boreholes owned by the Gedaref Water Corporation (GWC) in the wellfield areas to assess the effect of pumping on the groundwater levels at the wellfields;
- a set of water levels measured by GWC in 1996 at 13 boreholes in the wellfields of Azaza and Abu Naga.

As it is clear from the previous section, most boreholes are screened only through the main middle aquifer layer. Some boreholes that are filtered only along the upper or the lower-most layers indicated considerable differences in the water levels of the three aquifer layers. These are clearly visible at locations such as the boreholes at Umm-Higliga and the dug-well (3), which tap the upper aquifer layer; and at borehole Azaza3 and Naga 6, which tap the lowest layer. Depth to groundwater encountered in the upper, middle and lower aquifers ranges between 19.34–53.0 m, 43.2–76.37 m, 57.4–82.72 m respectively. On average, a vertical head difference of up to 20m is observed between the upper and the middle aquifer, while a lesser one of around 5m is estimated between the middle and the lower layers. Accordingly, downward leakage is expected to take place depending upon the thickness and the vertical hydraulic conductivity of the clayey beds separating the three layers.

Generally, the groundwater level in the sandstone aquifer rises-up between 0.09 - 30.94 m above the uppermost Mudstone layer. Looking at the filter position in different wells (see profiles above), and the corresponding rise of piezometric level, water rises in the different layers up to 0.5 m, 20.0 m and 30.0 m above the confining bed of the top, middle and lower aquifers respectively.

A regional piezometric map (referenced to mean sea level) is prepared for the middle sandstone aquifer (fig 4.12) using linear interpolation. Assuming low abstraction rates before 1992, the static water level contour is considered to represent the steady or equilibrium condition of the aquifer. The piezometric level slopes roughly to the southwest direction from about 565 to 470 m above sea level, along a non-uniform gradient between 0.1% to 0.5%.

Apart from some local trends, the piezometric surface indicates a general regional flow direction towards the west and the southwest. Groundwater levels show abrupt ups and downs within short distances across the flow direction, which reflect local groundwater divides in the contour pattern. This phenomenon could be attributed to the effect of tectonic pattern in the Nubian formation, which enhances recharge in some places and acts as barriers in others. Opposite to the regional flow, a minor flow direction towards the east is created by groundwater depressions at Azaza and Abu-Naga wellfields.

The piezometric map shows that the groundwater contours go parallel to the western edge of the basalt between Azaza airport and Jebel Twawa. The implication is that, the Basalt outflows recharge the aquifer along this boundary. Further to the south, east of Abu-Naga, the contour pattern also indicated inflow from the basalt, contrary to the effect of the throwdown fault indicated earlier by ELSEED (1987). This fault (RWC, 1989) is believed to separate the Nubian aquifer in the study area from the eastern one lying under basalts of more than 80m thickness.

4.3.2. Sources of Recharge

From the previous section, it can be concluded that, the aquifer system is recharged by underflow from the Basalt aquifer at the east, and from the northern extension of the Nubian aquifer. Additionally, infiltration of rainwater constitutes a major source of recharge to the

sandstone of the study area. Infiltration is expected to take place in waterlogged areas or a long streamlines. SULEIMAN (1968) estimated the annual recharge to Abu-Naga, through infiltration at exposed Nubian outcrop in the west, at 200×10^6 Gallon ($0.91 \times 10^6 m^3$).

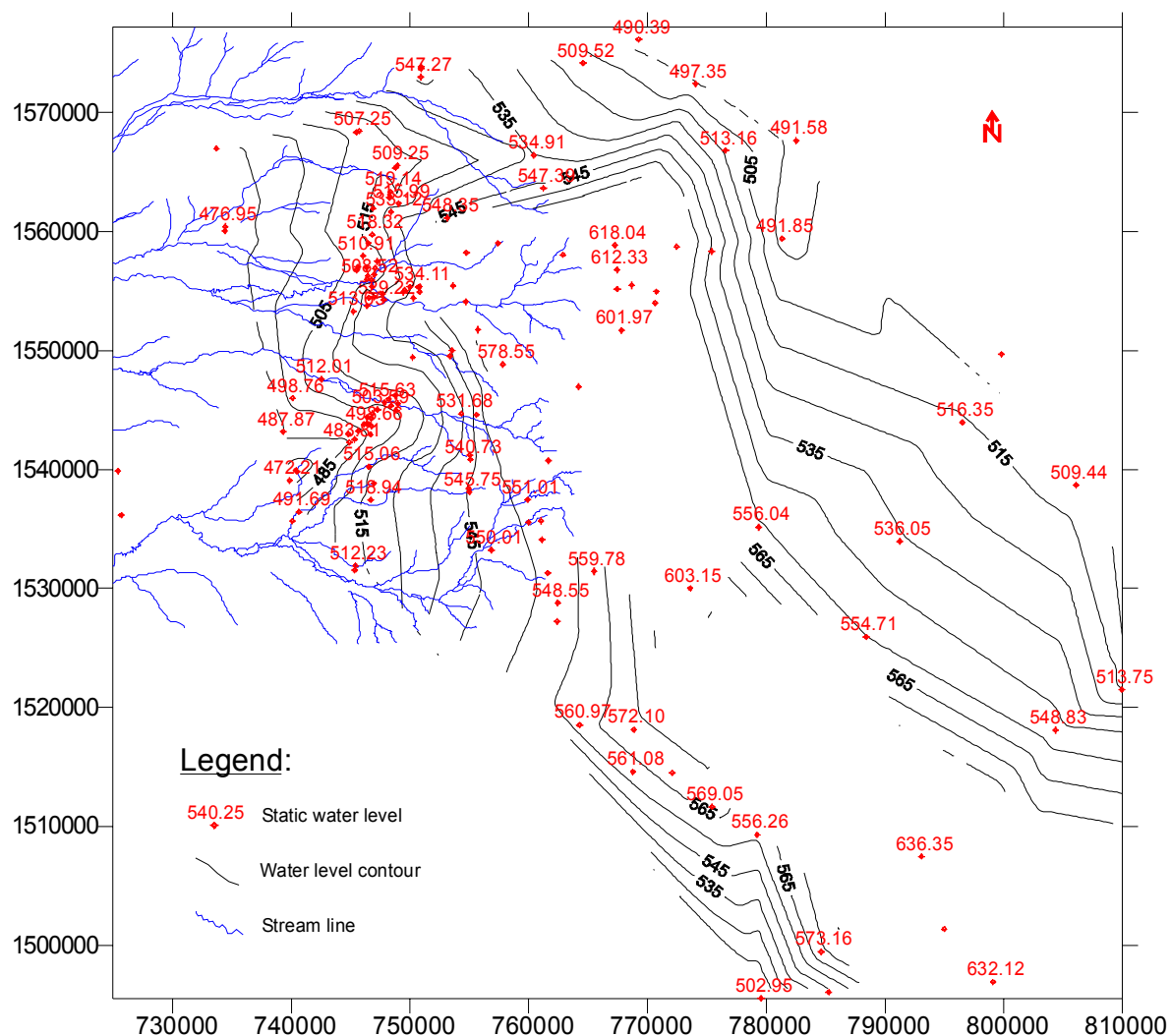


Fig. 4.12: Static water level in the Sandstone aquifer according to the archive record (1989-1992).

Vertical recharge to the sandstone aquifer varies in different locations across the basin. It occurs primarily through rain infiltration along the contact between the basalt and the sandstone formation, and along fracture zones within the outcropping Nubian formation. It is clear from the regional topography that, the study area (Azaza-Naga) is characterized with relatively low-lying areas with a very gentle slope towards the east and the southeast (see Topographic map). This has contributed to the accumulation of the high intensity rainwater during the rainy seasons (July-October). Based on imagery data, SKAP (1992) concluded that,

apart from the flash floods along the Khor lines the land between the Azaza and Abu-Naga Wellfield is flat to undulating, so low-lying places collect appreciable runoff such that they remain waterlogged for considerable periods during and after the rainy season.

Monthly monitoring of the water levels in 1996/1997 at selected boreholes (table 4.2, fig. 4.13) has indicated an increase in the groundwater level shortly after the begin of the rainy season during September and October. This could be interpreted as a result of the vertical recharge through the Basalt and the fracture zones in the area. Head variance during ten months in the monitored wells vary between 0.55 – 10.22 m², which indicates considerable spatial variation in groundwater recharge.

Another monthly monitoring during year 2000 (table 4.3) was carried out in both wellfields. However, measurements in Abu Naga are probably falsified by heavy pumping from neighboring boreholes. Fluctuations of groundwater levels caused by pumping do not reflect the natural recharge pattern. Nevertheless, fig 4.14 indicates that no significant drawdown occurred in the aquifer with the current pumping rate (3000m³/d). A constant groundwater level could be maintained during the year. However, increase in pumping rate in the period from October to December 2000 has caused rapid lowering of levels.

4.3.3. Abstraction rate

Groundwater abstraction from the sandstone aquifer in west Gedaref has started shortly before the sixties. Borehole drilling was only based on rural water demand, and hence located in the vicinity of settlements to satisfy the villages' need for drinking water. Abstraction rate was relatively low till the eighties. With the increasing population of the main city of Gedaref after the expansion in the mechanized farming, more attention is focused on the development of the sandstone aquifer to satisfy the city demand. The first constructed wellfield consisted of six boreholes (N1 to N6) in the vicinity of Abu Naga village, followed by more 12 boreholes in the eighties, and lately in 1991 a new wellfield of 15 boreholes was constructed at El Azaza 8 km north of Abu Naga.

There are no meter gauges installed to record the amount of abstraction from each well. Abstraction from the two wellfields as well as from the scattered rural supplies is estimated as follows:

Tables 4.2 & 4.3: Monthly monitoring of groundwater depth (in meters) at Azaza and Abu-Naga areas in years 1996 and 2000.

Location	Jun. 96	Jul. 96	Aug. 96	Sep. 96	Okt. 96	Nov. 96	Dez. 96	Jan. 97	Apr. 97	Dez. 97
DW1	27.46	27.45	27.40	29.14	29.15	26.83	27.48	27.28		D
Aza 7	54.73	45.23	53.70	55.53	55.73	53.83		53.88	54.73	52.97
Aza 9	49.48	49.27	48.90	49.91	49.47	47.25	48.10	47.56	49.24	46.08
Aza 12	46.28	46.10	45.78	46.93	46.48	44.14	44.71	44.52	44.85	43.31
Aza 14	25.10	24.81	24.41	25.84	25.94	24.65	25.12	25.00	26.60	23.60
Aza 16	45.17	43.91	43.17	41.14	39.53	37.62	36.71	36.72	43.65	38.67
DW3	21.62	21.79	22.13	23.06	23.49	21.35	21.65	21.75	22.66	22.54
Naga3	76.73	77.23	77.73	77.77	77.62	74.95	76.80	76.69	80.19	74.90
Naga5	78.86	79.47	81.05	79.19	79.81	76.84	80.00	79.93	81.00	83.36
Naga10	70.35	72.43	71.46	71.17	71.33	69.27	70.82		73.98	69.97
Naga13	75.03	75.34	75.75	75.97	75.86	73.70	74.92	74.64		74.45
Naga15	87.78	87.37	88.35	88.09	84.79	82.51	85.59	85.89	86.30	86.02
Naga16	45.86	45.84	46.30	D	D	D	D	D	45.76	45.93
Naga17	65.77	65.75	66.64	66.78	66.27	63.92	64.95	64.72	65.00	65.20
D-Elnus	37.14	37.78	38.92	40.12	40.18	34.66	37.68	37.49	36.99	D
El-Sarra		75.03	75.34	75.75	75.97	75.86	76.34	76.29	75.68	77.17

Location	Dez. 99	Feb. 00	Mrz. 00	Apr. 00	Mai. 00	Jun. 00	Jul. 00	Aug. 00	Sep. 00	Dez. 00	Jan. 01
Aza4	47.13	46.69	46.68	46.68	46.68		46.68				46.55
Aza3	56.58	56.61	56.57	56.63	56.60		56.59				56.57
Aza2	47.55	47.65	47.64	47.76	47.70		47.77				47.75
Aza7		51.42	51.38	51.55	51.41		51.37				51.42
Aza12	47.33	47.42	47.69	47.81	47.55		47.86				47.52
Aza10			48.61	48.81			48.82				48.37
Aza11	49.00	49.35	49.47	49.40	49.41		49.53				49.27
Naga3	83.10	84.21	83.81	83.71	83.55	82.92	83.84	83.53	83.45	86.37	85.53
Naga8		82.48	81.41	81.71	81.67	81.83	84.30	84.86	84.10	97.85	103.45
Naga13			76.48				77.30				78.70
Naga14	99.25	97.21	93.64	100.91	100.27	99.37	98.65	100.12	99.31	105.93	111.70
Naga22	98.53	96.89	94.48	100.14	99.92	99.07	97.80	99.96	99.04	105.65	110.97
Naga23	87.23	86.43	84.88	88.92	89.00	89.42	89.80	91.21	88.55	102.21	105.17
Naga11	61.46	61.18	61.27	61.52	61.55	61.78	61.30	61.29	61.55		
Naga18	44.08	44.18	44.16	44.16	44.19	44.45	89.80	91.21			

Remark: Unit of measurement is meter, D stands for dry, _ indicates missing value.

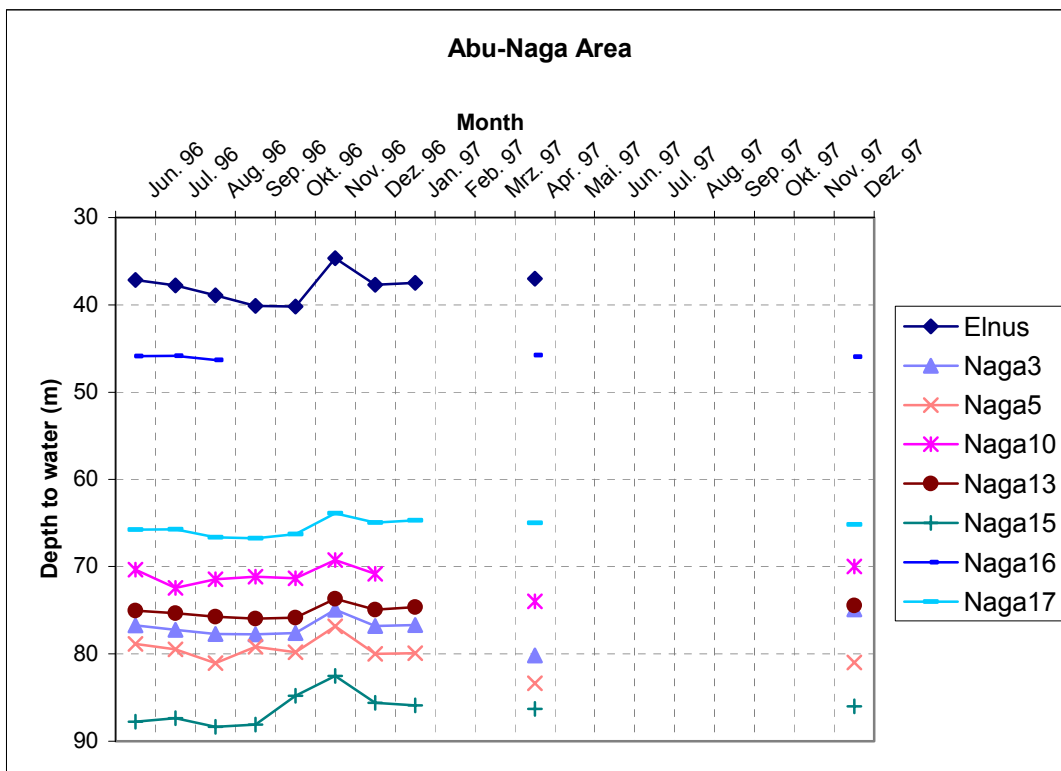
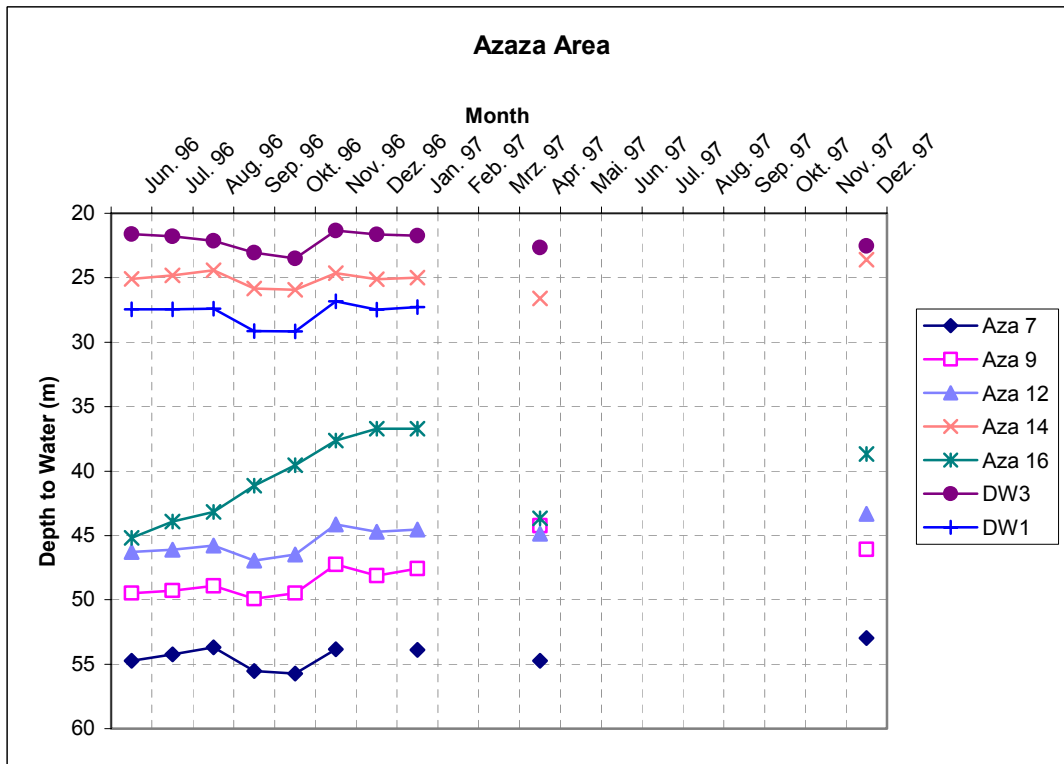


Fig 4.13: Groundwater hydrographs of monitored boreholes at the Azaza and Abu-Naga wellfields in 1996 (Plotted values are found in table 4.2).

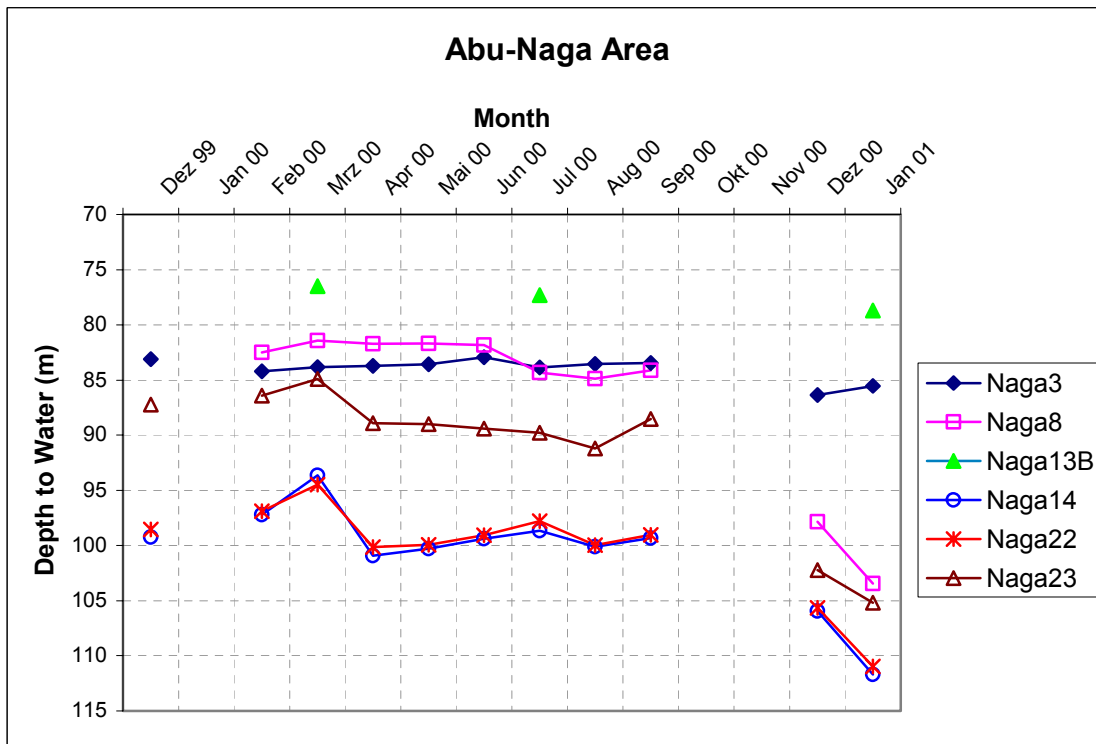
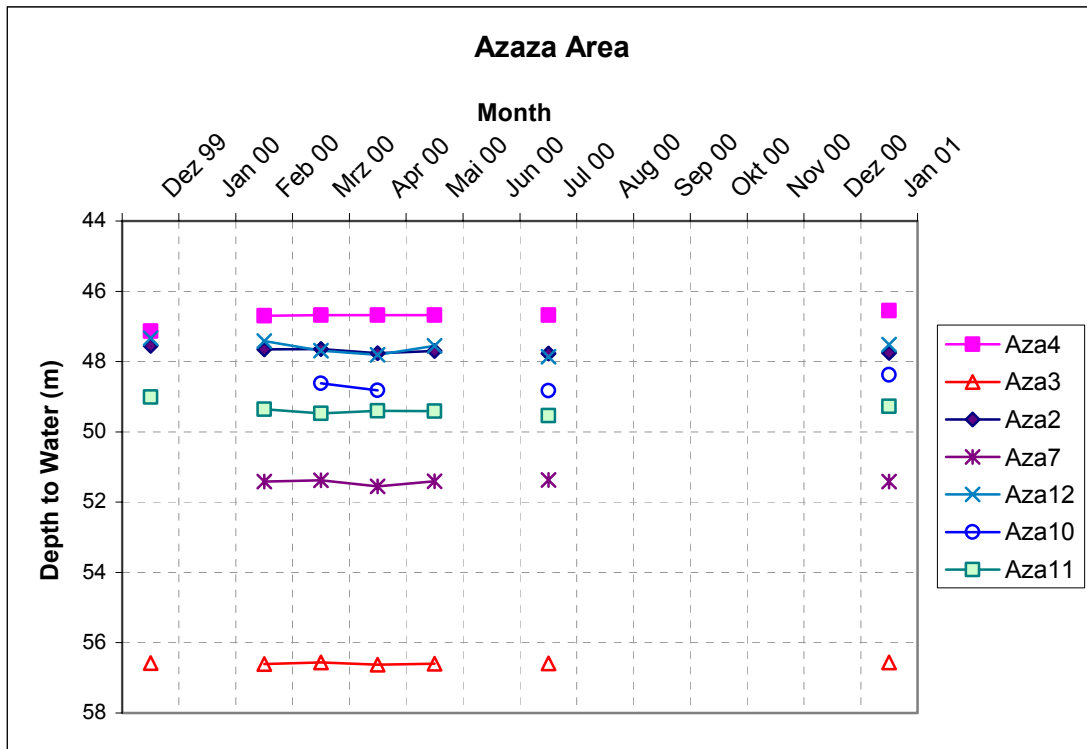


Fig 4.14: Groundwater hydrographs of monitored boreholes at the Azaza and Abu-Naga wellfields in 2000 (Plotted values are found in table 4.3).

- 1- Abstraction from the wellfields is estimated from the capacity of the high-pressure booster pumps, which deliver the pumped water from the collecting tanks at the two wellfields to the city distribution network. According to the Gedaref city water authority, a total of 3000 m^3 is pumped daily from Abu Naga tanks, and a between $2000 - 3000 \text{ m}^3$ from El Azaza tanks. The above quantities are pumped from 8 boreholes in Abu-Naga, and 3 to 5 boreholes in El Azaza, which give rise to an average pumping rate of $350 \text{ m}^3/d$ and $400 - 600 \text{ m}^3/d$ respectively.
- 2- Abstraction from the single wells supplying the villages is considered as $100 \text{ m}^3/d$ from each borehole, estimated by the rural water office (SALEEM, 1998) from the capacity of the water tanks and the number of times these tanks are filled each day.

4.4. Hydraulic characteristics

4.4.1. Transmissivity

A total number of 27 pumping and recovery tests were analyzed. 25 tests are single-well tests and only two tests used a near by observation well. The test results are analyzed considering the characteristics of the aquifer system and the well design. Specific attention is paid to the aquifer extension/geometry and lateral boundaries, and to the filtered length/position. Regarding the multi-layer aquifer system defined earlier from the correlation of the drilling logs (see section 4.2.1), all boreholes under consideration are mainly catching the middle sandstone layer. This aquifer layer is relatively thick; therefore the wells are designed with partially penetrating filters of 168 mm diameter and average length between 18-24 m. In some of the boreholes the upper and the lower sandstone layers are also filtered beside the main middle aquifer. As mentioned earlier, the water level in the wells rises above the top of the filtered layer indicating confined leaky conditions. To assess the data quality, the pumping period and the drawdown pattern are observed. The pumping tests in each well continued for more than 20 hours, which is considered enough to reach steady state conditions compared to the time specified by KRUSEMAN (1991) for leaky aquifers. According to the mentioned reference, “under average conditions steady state is reached in leaky aquifers after 15 - 20 hours of pumping; in a confined aquifer it is good practice to pump for 24 hours“.

Both diagnostic log-log plots and specialized semi-log plots of the drawdown against the time are constructed. Considering the aquifer system, the drawdown behavior indicated leaky to confined conditions in Azaza and Abu-Naga respectively.

According to KRUSEMAN (1991), in confined and leaky aquifers, single-well tests can be analyzed with Jacob straight-line method without any corrections for non-linear well losses, provided that late time data (at $t > 25rc^2 / KD$, rc is the radius of the screened part) are available to avoid the effect of well-bore storage at the beginning of the test. Here the one and one-half rule of thumb introduced by RAMEY (1976) is used. According to this rule, the end of the unit slope straight-line is about 1.5 log cycle prior to the start of the semi-log straight line as used in Jacob's method.

Therefore, T is estimated from pumping tests considering the following Jacob's equation

$$KD = \frac{2.30Q}{4\pi\Delta s}$$

under the following conditions:

- The well does not penetrate the entire thickness of the aquifer;
- The flow to the well is in an unsteady state;
- The time of pumping is relatively long: $t > D^2(Ss)/2KD$.

FETTER, 1994, advised not to use a single-well test for estimating the Storativity value. Storativity is estimated from three pumping tests with observation wells, conducted by previous studies in the Azaza and Abu-Naga well-fields.

With partially penetrating wells, the condition of horizontal flow is not satisfied and vertical flow develops in the vicinity of the well. KRUSEMAN (1991) recommended to make corrections to the observed drawdown in case of partial penetration, to compensate for the head loss caused by higher velocities develop close to the well. He suggested the use of the Hantush's modification of the Theis method or of the Jacob method for confined aquifers under unsteady state conditions.

Alternatively, Jacob model can be used without corrections for head losses in confined and also in leaky aquifers. According to KRUSEMAN (1991) "In theory, Jacob's Method can also

be applied if the well is partially penetrating, provided that late time ($t > D^2S/2KD$) data are used“. This is justified by HANTUSH’s (1964) statement, that, “the additional drawdown due to partial penetration will be constant for $t > D^2(Ss)/2KD$ and hence will not influence the value of Δs_w as used in Jacob’s method“.

Using Jacob’s method for partially penetrating single-well pumping test, a range of transmissivity values (table 4.4) between $17.4 - 171.0 \text{ m}^2 / \text{d}$ is obtained from the analysis of the archive record. The average storage coefficient is considered as 2.4×10^{-3} . The hydraulic conductivity estimated from an average aquifer thickness of 40 m ranges between $0.44 - 4.28 \text{ m/d}$.

It is believed that transmissivities higher than those determined by pumping tests do exist along fracture zones, which are not reflected by the pumping tests. According to SINGHAL and GUPTA (1999) fractures can impart good hydraulic conductivity ($10^{-7} - 10^{-4} \text{ m/s}$) to impervious siltstone and fine-grained clastic rocks. He also mentioned that siltstones are capable of transmitting large quantities of water over contact areas by leakage across lithologic boundaries. Therefore a good mapping of fracture net is necessary to characterize the transmissivity distribution of the Nubian formation in West Gedaref aquifer.

Hydraulic parameters estimated above lie within the range of values mentioned in the literature for sandstone aquifers. Hydraulic conductivity between $6 \times 10^{-6} - 3 \times 10^{-10} \text{ m/s}$ is reported by DOMENICO and SCHWARTZ (1997); and a storage coefficient range between $0.05 - 10^{-5}$ is provided by MARSILY (1986).

4.4.2. Aquifer Yield and specific capacity

Table 4.5 shows the estimated yield and the corresponding dynamic level achieved during pumping tests conducted upon the construction of the wells. Registered well yield varies from $57.60 \text{ m}^3/\text{d}$ at the shallow basin boundaries to above $600 \text{ m}^3/\text{d}$ in the center of the Basin. On average the aquifer yield is considered moderate (HÖLTING, 1989). The average specific capacity is around $1.08 \text{ m}^2 / \text{h}$.

Table 4.4: Results of analyzing pumping test data from the archive record.

No.	Location	Easting	Northing	T (m ² /d)	S
1	Aza16	747796.19	1554253.38	40.8	
2	Aza15	746989.00	1554497.88	30.1	
3	Aza14	746548.81	1554419.38	47.6	
4	Aza13	746461.88	1556267.00	34.6	
5	Aza12	746374.81	1555998.25	30.0	
6	Aza11	746779.44	1555369.13	30.1	
7	Aza10	746743.63	1555943.25	34.7	
8	Aza9	746982.50	1556382.75	37.8	
9	Aza8	747068.19	1556906.00	31.1	
10	Aza7	747241.81	1557488.75	73.2	
11	Aza6	748399.13	1561654.13	35.5	
12	Aza4	746821.63	1559726.13	35.6	
13	Aza2	746051.88	1557951.00	166.0	
14	Terria-old	742540.69	1547577.25	54.3	
15	Naga2	748207.31	1545894.50	75.9	2.40*10-3
16	Naga3	747853.00	1545620.50	24.4	
17	naga4	748404.88	1545352.38	19.2	
18	Naga5	748849.81	1544962.75	38.5	
19	Naga6	748985.88	1545511.88	24.5	
20	Naga9B	746390.31	1544370.38	100.0	
21	Naga10	746119.81	1543784.13	142.0	
22	Naga12	747254.88	1545024.38	36.5	
23	Naga13B	746721.56	1544281.38	171.0	
24	Naga14	746764.00	1543629.88	149.0	
25	Naga15	746674.75	1542928.13	17.4	2.87*10-5
26	Naga17	744797.31	1542990.00	21.7	
Geometric Mean				45.1	

4.5. Aquifer reserve

According to MARSILY (1986) the reserve of a confined aquifer is the product of the storage coefficient S , the area of the aquifer and the difference between the present piezometric surface and that to which it is agreed to draw down the head in the confined aquifer. Considering pumping down to a level above the confining beds, 50.5 m average reserve is available above our target minimum level. Considering only the area between Azaza airport

and Toria village (200 km^2), storage capacity of 2.4×10^{-3} , the aquifer reserve is around $24.2 \times 10^6 \text{ m}^3$. However, this amount is amended with the annual recharge to the system indicated in section 4.3.2

4.6. Groundwater Type

It has been known that the chemical composition of groundwater is affected by the petrographic composition of the aquifer. According to FREEZE and CHERRY (1979), the dominant ions in the cretaceous sandstone formation are Na^+ and HCO_3^- . This is explained by the combined effects of cation exchange and the dissolution of calcite or dolomite and clay minerals with exchangeable Na^+ . As groundwater moves along its flow path in the saturated zone, increases of total dissolved solids and most of major ions normally occur, FREEZE and CHERRY (1979).

36 water samples are collected from wells around and inside the study area (fig. 4.15). Water samples are analyzed to confirm the source of groundwater recharge in the Azaza Abu-Naga sub-basin. The composition of the groundwater (table 4.6, Appendix), indicated by the analysis is interpreted using hydrochemical maps and diagrams. Fair accuracy is indicated by the balance calculation (table 4.5) due to the limited sampling facilities available in the field. However, the results are considered good enough to interpret the general pattern required for the purpose of this study (fig 4.17).

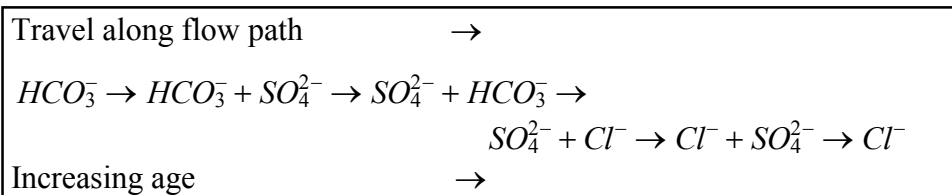
The analytical data is plotted in Piper diagram (fig. 4.16), as it better represents noisy data (DOMENICO and SCHWARTZ, 1997). Accordingly, the groundwater in the area could be classified as $\text{Na} - \text{HCO}_3$ type in the center, and $\text{Ca} - \text{HCO}_3$ at the peripheries as well as in the upper layer. One sample in the lower-most aquifer is classified as $\text{Ca} - \text{Cl}$ type.

Table 4.5: Aquifer yield estimated from the above pumping test, source: well archive.

Location	X	Y	SWL	DWL	Yield(m ³ /h)	SC (m ² /h)
Wad-Kabo	769265.31	1576150.00	107.31	114.04	7.30	1.08
karadis	750935.06	1573672.88	79.00	84.60	2.40	0.43
Ummkhanger	745737.50	1568443.88	69.18	80.31	5.40	0.49
Aza-Madrassa	748945.88	1565548.38	67.37	74.53	6.80	0.95
Aza-Matar	748358.31	1563328.88	58.95	67.37	5.30	0.63
Aza1	749043.69	1562357.75	63.48	88.01	22.72	0.93
Aza6	748399.13	1561654.13	43.20	75.64	26.18	0.81
Aza4	746821.63	1559726.13	48.28	68.52	26.18	1.29
Aza3	746483.88	1559021.13	57.40	93.52	16.36	0.45
AlAgool	772455.06	1558719.00	114.20	130.05	9.00	0.57
Aza2	746051.88	1557951.00	46.98	56.52	26.18	2.74
Aza7	747241.81	1557488.75	49.43	61.79	23.10	1.87
Aza8	747068.19	1556906.00	48.89	71.73	19.64	0.86
UmmGulga	745493.44	1556786.00	46.10	54.80	10.35	1.19
Aza9	746982.50	1556382.75	47.08	65.00	22.44	1.25
Aza13	746461.88	1556267.00	44.90	65.81	22.44	1.07
Aza12	746374.81	1555998.25	46.28	67.97	26.18	1.21
Aza10	746743.63	1555943.25	45.25	57.01	15.71	1.34
Twawa-Uni	750822.56	1555374.50	36.34	69.58	27.27	0.82
Aza11	746779.44	1555369.13	45.80	68.99	22.44	0.97
Twawa_HB	749559.38	1555039.13	46.10	54.80	27.28	3.14
Aza15	746989.00	1554497.88	29.31	54.90	17.85	0.70
Aza14	746548.81	1554419.38	19.34	42.13	27.27	1.20
Aza16	747796.19	1554253.38	29.96	57.07	26.18	0.97
Wad-Wadida	750220.44	1549419.13	54.00		4.22	
Terria-old	742540.69	1547577.25	45.64	65.00	12.24	0.63
Terria-new	740112.19	1545989.38	56.80	72.54	14.40	0.91
Naga3	747853.00	1545620.50	58.99	92.78	16.36	0.48
Naga6	748985.88	1545511.88	82.42	110.61	16.36	0.58
Naga4	748404.88	1545352.38	60.49	83.06	13.63	0.60
Naga12	747254.88	1545024.38	69.52	99.08	21.82	0.74
Naga5	748849.81	1544962.75	60.07	85.86	21.82	0.85
Naga8	746838.06	1544682.13	67.36	88.16	18.70	0.90
Ghreigana	755594.75	1544595.75	102.94	110.28	10.50	1.43
Naga9B	746390.31	1544370.38	68.15	75.58	26.18	3.52
Naga13B	746721.56	1544281.38	69.58	76.26	21.82	3.27
Naga10	746119.81	1543784.13	67.92	75.55	21.82	2.86
Naga14	746764.00	1543629.88	74.00	81.55	26.18	3.47
Naga11	745650.44	1543226.25	60.36	79.35	16.36	0.86
Naga17	744797.31	1542990.00	57.41	84.97	21.82	0.79
Naga15	746674.75	1542928.13	76.92	81.55	5.45	1.18
Naga16	745342.56	1542528.13	48.24	100.37	16.36	0.31
Naga18	744902.75	1542271.75	81.89	102.77	16.36	0.78
AsSarraf	755028.00	1541183.50	77.10	86.67	18.00	1.88
W/Huri	740482.19	1539825.63	76.20	80.85	2.40	0.52
Jana-Barra	746975.19	1538826.50	26.48	39.11	28.06	2.22
Wad-Kabarus	754935.63	1538396.75	62.26	73.77	13.80	1.20
Wad-Kabarus	754998.31	1538108.38	65.63	78.57	9.60	0.74
Kagara	759912.81	1537462.75	69.50	82.63	15.12	1.15
Abulraif	746697.13	1537443.38	44.59	74.87	12.64	0.42
Kamadeib	740652.13	1536420.75	48.28	90.47	11.93	0.28
Assar	761036.25	1535675.25	83.28	98.28	13.09	0.87
Wad-Daif	756843.44	1533225.63	42.63	61.58	15.00	0.79
Saseib	745404.63	1531903.13	35.54	47.14	15.44	1.33
Genan	765501.75	1531431.38	93.90	115.46	9.12	0.42
Kassab	761591.50	1531284.00	67.50	88.36	12.24	0.59
WadelHalangi	762389.88	1527217.88	67.42	92.00	9.12	0.37
Mahal	764283.50	1518505.38	28.27	62.35	6.00	0.18
Qureisha	815549.69	1518244.63	51.40	84.60	18.00	0.54
ZreiqalHila	768856.88	1518121.63	48.25	74.91	15.12	0.57
ZreiqalDonki	772080.88	1514495.75	38.20	66.80	7.28	0.25
Tawarit	784631.69	1499437.63	22.90	36.45	12.24	0.90
Rashid	785268.06	1496060.75	14.63	42.77	15.00	0.53

Groundwater samples exhibit both lateral and vertical variation in their major chemical constituents. Samples from two wells tapping only the upper sandstone layer show electrical conductivity (EC) values of $636 \mu S/cm$ at Jana-Bara and $920 \mu S/cm$ at Umm-Higliga near the Basalt boundary east of Azaza. A EC value of $1820 \mu S/cm$ is registered for the lowermost aquifer layer at Twawa gardens. The horizontal distribution of the EC in the main middle aquifer is plotted in figure 4.18a. Lower EC values encountered at the northeast, the southeast, and in the area between Azaza and Abu-Naga wellfields. This confirms the flow pattern indicated by the piezometric map. It also indicates the occurrence of fresh water recharge in the low-lying area of Al Laya khor system probably due to dense fracturing net between the two wellfields.

The regional changes of Chloride observed along the flow path (see figure 4.18b) compares well with the Chebotarev conclusion (FREEZE & CHERRY, 1979).



The above relation shows that the recharge to the Azaza area is probably coming from the northeast around borehole A6. It also showed that south of the Azaza area receiving fresh recharge, which could have come from fractures near boreholes A14, A15 and A16, interrupts this evolution.

4.7. Conclusion

The above characterization clearly allows for the delineation of different hydrogeologic units, hence the boundaries of the aquifer system in the study area.

It is shown that, the lateral extension of the investigated Nubian subbasin has a width of about 30 km from the Basalt ridge in the east to the shallow Basement rocks in the west. It extends along a north northeast south-southwest axis for about 45 km, from El Karadis to Seseib. The sub-basin is divided along its axis into three hydraulically connected aquifer systems.

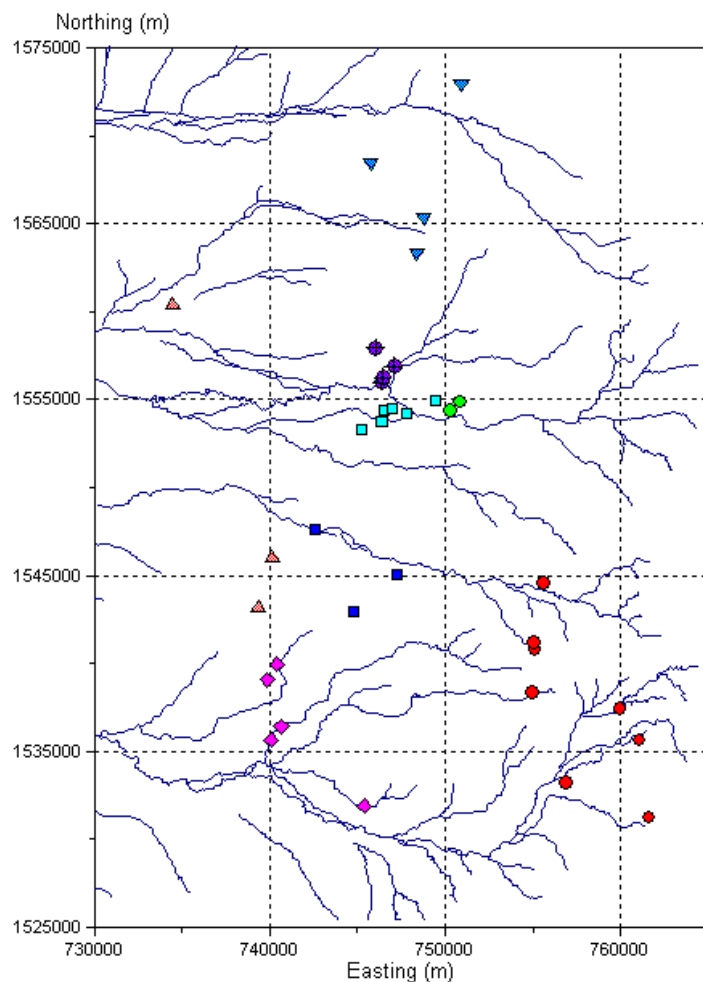


Fig. 4.15: Location of sampled wells.

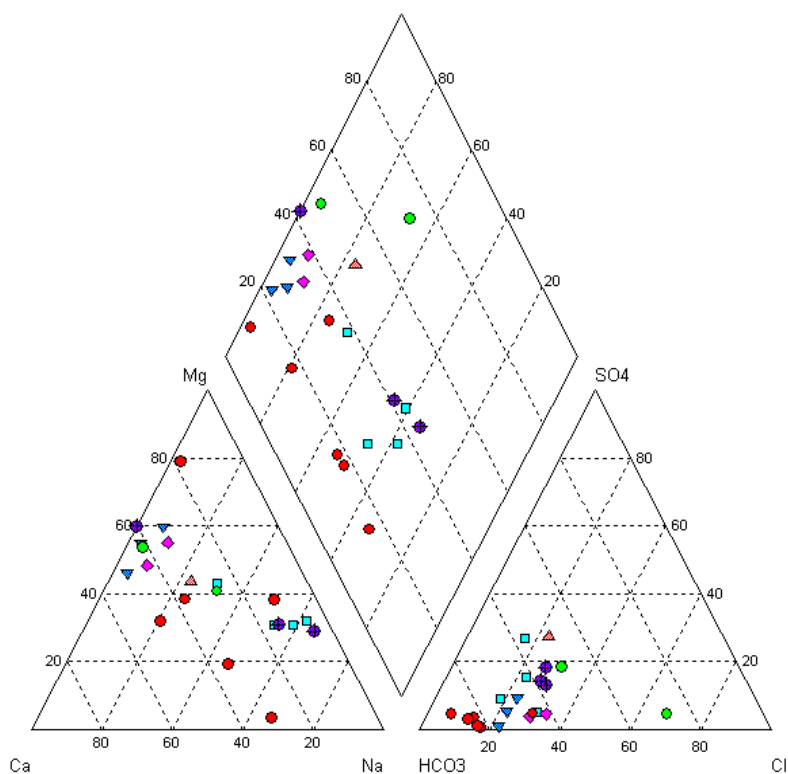


Fig. 4.16: Piper diagram showing hydrochemical facies in the Sandstone aquifer.

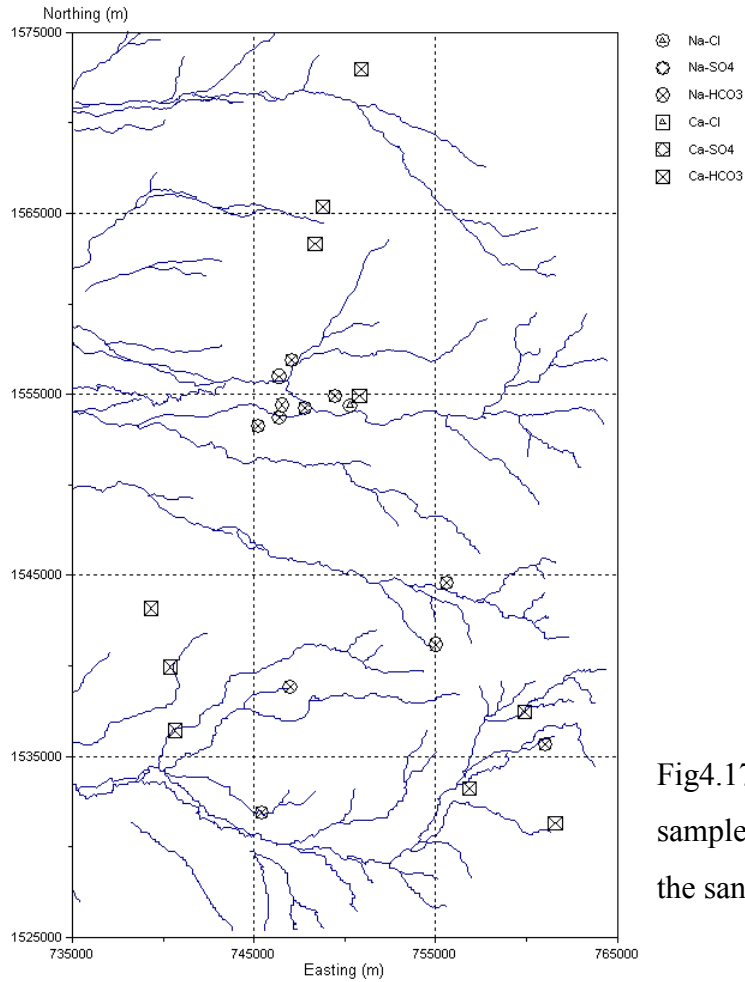


Fig4.17: Water facies at sampled boreholes in the sandstone aquifer.

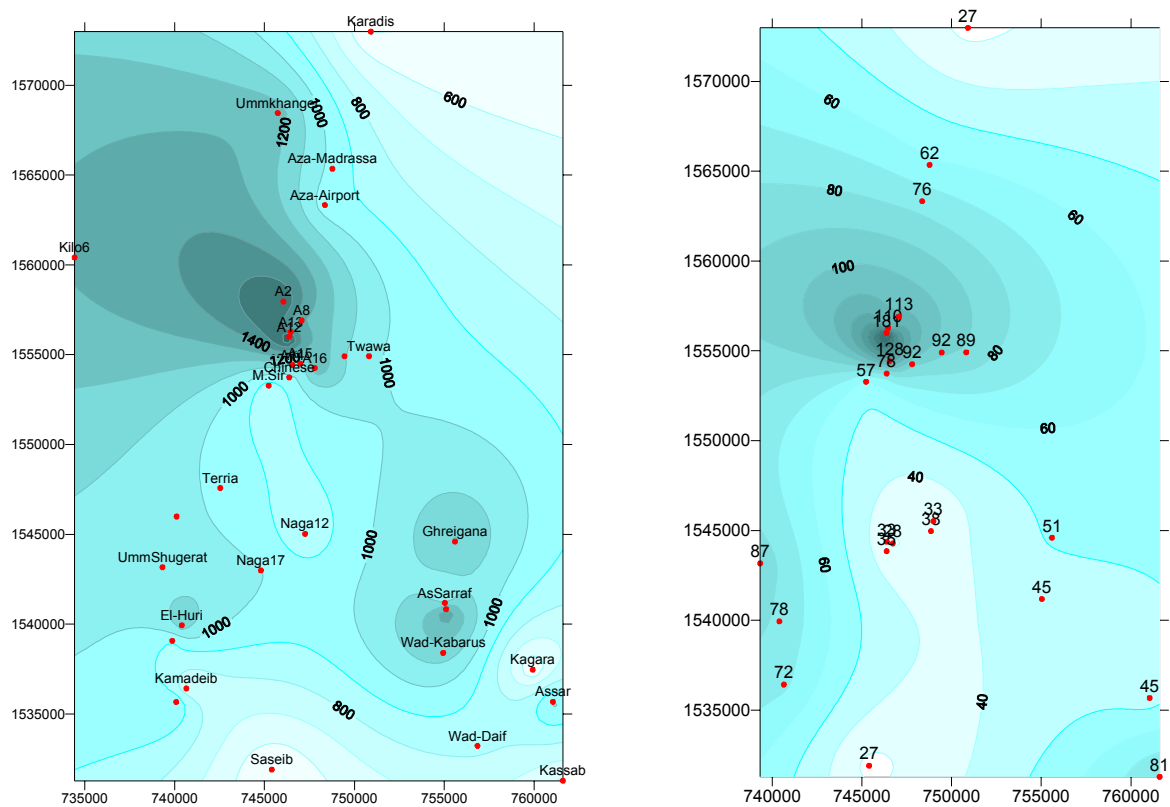


Fig. 4.18: Spatial distribution of a) EC values and b) Chloride sampled in 1999.

The configuration of the Azaza-Naga Aquifer is defined as a multi-aquifer system consisting of three sandstone layers separated by two aquitards. This has been proved by comparing the variation in Water level, the water type and the drilling logs of wells capturing one layer only, e.g. Umm-Higliga well in the top layer, Azaza16 and Naga14 in the middle main layer, and Azaza3 and Naga6 in the bottom aquifer layer.

The analysis of the aquifer properties gives rise to an average transmissivity of $5.22 \times 10^{-4} \text{ m}^2 / \text{s}$; Storativity of around 2.4×10^{-3} and average specific yield of $1.08 \text{ m}^3 / \text{h/m}$.

The Water facies classification has confirmed the direction of flow and pointed the possible recharge areas.

5. A conceptual framework for quantitative analysis and model design

5.1. Introduction

A typical modeling process starts with data integration and description of the hydrogeological setup, then the definition of the conceptual framework for analysis, and finally comes the numerical simulation/approximation. The conceptual framework represents an important phase in defining the quantitative framework within which a numerical scheme works. It identifies and specifies the different steps, which can be taken in the process of formulating, analysis, evaluating and presenting alternative models (KOUDESTAAL, 1992). According to SUN (1994) application of sound hydrologic reasoning during the development of an appropriate conceptual model of flow represents a full 90 % of the solution to most hydrogeologic problems.

Three components are discussed in the development of a conceptual framework for flow modeling. These are the hydrogeologic framework in section 5.2, the nature of the flow system parameters, including the hydraulic and physical properties in section 5.3, and the water budget over a specified domain in section 5.4.

5.2. The Geohydrological Framework

The geohydrological framework includes the outline of a model geometry, and the different hydrogeologic units.

5.2.1. Model Areas confines

The appropriate space and time scales are chosen in relation to the heterogeneity of the system under study and the data available for calibration.

From the previous chapter, it was indicated that the groundwater flow in west-Gedaref is dominated by local and sub-regional flow systems. Efforts to artificially generate regional flow for the whole investigated area is expected to fail in simulating important sub regional features. This coincides with RUSHTON (1979) conclusion on scaling of regional flow models. He concluded that there is no regional movement of groundwater in hard rocks of transmissivity less than $100 \text{ m}^2/\text{d}$. He argued that in addition to the slow movement of water,

the groundwater gradient in hard rock aquifers is dominated by the topography with groundwater movement mainly towards the nearest valley.

Referring to the subsurface geology of the west Gedaref (section 4.2), it became visible that, the basin is divided into three sub-areas of varying sandstone thickness. This is clearly seen from the north-northeast south-southwest profiles (fig. 4.7) in the previous chapter. Although data from Azaza and Abu-Naga wellfields show different stratigraphic characteristic, it appeared that they are hydraulically connected. Hence, the two wellfields are tapping a single aquifer.

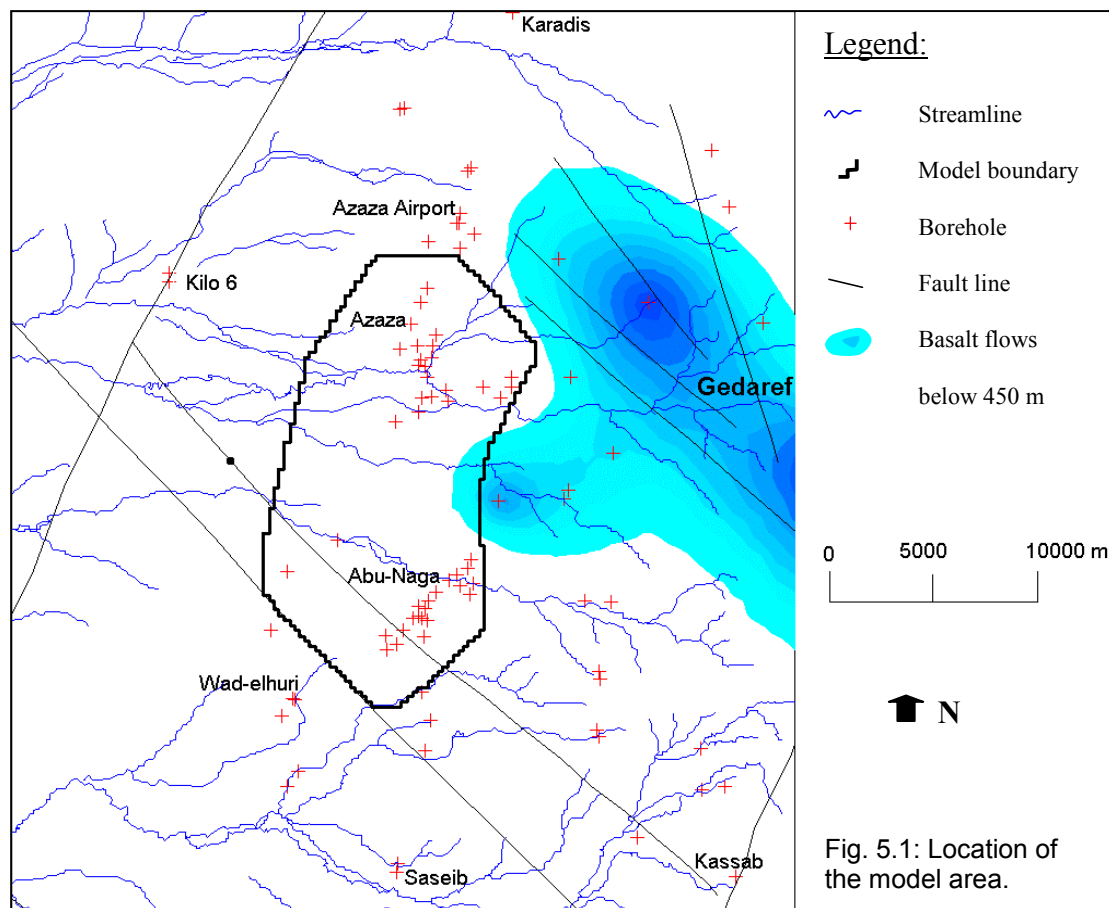


Fig. 5.1: Location of the model area.

Mainly hydraulic boundaries are chosen, as physical boundaries of the basin are far and not enough information is available. The model boundaries were chosen to coincide closely with the limits of the continuous/regional Nubian sandstone at the east. At the west, the boundary is limited roughly to the maximum possible range for extrapolation of available information. Both to the north and to the south the selected boundaries coincide with clear changes in the Nubian aquifer characteristics, which are believed to mark the subbasin boundaries. The

selected model area encompasses around 200 km. It extends 10 km to the west of the Basalt Nubian contact, and 20 km along a north-south axis from Azaza Airport to the southern edge of the Abu-Naga wellfield. The selected boundaries shown in figure 5.1 coincide with some physical features, including a water divide in the north, Basalt thickness contour of 440 m above mean sea level at the northeastern boundary, thin Nubian formation of less than 100 m at the southwest, and inferred fault lines at the south and the southeast.

5.2.2. Defining the Hydrogeologic units

Two types of hydrogeologic units are identified for the purpose of modeling the Gedaref system. The first type is based on the stratigraphic units. The classical method (DE MARSILY et al., 1998) is followed to represent the complex geologic formation within the Azaza-Naga sedimentary basin. With the main purpose to simulate the hydrogeologic behavior, the geologic formation is decomposed into aquifers and aquitards, and then the system is represented schematically as a multi-layered. A second type of hydrogeologic units is introduced in the model to compensate for the lack of data on fractures conductivity. It is used due to the need to characterize the fractures effect using the inverse modeling without prior interpretation of field data. Thus, the fracture system is defined in terms of hydrogeologic units. According to LONG et al. (1997) this will eliminate the need for an intermediate conceptual model to interpret the structural data and may result in a parameter that has little relevance to any flow system.

As described in the previous chapter, the geology consists of interbedded sandstone and mudstone of the Gedaref Formation. Using stratigraphic boundaries and regional head data together with the filter position, hydrostratigraphic units of similar properties are identified. The aquifer system is composed of three layers and confining units. The upper aquifer zone lies at 60 – 80 m below ground level (BGL), the middle at 90 – 135 m BGL, and the lower is at 140 – 230 m BGL. Figure 5.2 shows the layering scheme along a North South direction.

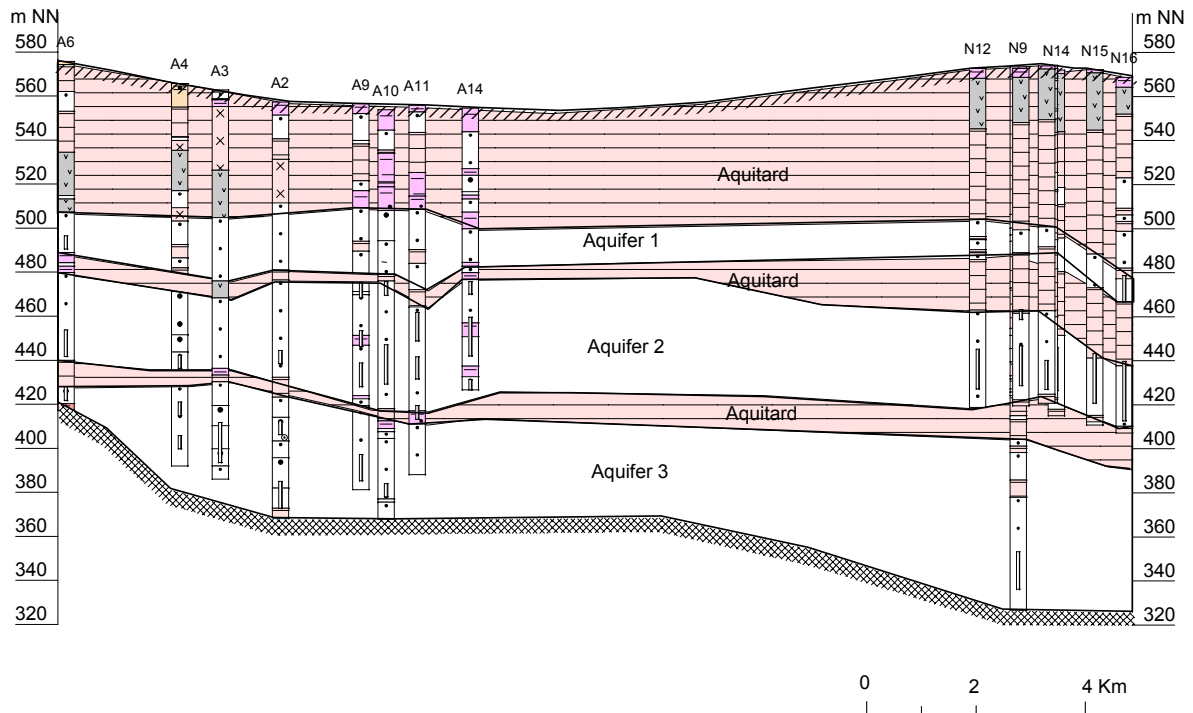


Fig. 5.2: Scheme of the Hydrostratigraphic units identified in the model area.

The above configuration has taken into account the validity of the governing equations for multi-layered aquifers as studied by CONNORTON (1985). In the case of multi-layered aquifers it is recommended to split-up the total range of integration over z (vertically) such that q_x , q_y are sufficiently smooth over each sub-interval of integration. Leakage to and from each layer can be incorporated into the upper and/or lower boundary conditions for each layer

Three hydrostratigraphic units are considered for the proposed flow model, forming a confined aquifer (the middle layer) and two confining beds. The top and bottom aquifers are not explicitly represented in the model because of lack of information about their properties. The middle aquifer layer is modeled as a leaky confined aquifer. Leakage through the confining Mudstone (which has a vertical hydraulic conductivity much lower than that of the Sandstone aquifer) is modeled with a source/sink term.

The leakage rate from/to the upper/lower aquifer layers depends on the vertical conductivity of the confining beds. Areas with thick mudstone beds (e.g. around Abu-Naga) are assigned zero leakage. However, high leakage is considered at borings screened along two or three layers to account for vertical flow between these layers at well locations.

The configuration of fractures considered as hydrogeologic units in the model is conformed to those identified in the previous chapter. However the final adopted units will depend on their effect on the calibrated numerical model (chapter 6).

5.2.3. The flow system conception

The flow system conceptual model is based on the assessment of information available from head and transmissivity data combined with the lithological data.

The flow system in the area is controlled by the multi-layer aquifer system defined above. Focusing on the selected model layer, the scheme below (fig. 5.3) is meant to describe the flow pattern.

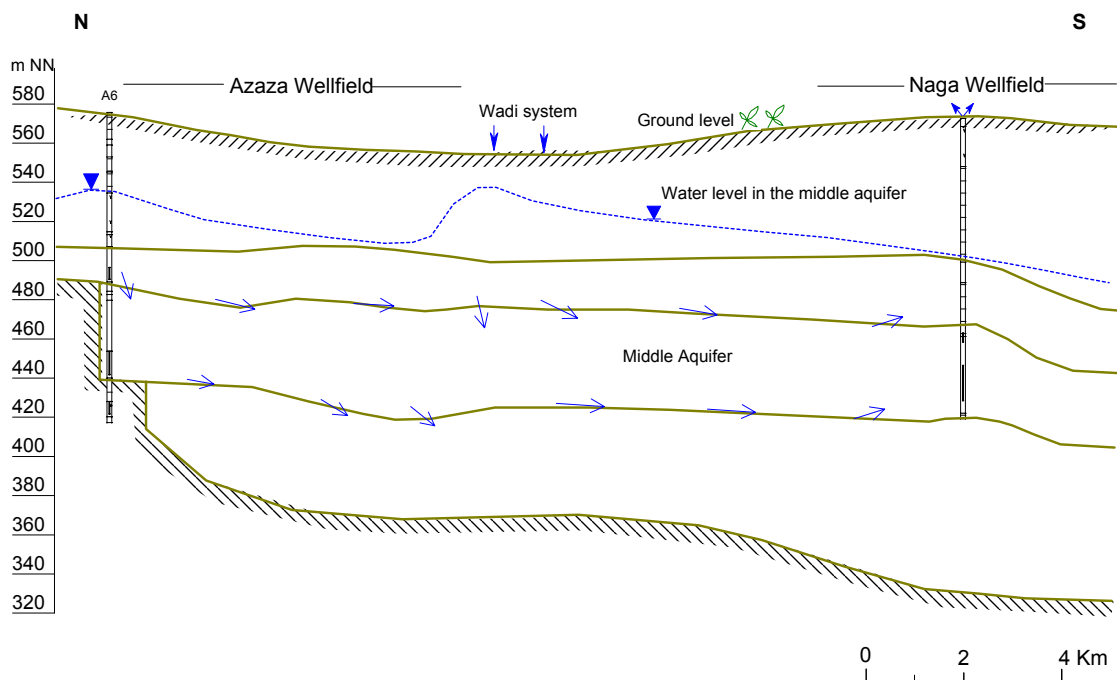


Fig. 5.3: Schematic diagram showing horizontal and vertical flows in the model layer.

The following assumptions are considered to enable the subsequent quantification of flow components:

- The flow occurs under confined to leaky condition, with leakage varying in space;
- The aquifer is under steady conditions before 1992 (base year), unsteady flow regime prevails in the aquifer after 1992, due to the extensive pumping, and to seasonal variation of natural gradients;

- The flow in the aquifer is horizontal, and is represented with a planar depth averaged, two dimensional model (see equation in section 2.2);
- The interaction between the model and the upper/ lower aquifers is approximated by a source/ sink leakage on top/bottom of the model;
- the aquifer is heterogeneous and can be represented by zoned or continuous heterogeneity;
- Horizontally, the flow direction in the porous matrix is probably affected by the prevailing structural pattern;
- fractures in the sandstone formation are modeled as discrete units or as equivalent continuum.

5.3. Parameterization and uncertainty analysis

This step comprises the estimation of the values of different parameters characterizing the system model described above.

Two types of information will be considered, namely:

- 1- Sample information: These are state variables such as head distribution and fluxes estimated from available field measurements. Uncertainty analysis is also included to establish the plausible range of errors in the estimated parameters. (to be used as calibration targets for the numerical simulator).
- 2- Prior information: These are estimates of the system parameters. Such parameters are separated into distributed ones in space such as transmissivity, storativity, and discrete parameters such as well discharge and constant values of head and recharge at the boundaries.

As a rule, the above information/ parameters are not known accurately and their values are affected by uncertainty. Uncertainty associated with different parameters will be handled differently in the following sections.

5.3.1. Head Distribution

Here the head distribution and expected errors are estimated. As known, head values show a spatial drift in the direction of flow; hence its distribution is handled using the universal kriging method. The spatial drift model is chosen according to the final interpolation results. Analysis indicated that head distribution with linear or quadratic drift provides comparable

average residuals variance of 83.00 m^2 ($\pm 9.11 \text{ m}$ standard deviation). However, the standard deviation of kriging map (figure 5.4d) is lower for the linear drift. The variogram structure, the resulting head and standard deviation map for the base year 1992, are given in figures 5.4. Due to the lack of data on the western boundary, different contour pattern resulted for different combination of neighboring points (search radius). However, the head distribution in fig. 5.4c is considered more realistic, taking into account other hydrogeological information.

Beside the aquifer heterogeneity, several sources of errors contribute to the typical large variance of the head values in Gedaref case. These include:

- well design (called scale effect) caused by the varying length and position of the filter. Here wells tapping more than one aquifer layer don't reflect the true head due to the enhanced leakage,
- transient effect due to pumping or seasonal recharge showed a variance of 0.55 to 2.22 m^2 (standard deviation of $0.74 - 1.80 \text{ m}$) reaching an extreme value of 3.20 m at A16 in 1996 close to two khor lines (see table 4.2),
- accuracy of the reference ground elevation,
- measurement error in the range of $\mp 0.05 \text{ m}$ is a possible human/instrument error,
- and finally interpretation errors due to the sample configuration are showed by figure 5.4d.

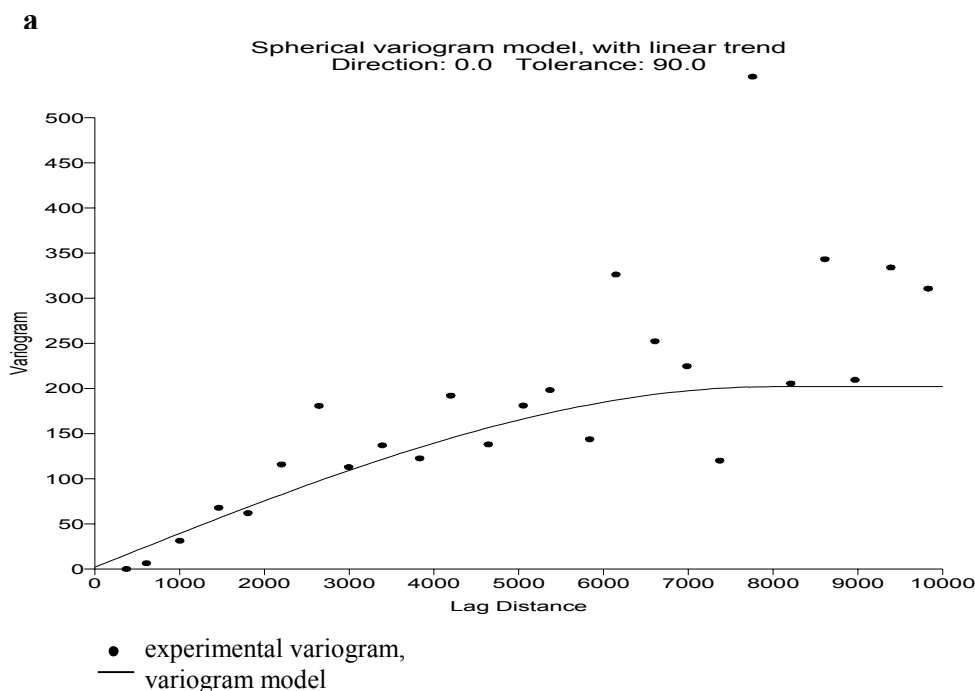


Fig.5.4: a) The variogram model fitted to the head data of 1992.

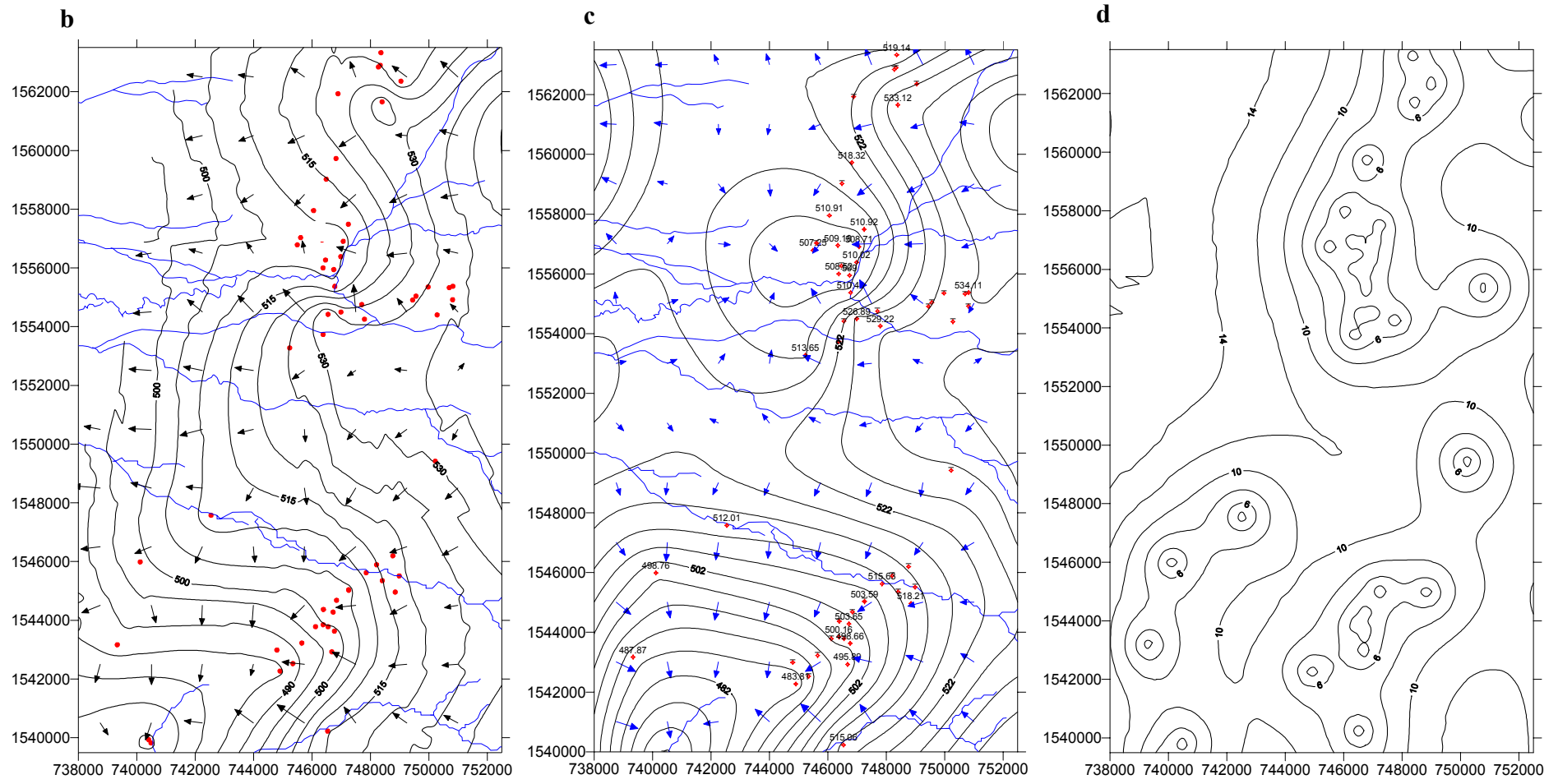


Fig. 5.4: (b) and (c): Two alternative head distributions representing predevelopment conditions (1992) in the model area; (d) standard deviation map of the estimated head.

Using MIZEL's (1982) theoretical head variance a lower estimate of 39.69 m^2 (standard deviation of $\pm 6.30 \text{ m}$) is provided for the case of 2D steady flow conditions. Where, the incorporation of the knowledge on logT variability reduces the uncertainty about the head values. Below is the values considered for the calculation of MINZEL's variance above.

$$\sigma_H^2 = \frac{8}{\pi^2} J^2 \lambda^2 \sigma_{\ln T}^2$$

$$J = 0.00154 .$$

$\lambda = 8 \text{ km}$ according to the head variogram-model above.

$$\sigma_{\ln T}^2 = 0.34 .$$

Therefore, head residuals of the intended 2D simulation results at measurement locations are tolerated within a range of between $\pm 6.30 \text{ m}$. This figure accounts for the expected errors in the head sample due the sources discussed above.

The standard deviation map obtained as a result of Kriging interpolation clearly indicates high uncertainty in the head estimates associated with large data gaps between the two wellfield and at the western margin of the model area. This demonstrates that additional measurement points are needed to increase the accuracy of the head distribution map.

Head distribution after 8 years (1999) of aquifer development is interpolated as in figures 5.5.

5.3.2. Transmissivity distribution

The above contouring of head data suggested the existence of sharp transmissivity contrasts as reflected by the non-uniform flow pattern (varying hydraulic gradient). This phenomenon is also partly due to the effect of jointing defined earlier. Dealing with a fractured porous media, two approaches are followed to produce the transmissivity distribution within the aquifer.

The first approach is a deterministic one. Here the identified discrete units (sub-aquifer units and/or fractures) are assumed to have unique transmissivity values to be provided by the inverse solution. Hence there is no need for prior interpolation of field data.

In the second approach, T of the porous sandstone matrix is regarded as continuous (i.e. spatially correlated) random variable affected with uncertainty. Therefore, its spatial variability can be described through geostatistics methods. Two models are tested to describe

the continuous heterogeneity pattern of T. These are the intrinsic model with nested scales of heterogeneity and NEUMAN's lumped scaling model.

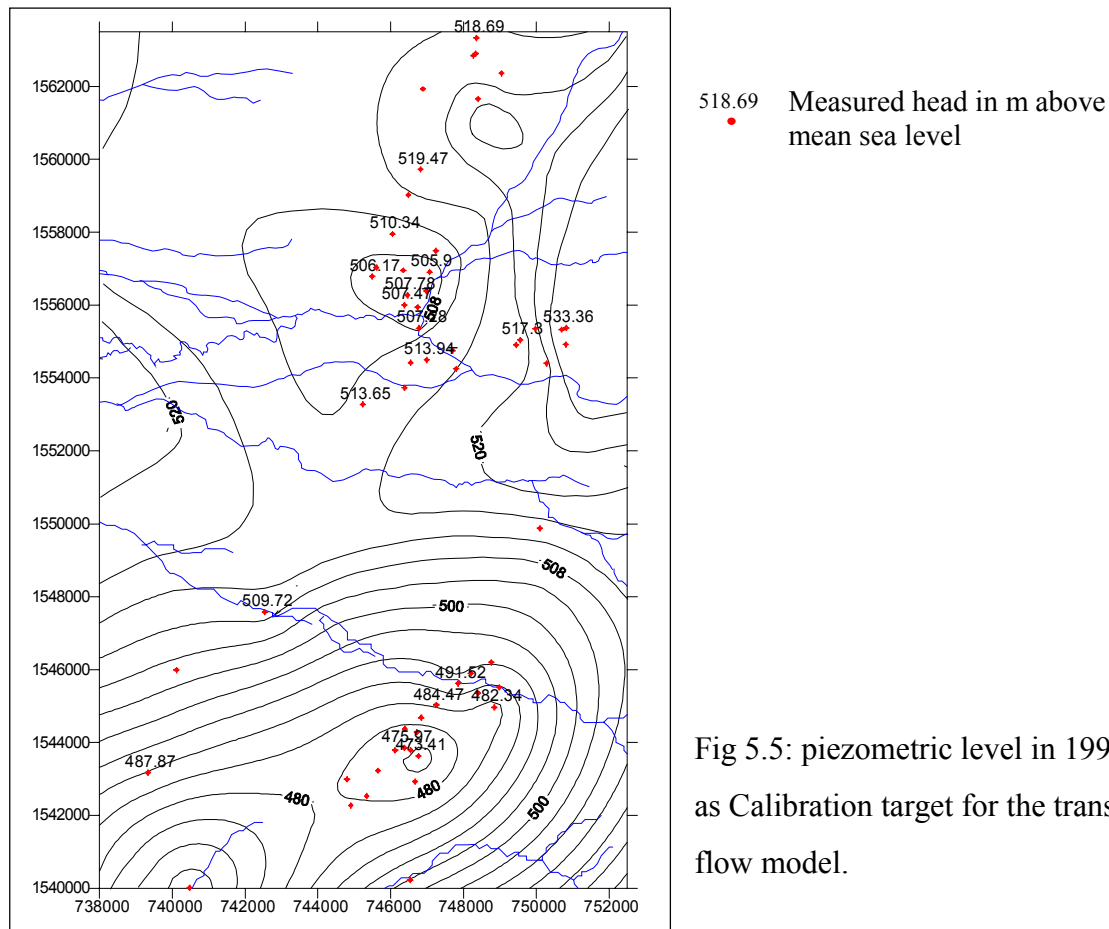


Fig 5.5: piezometric level in 1999 used as Calibration target for the transient flow model.

Two geostatistical methods are applied to compute the transmissivity field using the above models of heterogeneity, namely: kriging interpolation and conditional stochastic simulation. In the following the adopted transmissivity models are presented.

The transmissivity data are first expanded from 23 to 51 locations using the specific capacity estimates. Figure 5.6 shows the result of regression between log transmissivity and log specific capacity using 23 available pairs of data. The variance of the error of prediction derived from the regression equation is 0.06, which is considered as measurements error variance for further kriging and simulation estimates.

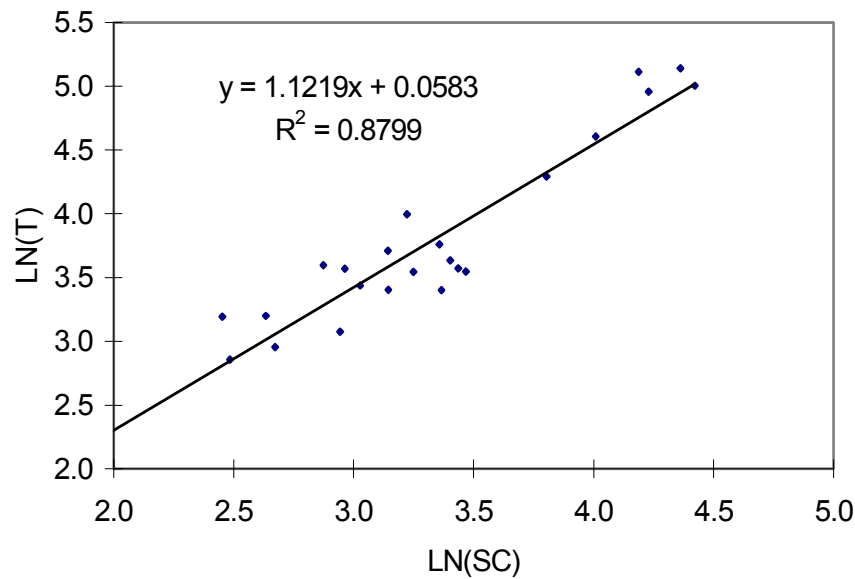


Fig. 5.6: Regression of log Transmissivities on log Specific Capacity.

The extended T values give rise to an average transmissivity of $4.29 \times 10^{-4} \text{ m}^2 / \text{s}$. Also, the increase in data has its effect on the resulting histogram as shown in figure 5.7.

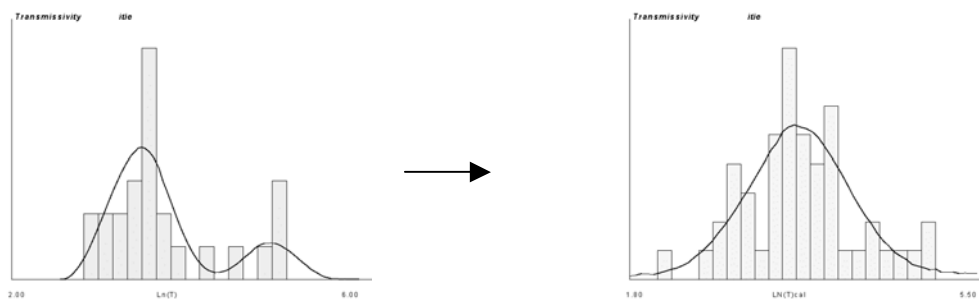


Fig. 5.7: Histogram of ln T, a) from pumping tests, b) extends lnT from regression.

The existence of high T zones deduced the bimodal histogram in the case of limited T points, which is normalized by adding more data from the correlation with the specific capacity.

The first step towards the spatial analysis was to fit a theoretical variogram model to the LnT values. Two alternative models are fitted to be differentiated according to their end results. Adopting NEUMAN's (1991, 1994) generalized power law model. The variogram model fitted to the sandstone transmissivity is presented in figure 5.8a. Fig. 5.8b shows the alternative

nested-structure isotropic variogram model. The theoretical models fitted in figure 5.8 are formulated as follows (PANNATIER, 1998):

$$\gamma(h) = C_o + C|h|^a \quad (\text{power model})$$

with the parameters, $C_o = 0.06$, $C = 0.00315$, $a = 0.5$.

$$\gamma(h) = C_o + C \left[\frac{3h}{2a} - \frac{1}{2} \frac{h^3}{a^3} \right] \quad \text{for } |h| \leq a \quad (\text{spherical model})$$

with $C_o = 0.06$, and the parameters of the nested three spherical variogram models are: $a_1 = 1100$, $a_2 = 3000m$, $a_3 = 10000m$, and sill values of $C_1 = 0.045$, $C_2 = 0.10$, $C_3 = 0.135$.

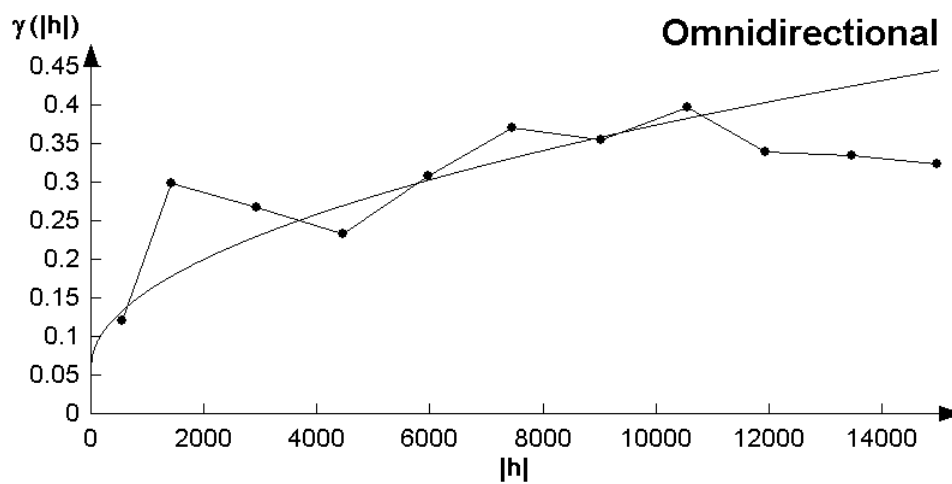


Figure 5.8a: A universal power model fitted to the mean variogram of lnT.

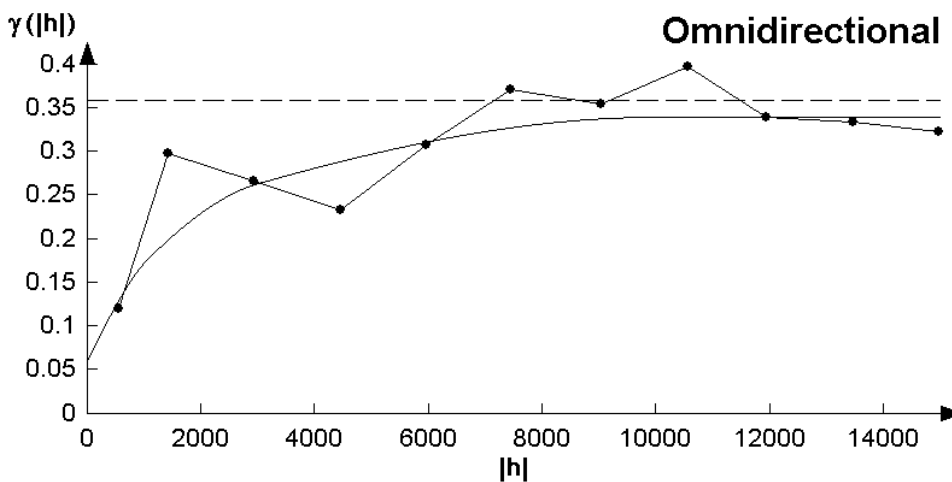


Fig. 5.8 b: The mean variogram of lnT, and the fitted nested-structure model.

1\ Kriging Interpolation

Kriging combined with linear regression (AHMED & MARSILY 1989) is used. In the method, the transmissivity data are considered as local values, which is then interpolated using the fitted variogram models above. The resulting transmissivity distribution using ordinary kriging is shown in fig 5.9a & b.

Although Kriging honors local measurements, it provides smooth spatial variation of T that is hardly natural. The kriging interpolation gives average estimates of T suitable only for simulating the general regional trend. However, it is not expected to simulate natural transmissivity variations. Additional shortcoming in using Kriging in modeling is that it does not allow for uncertainty evaluation in the predicted model results. According to MARSILY, et al. (1998) this traditional approach tends to exaggerate the internal hydraulic conductivity in the water-bearing layer. Therefore representation of heterogeneity is considered in a second approach. The kriging standard deviation map (fig. 5.9c) accounts for the range of certainty in the interpolated field.

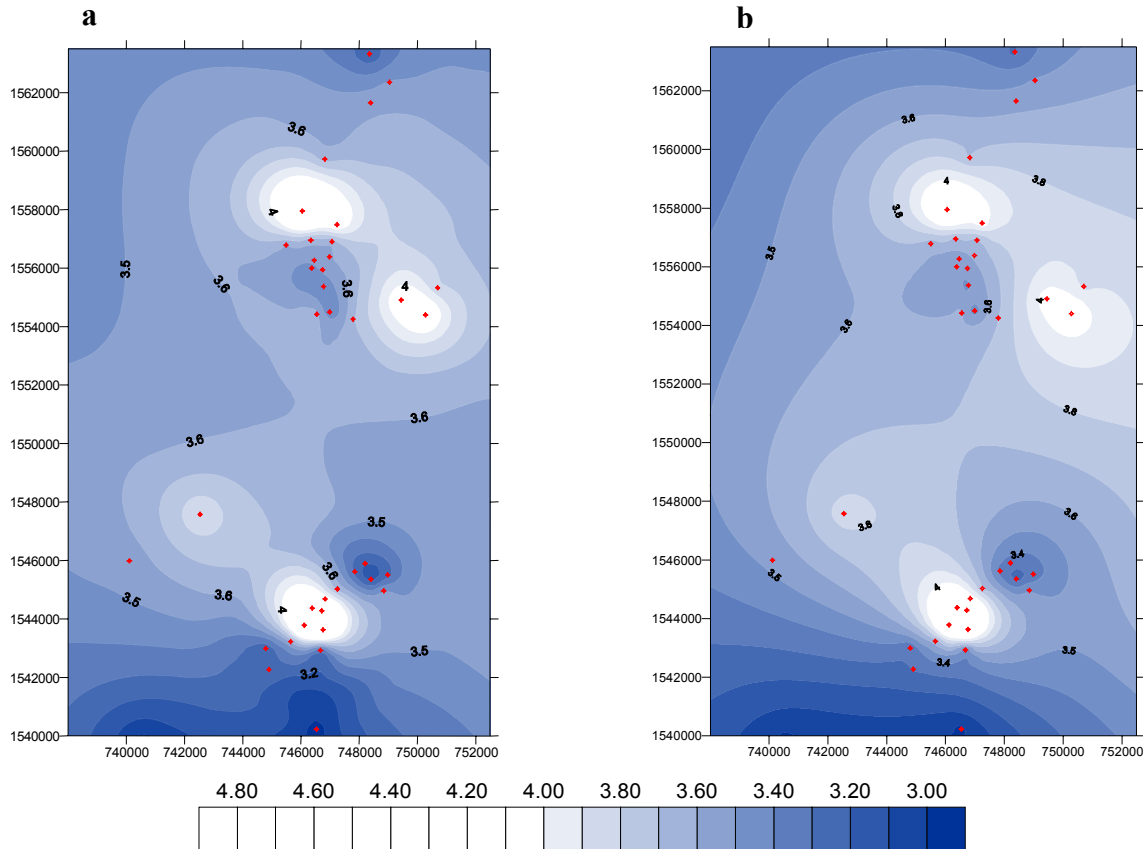


Fig. 5.9: Kriging estimates of ln Transmissivity values using: a) the nested, and b) the universal variograms.

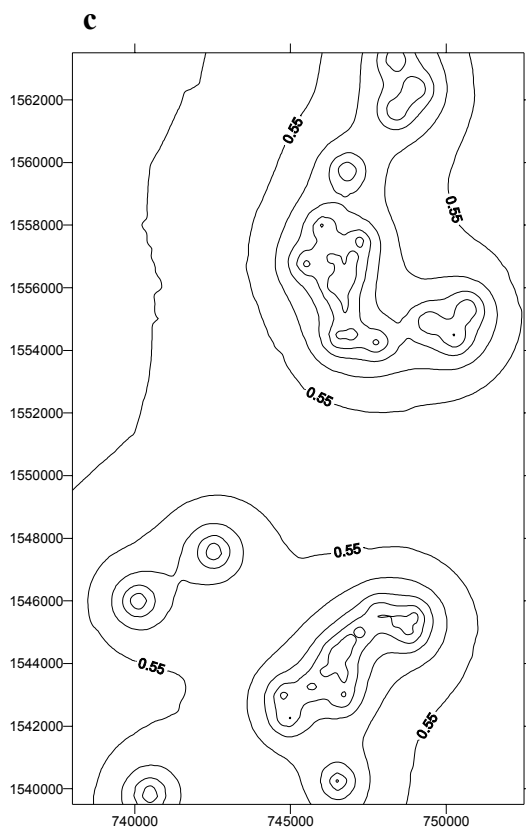


Fig 5.9c: The standard deviation of kriging estimates (fig. 5.9a) using the nested variograms.

2\ Stochastic simulations

In the second approach, the conditional simulation technique “Simulated Annealing” described in chapter 2 is applied to simulate the transmissivity field honoring both the measurements and the spatial continuity modeled above (fig.5.8). Referring to the transmissivity data at borehole locations, it is clear that the data is clustered in the two areas of the Azaza and Abu-Naga wellfields, and large gabs of information exist between the above mentioned locations

This data constraint has been a typical phenomenon in hydrogeology where borehole locations are always guided by demand rather than systematic research-oriented planning. Conditional simulation handles this problem by constraining the resulting distribution to the variogram model fitted to smallest available data spacing. Simulation results (figure 5.10) fill the data gabs according to the histogram and the variogram models above, within a range of $\ln T$ values between 2.00 to 5.20 (limits of $\ln T$ data).

3\ Zoned heterogeneity Approach

A third approach is based on the definition of homogeneous zones in the aquifer. As no enough geologic information to support the zonal heterogeneity, Kriging is used to shape the zonal pattern. Additionally, the head gradient is also used in the delineation of the zones. T is then averaged over the identified homogenous zones. The identified homogenous sub-units and their average T values are given below in table 5.1.

Based on the (first) suggested T-zones, four prior estimates of the average T are considered to represent the range of magnitude of the transmissivity exists in the model area. These give rise to a very low T-zone, a low, middle and a high one. The orders of magnitude of the four values are 2.8, 3.7, 5.0 and 10.0 $10^{-4} m^2 / s$ respectively. Far from certain, the zonation pattern is first outlined after several runs of adjustment during the calibration of the numerical model next chapter. The overall coefficient of variation of T (equals ± 0.05) indicates the plausible range in the above transmissivity estimates.

Table5.1: Average zonal transmissivity estimated from pumping test results.

Aquifer subunit	T in $m^2 / s \times 10^{-4}$
North Azaza	3.7
Azaza wellfield	5.0
Abu-Naga wellfield	10.0
South Abu-Naga	2.8

5.3.3. Hydrogeologic Stresses

Hydrogeologic stresses include natural and man-made induced recharge and discharge.

No measurements of the stresses are available in the Gedaref area. Estimates will be provided in the next section by calculating the steady state water budget based on T and h data. Discharge due to well abstraction in the model area is estimated (as mentioned earlier) from the capacity of the water tanks and the approximate pumping duration. The total abstraction in the area before construction of Azaza wellfield in 1992 is estimated at around 3600 m^3/d . After 1992 pumping increased to around 7200 m^3/d (2.60 Million m^3/y , or about 2% of the annual precipitation in the area).

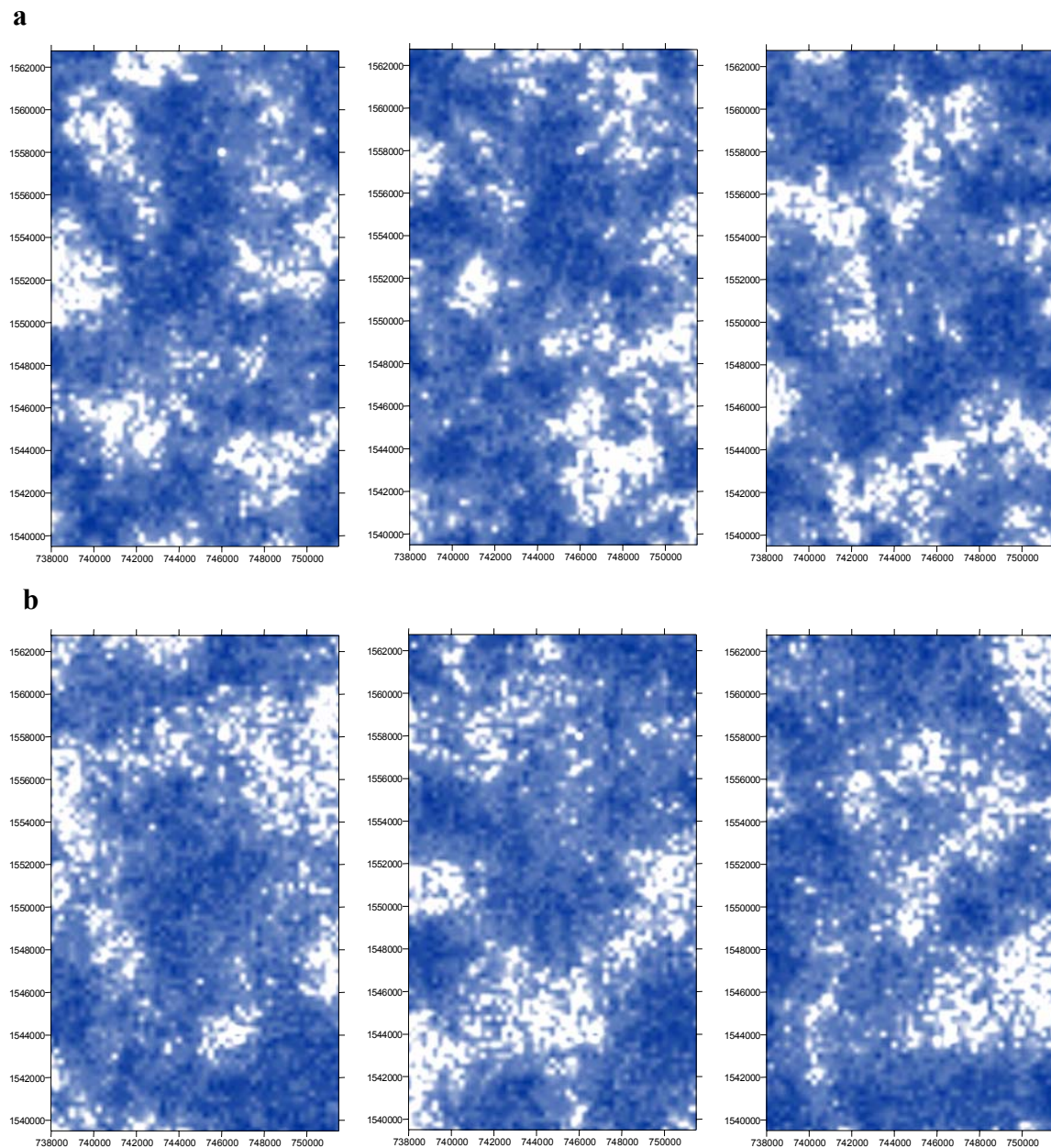


Fig. 5.10: Different random T fields resulting from stochastic simulations using: a) nested variogram model, b) lumped power variogram. (the lighter the color the higher the T value)

5.4. The Water Budget

This section focuses on the estimation of the water budget components including inflow and outflow within the model domain.

The flow balance is an essential feature of any groundwater problem. The appropriate balance equation must be satisfied at zero time of simulation. As the starting conditions in groundwater simulation refer to a particular time in a continuous process, the base year 1992 is considered for the balance calculations.

Recharge in the aquifer is mainly due to vertical leakage across the overlying aquitard, in addition to the influx across the boundaries, whereas discharge components include pumping, out-flux, and downward leakage to the lower aquifer layer. Beside the estimation of the lateral in/out flux through the model boundaries, the spatial variations in recharge are modeled by defining recharge zones. Typically, there is not enough hydrogeological information to define the extent of recharge zones, and to assign recharge rates to each zone. Prior estimates are calculated based on certain assumptions, which will be justified on the basis of the calibration results (next chapter).

Assuming 2D isotropic regional groundwater flow conditions, the flow balance is described by the differential equation:

$$\frac{\partial}{\partial x} \left(T \frac{\partial h}{\partial x} \right) + \frac{\partial}{\partial y} \left(T \frac{\partial h}{\partial y} \right) = S \frac{\partial h}{\partial t} - Q(x, y)$$

Where, h is the hydraulic head [L], T is the transmissivity [L^2T^{-1}], S is the dimension-less storage coefficient and Q is source/sink term per unit area of the aquifer [LT^{-1}]. The left-hand terms represent the lateral flow, and the right-hand terms represent inflows and water release from storage. Assuming that before 1992 the groundwater system in the model area existed in a state of dynamic equilibrium with negligible head variation, a steady state model can be used to simulate the starting conditions. This implies a long-term balance between natural recharge and discharge in the area. Therefore, the term $\frac{\partial h}{\partial t}$ in the balance equation above is neglected.

A tentative water balance is calculated with the help of a computerized method recommended by STOERTZ and BRADBURY in 1989 (ANDERSON, 1992). Using the model grid (chapter 6), all finite element nodes are given specified head values as interpolated earlier. The water balance module of FEFLOW is used to calculate the total in/out flow through the boundaries, and to roughly define the recharge/discharge zones. The flux analyzer is then used to estimate the vertical component of the flux.

The total in/out flow in the modeled aquifer is calculated by FEFLOW water budget module amounts to 7183 m³/d. However, this budget is highly dependent on the estimated average

transmissivity of $4.29 \times 10^{-4} \text{ m}^2/\text{s}$ and on the interpolated heads taken from the water level contour map (fig 5.4). They are also dependent on the scale of the model. Therefore, the total in/outflow in the calibrated model is accepted within $\pm 10\%$ of the estimated value.

Low-lying areas around Al-Laya wadi system resulted significant vertical flow component estimated at $3623 \text{ m}^3/\text{d}$ by the flux analyzer of FEFLOW. This vertical component will be added as source term ($Q(x, y)$) in the 2D water budget equation above. Upward (-ve) flux typically shows up around the two wellfields indicating the capture zones of pumping wells, and leakage to the underlying aquifer. This is calculated as $3855 \text{ m}^3/\text{d}$.

5.5. Conclusion

In this chapter, a complete design of the flow model is provided within a prescribed framework. Decisions are made on the model area and the boundary conditions. Estimates of the state variables (head and water budget) as well as prior estimates of transmissivity and hydrologic stresses are given based on continuous or discrete structural analysis.

Following the modeling approach outlined in chapter two, this chapter emphasized the supportive role of geostatistics in applying groundwater models. Transmissivity maps are produced using external data through the combination of ordinary kriging with linear regression. Additionally, conditional stochastic simulation is applied to provide alternative heterogeneous T maps. Universal kriging is used to produce head distribution characterized with a drift component. Finally, an assessment of the uncertainty in the estimated data is presented to provide a control on further numerical estimation results.

6. The Numerical Simulation

6.1. Introduction

The numerical modeling is one of several methods used to assess the Gedaref hydrologic system. With the absence of enough hydrogeological data, a hydrogeological model is expected to simulate the average behavior of the sandstone aquifer, and allow testing several scenarios to enable a decision on the important flow elements in the aquifer. The use of numerical analyses provided a good tool that helped to confirm the assumptions made in the previous parts, and to put across the range of potential future conditions.

Being interested in the groundwater potential close to existing over-pumped wellfields, the objectives of the numerical modeling effort is to determine the values of the hydraulic parameters and hydrologic stresses from information about head, i.e. to solve the inverse problem to provide check for the assumptions underlying the conceptual model. This would ultimately lead to the estimation of:

- Transmissivity and storativity, and their spatial distribution,
- Vertical recharge/leakage rates,
- Boundary conditions, namely: in and outflow across the model boundaries.

Subsequently, predictions provided by a calibrated model would contribute to the management objective realized by specific development scenarios.

The finite element method imbedded in FEFLOW software is applied to solve the flow equations adopted for the Gedaref aquifer system. The discretization of the model domain is discussed in section 6.2. Section 6.3 presents the boundary conditions used for the solution of the numerical scheme. In section 6.4, the results of the calibrated quasi three-dimensional distributed model are presented. A full 3-dimensional model is not considered, as it would require many assumptions, which is difficult to pack with real measurements.

6.2. Horizontal and vertical discretization

The model area is discretized using a uniform, rectangular grid to facilitate the import of the transmissivity fields estimated from different methods (see last chapter). A deformed triangular grid is expected to accurately locate pumping wells and recharge from seasonal streams. However, within the estimated model accuracy, the latter grid is not considered for the current study.

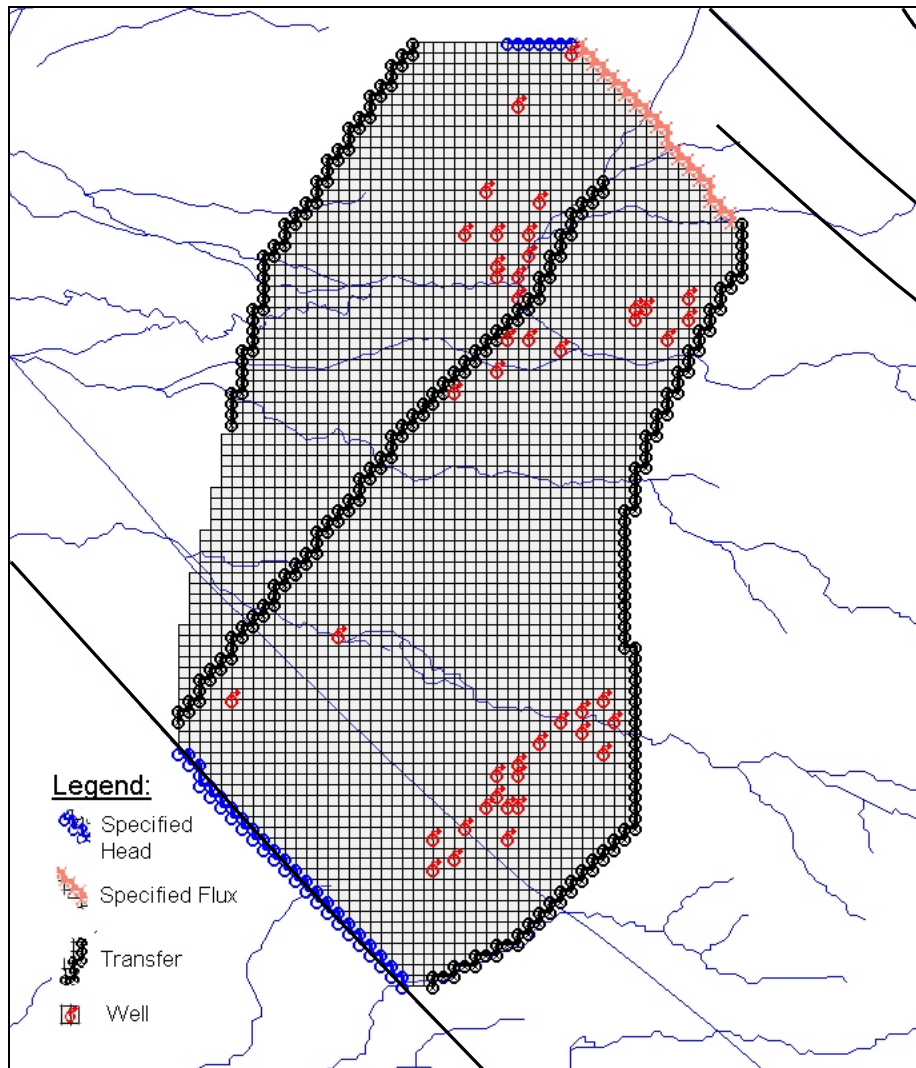


Fig. 6.1: Finite element grids used for numerical approximation.

As recommended by ANDERSON and WOSSNER (1992) the size of the grid is chosen considering the curvature of the piezometric surface, the variability in the aquifer properties as provided from the available information, and the variability of pumping nodes, recharge nodes (streams and possible faults).

The outline of the grid is determined roughly by the hydraulic boundaries identified in section 5.2. Fitting the grid to the exact shape of the sandstone is not critical to the modeling effort, because concern focuses on the stressed interior part of the system. Hence, the western boundary is placed sufficiently far from the center of the grid, so that pumping effect does not reach the boundary within the time period used in transient simulation.

The rectangular mesh is composed of 3158 elements. The grid cells are designed with uniform dimensions $\Delta r_j = \Delta c_i = 250\text{m}$. According to the schematic stratigraphy (fig. 5.2), the model layers are simulated differently as allowed by the data. A quasi-three dimensional model is

designed to simulate the multilayer Nubian system. The middle (main) sandstone aquifer identified in the previous chapter is simulated with a 2D model layer integrating the hydraulic conductivity over the aquifer depth, and assuming negligible vertical head gradients. Both the upper and the lower aquifers and the aquitards confining the main layer are simulated as downward leakage (source/sink). In spite of the lack of data for the overlying/underlying aquifer; they could be included in the model by calibrating their contribution at wells tapping more than one layer.

6.3. Boundary conditions

According to the above model design, the numerical scheme for the groundwater system in the Gedaref sandstone is based on the so called the aquifer viewpoint (ANDERSON, 1992). The flow governing equation takes the following general form considering an inhomogeneous, isotropic leaky confined aquifer under the aquifer viewpoint:

$$\frac{\partial}{\partial x} \left(T \frac{\partial}{\partial x} \right) + \frac{\partial}{\partial y} \left(T \frac{\partial}{\partial y} \right) = S \frac{\partial h}{\partial t} - R + L$$

and

$$L = -K'_z (h_{source} - h) / b'$$

Where,

1. Groundwater flow is assumed to be strictly horizontal through the aquifers and strictly vertical through confining beds.
2. The hydraulic conductivity is integrated in the vertical dimension to give an average transmissivity.
3. The vertical flow through confining beds is represented by a leakage term ($L_{i,j}$) that adds or extracts water from the aquifer. Confining beds are not explicitly modeled and heads in the source and bottom aquifers are not calculated. Release of water from storage within the confining bed is not considered in this approach.

Starting with a steady state simulation, the boundary conditions largely determine the flow pattern. As indicated in figure 6.1 the following boundary conditions are considered.

- Inflow through low permeable walls in the eastern (Basalt Nubian contact zone) and the western (thin Nubian formation) boundaries is simulated using Cauchy boundary condition.

$$q_m(x_i, t) = -\bar{\Phi} h(h_2^R - h)$$

In this type a reference hydraulic head (a variable flux boundary) is assigned. The reference head is combined with a transfer rate to simulate the imperfect contact between the simulated domain and its boundaries. In/Out transfer between the aquifer and Cauchy boundary type is proportional to the transmissivity of the boundary formation.

- prescribed fluxes (Neuman type) are assigned at the northeast border to simulate drift underflow from the bordering aquifer environments.

$$\bar{q}_{n_h}(x_i, t) = \bar{q}_h^R(t) = -T_{ij} \frac{\partial h}{\partial x_j} n_i$$

- Fixed/time-varying hydraulic head (Dirichlet type) at the northern and southern boundaries to help achieving a unique solution of the head distribution within the model area.

$$h(x_i, t) = h_1^R(t)$$

- Additionally, singular point sources are assigned at borehole locations to simulate pumping rate, or interaction between aquifer layers at boreholes tapping more than one layer.

Vertical fluxes across the piezometric level are treated as an internal source or sink. An array of fluxes is assigned where leakage is expected.

The adopted mathematical models (governing equations, boundary conditions, and initial conditions) are solved using the numerical approximation method the finite element. The computer code FEFLOW solved the set of algebraic equations generated by numerical solution of the partial differential equations, and processed the results as will be presented in the calibration process.

6.4. Calibration targets

It is generally believed that regional models at best simulate the average head or the drift (CHRISTINSEN and COOLEY, 1999). Therefore, it is expected that the variance of the residuals between the simulated and the measured head lies within the range of the head variance as calculated in section .5.3.1.

In steady flow conditions, the estimated head variance of $(\pm 6.30)^2 m^2$ provides an estimate of the expected range of model residuals $(h_{simulated} - h_{measured})$.

Relating the above variance estimates to the 60 m head loss over the model area, an error range of 10 –15% is tolerant in the modeling results. This demonstrates a wide calibration target, and hence indicates a danger of non-uniqueness. This is compensated by the water balance calculation, which provides an additional control on the modeling results.

The reliability of the head observations is represented by a weighting factor. Weights are assigned to head measurements to account for the uncertainties associated with errors discussed earlier. Head values in Abu-Naga boreholes, Twawa and Umm Gulga are assigned weights of 0.8 to account for scale effect at wells filtered along the top source aquifer, and for transient effect caused by pumping in nearby wells, as well as for longer development periods. In the above locations development has started up to two decades before the rest of the wells in the model area. A similar weight is assigned where high gradients exist and extreme local mounds cannot be represented by the regional drift model. This is specifically met south of Azaza wellfield where the confining aquitard is thinning out giving rise to considerable vertical permeability between the upper and the middle aquifer.

The boundary fluxes estimated in the previous chapter within the water budget calculations are highly uncertain. Up to 10 % coefficient of variation would be acceptable in Gedaref model.

Plausible transmissivity estimates is considered within a range equivalent to 0.05 coefficient of variation (chapter 5).

6.5. Calibration assessment

Model calibration involved the adjustment of the following parameter:

- Vertical leakage rate
- Boundary flow rate
- Transmissivity distribution

Model fit to the calibration targets is assessed according to the below specified criteria.

- Root mean square error (RMS)

$$RMS = \sqrt{\frac{\sum_{i=1}^n (WF)_i (h_m - h_s)_i^2}{n}}$$

where, WF is a weighting factor used to estimate the reliability of measure head h_m value.

- Scatterplot of measured and simulated heads close to a 45° sloping line.
- Distribution of the head residuals from 22 target borehole locations.

Qualitative (visual) comparison between measured and simulated head contour is found to be of no significance given the effect of the data configuration on the interpolated contours. However, the overall flow pattern demonstrated by the head contour is taken into consideration.

6.5.1. Steady state

A steady state is first calibrated against the head measurements of the year 1992 as detailed below. Following Yeh's calibration rationale (chapter. 2), first the boundary fluxes, then the recharge rate and finally the transmissivity distribution are calibrated under steady conditions. Areas of uniform flow are assigned constant transmissivities to represent homogenous aquifer sub-units. By fixing the transmissivity at a uniform value equal to the geometric mean of the available T data (table 5.1) in each sub-unit, the governing flow equation is reduced to a boundary value problem. In areas where no data exist, T values are assigned within the identified T range considering other hydrogeological information.

Calibration started with the elimination of the bias by adjusting the boundary conditions and then the recharge rates while keeping a constant zonal transmissivity, until a scatter-plot roughly coinciding with a 45° line is obtained. Assigning a pumping rate of 2350 m³/d (in 1992), the calibrated total leakage on top of the main model layer amounts to 4087 m³/d. Steady state estimates of boundary influx and outflux are 1973 and 2693 m³/d respectively.

Compared to the prior estimate of the total budget in the previous chapter, the water balance estimated by the numerical model lie within the tolerable range specified in the previous chapter.

After calibrating the boundary conditions and the recharge rate, the second step focused on reducing the head variance by adjusting the transmissivity distribution in order to reproduce the head measurements. T values are changed within the estimated coefficient of variation (0.05). The shape and the number of the sub-units are also modified to improve the model fit.

The scatter plot of the calibrated model is given in figure 6.2, showing a RMS of 1.02 m excluding boreholes tapping the upper layer.

The parameter estimated by the numerical model include the water budget components (fig. 6.3), the extension of the leakage area (fig. 6.4), the transmissivity zones (fig. 6.5). Typical head distribution resulting from the above calibrated model parameters is shown in fig. 6.6.

The numerical model is then run under steady state condition using the geostatistical methods of Kriging and conditional stochastic simulation to account for the random nature of the transmissivity field, as well as the conditioning effect of transmissivity measurements. Testing the alternative transmissivity distributions modeled with Kriging and stochastic simulation (see the previous chapter), the resulting RMS amount to 2.35 m for kriged T, and 2.58 m and 2.30 m for T-fields created by the simulated annealing method using power and nested variograms respectively.

Varying transmissivity along identified fracture zones was not sensitive to the modeling results, as there are no control measurements close to the modeled fractures. However, their effect on the flow pattern is simulated with internal boundary conditions.

6.5.2. Transient conditions

Starting from the calibrated steady flow model, a transient run is simulated from 1992 to 1999, and calibrated against the head measurements obtained from the field visit in December 1999 with RMS of 1.71 m. Figure 6.7 below shows the transient water balance and the resulting scatter plot. The simulated piezometric level and the particle-tracking plot are shown in figure 6.8.

The mean storativity estimated by the transient model is about 2.0×10^{-3} . The calibrated transient model resulted higher inflow rates and lower outflow as compared to the steady one. This is justifiable due to the increased hydraulic gradient caused by the pumping effect. An imbalance of around 172 m³/d in the transient water budget is expected to gradually reach equilibrium on the account of the model outflows.

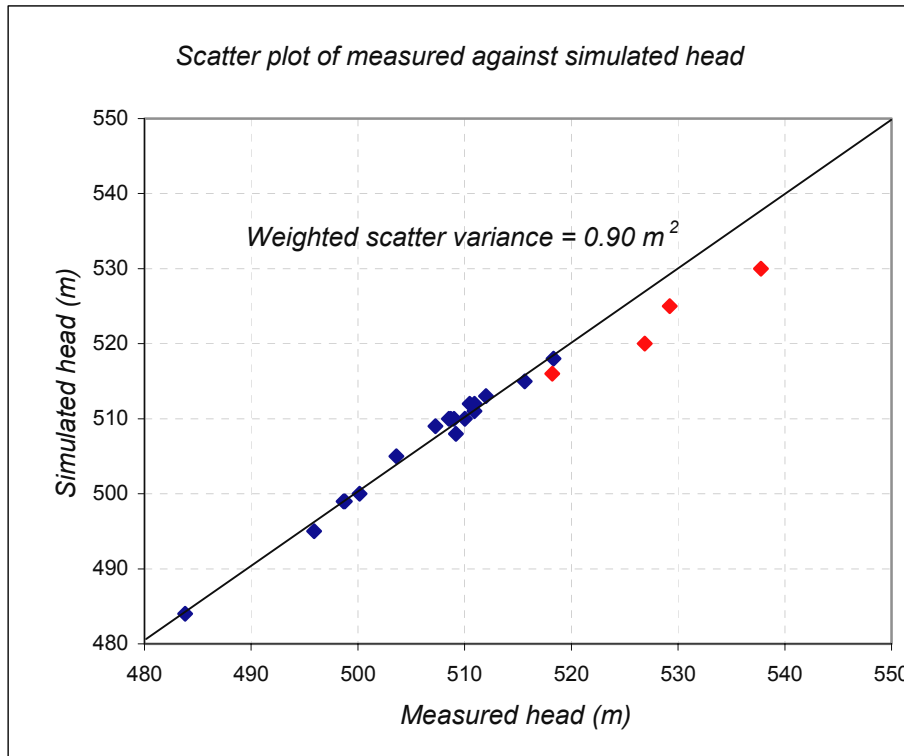


Figure 6.2: A scatter plot showing the steady flow model fit.

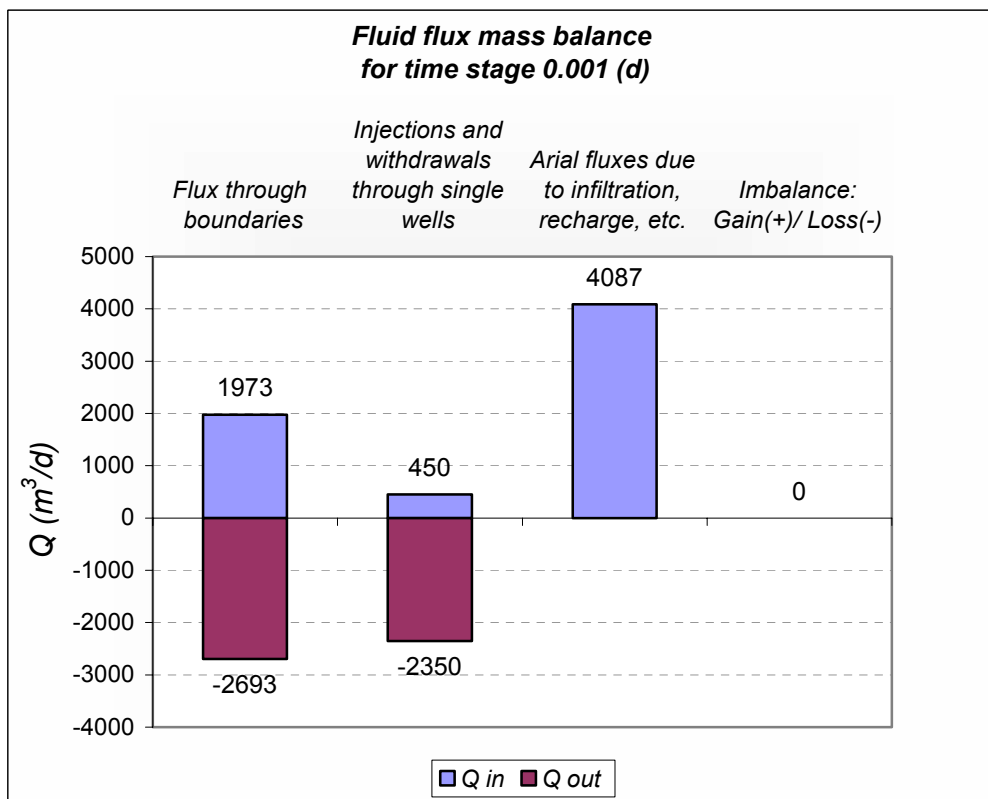


Fig. 6.3: The water budget resulting from steady state calibration of recharge rates and boundary fluxes.

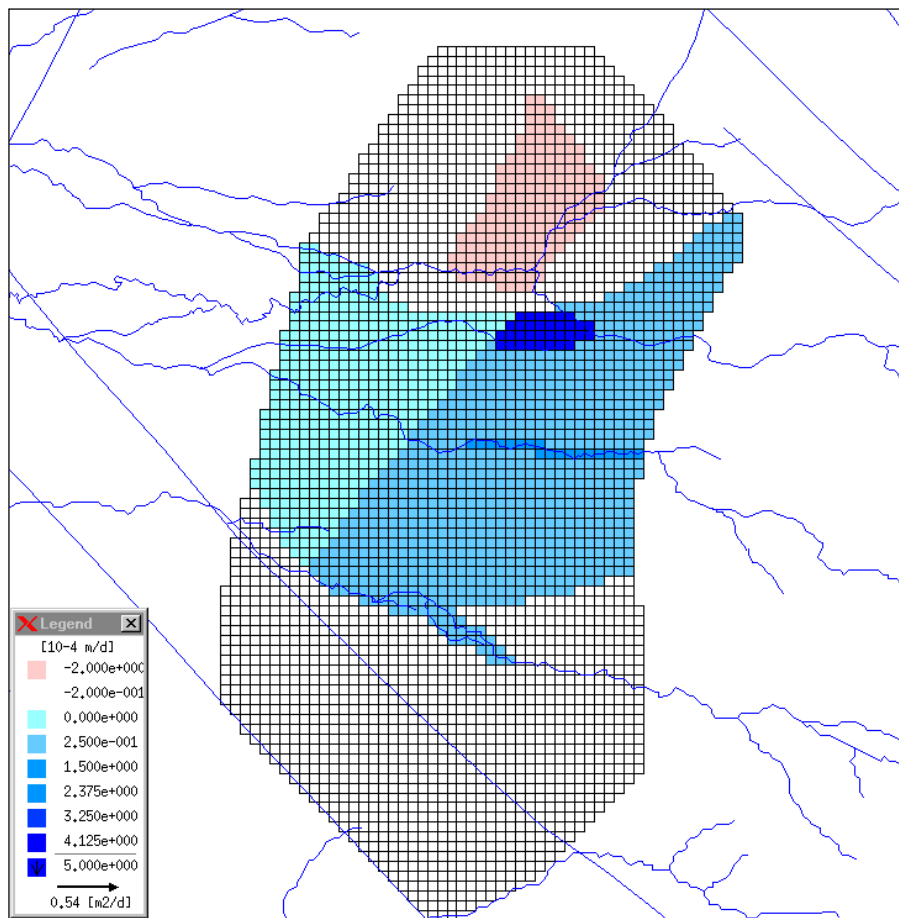


Fig.6.4: Extension of the downward leakage to/from the main aquifer layer.

According to the calibration results, only 5400 m³/d (4200 from the wellfields and 1200 from scattered wells) is pumped from the simulated main aquifer layer. The secondary overlying and underlying aquifer layers deliver the additional pumpage. The model clearly indicates the large contribution of the upper aquifer in the area south of Azaza wellfield. The modeled layer contributes only 1200 m³/d compared to the total abstraction of 3000 m³/d provided by the Azaza wellfield. This is also noticed at a lesser potential at boreholes tapping the upper aquifer horizon in Abu-Naga wellfield.

Within the specified range of accuracy, the calibrated transient model is believed to give a good estimate of the average balanced dynamic conditions in the area with an estimated water budget of 7500 m³/d and negligible deficit of 172 m³/d (see fig. 6.7). The model will then be used to predict the consequences of future development strategies. However, the predictive simulations will be limited to only twice the calibration period (i.e. not more than 20 years) to avoid the violation of the model boundary conditions.

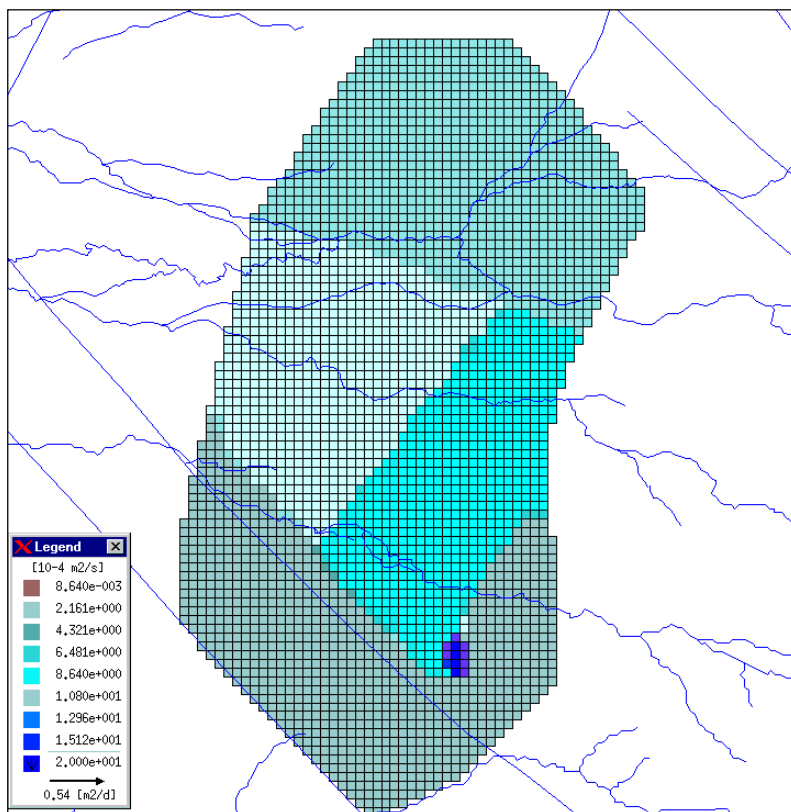


Fig. 6.5. Transmissivity sub units resulted from the steady flow model.

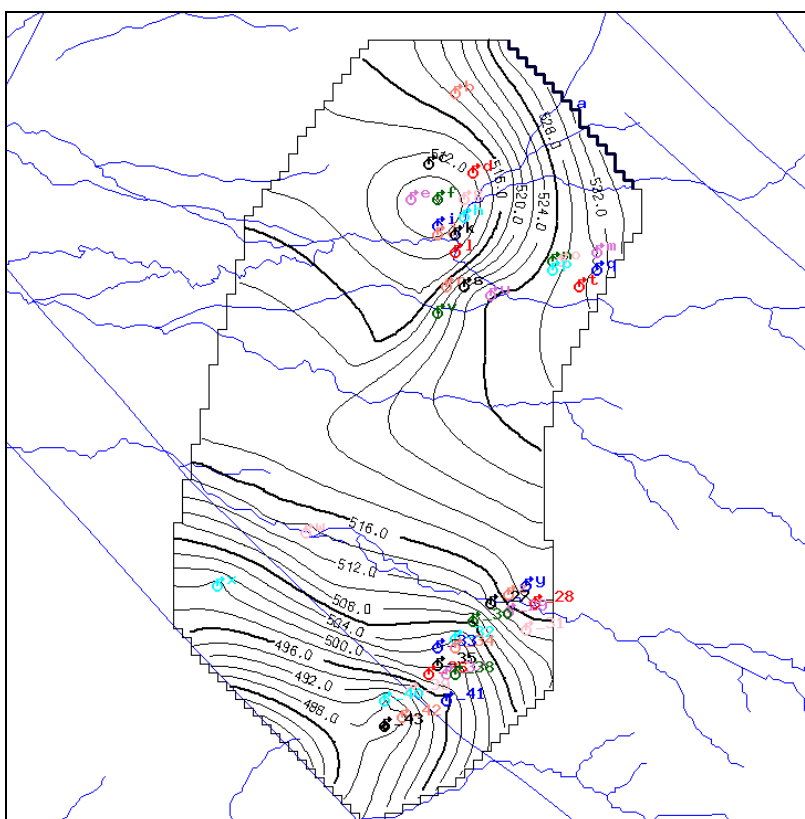


Fig. 6.6: Head distribution of the calibrated steady flow model.

6.6. Model predictions and Aquifer potential

Comparing the model estimate of the well discharge from the middle layer (5400 m³/d) to the actual pumpage (7200 m³/d) estimated earlier from tank capacities, it appeared that considerable amount is provided by the upper and lower layer. This reached up to 350 m³/d for a well in the valley of Al Laya khor south of Azaza wellfield. Further to the south of the Azaza, wells tapping the upper aquifer is expected to produce considerable amounts during the rainy season as indicated by wells N1, N11, N16. Un-modeled potential in the lower aquifer horizon becomes evident from the well yield of the boreholes N5, N6, N9, N10, & N17.

Two scenarios are considered to predict the consequences of future development in the model area. First, future abstraction at the current pumping rate is found to balance the inflows from vertical leakage and boundary fluxes for the coming 20 years with 13 m maximum decline in groundwater levels at Abu-Naga. Additional pumping of 3000 m³/d from 10 existing (non-operated) wells in the Azaza wellfield lead to 19 m drop in groundwater level to reach a minimum of 488m (8 m above the aquifer top). The later simulation results are shown in fig. 6.9. Increase of abstraction in Abu-Naga is expected to lead to excessive lowering of groundwater levels around the wellfield.

A second scenario focused on testing new developments in potential areas recognised from the calibrated model. Selected location west of the Azaza wellfield could contribute up to 2000 m³/d under confined conditions above 480m (fig. 6.10).

The eastern portion of the model area draws influx from the Basalt aquifer to the east. This part is expected to contribute high quantities during the rainy season. Wells tapping the upper aquifer are recommended in this part, to avoid deeper lowering of the groundwater head in the middle layer.

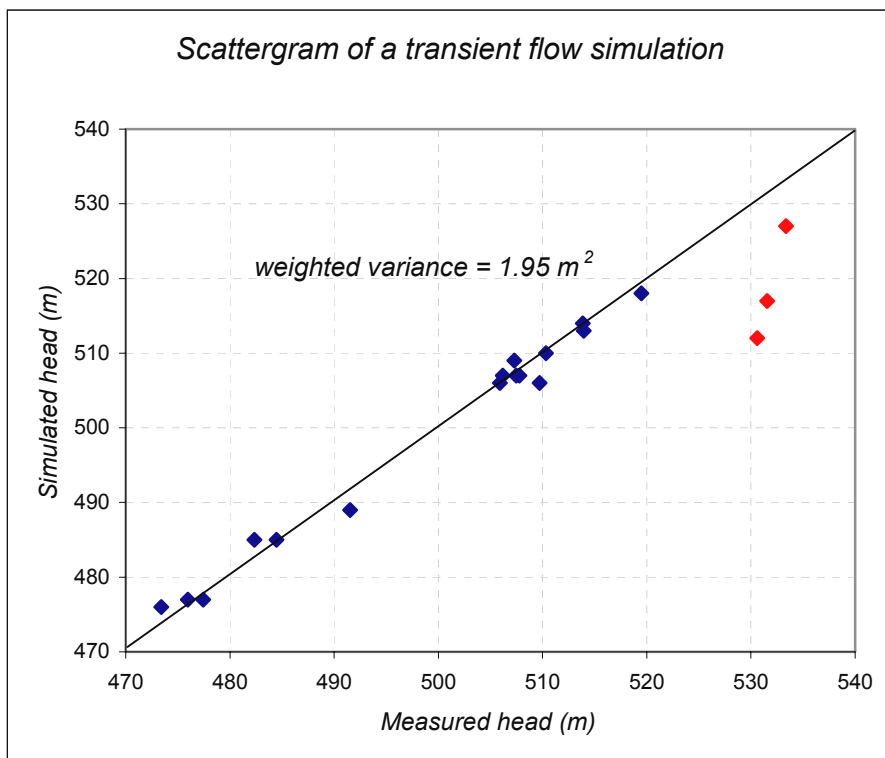
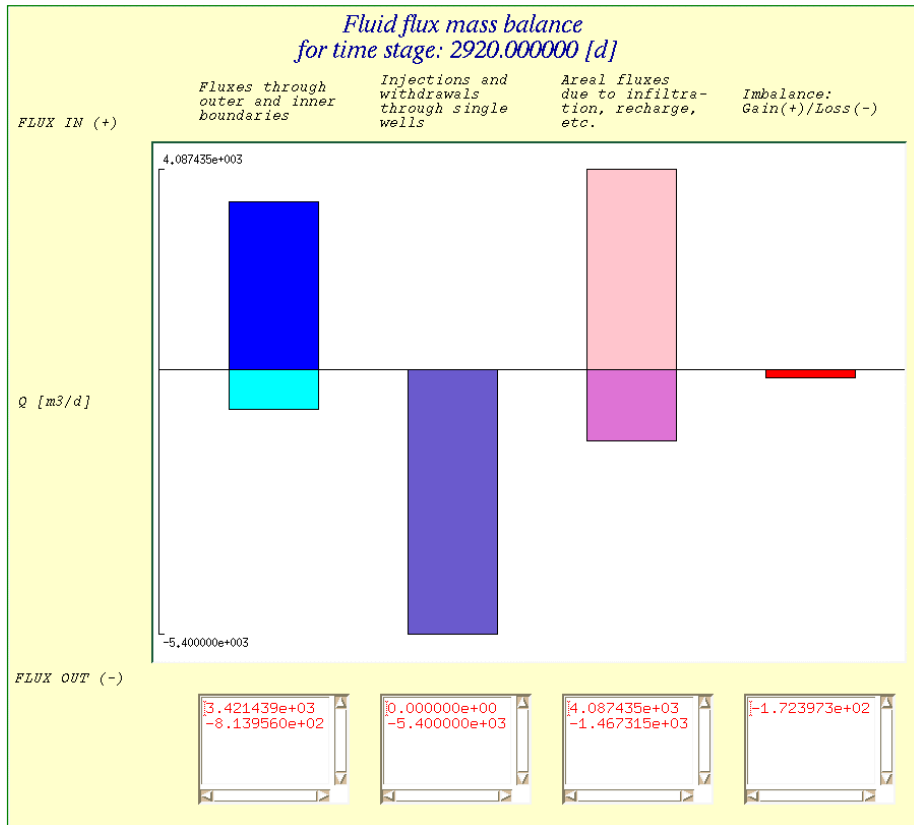


Fig. 6.7: The water balance and the scatter plot of the calibrated 8 years transient model.

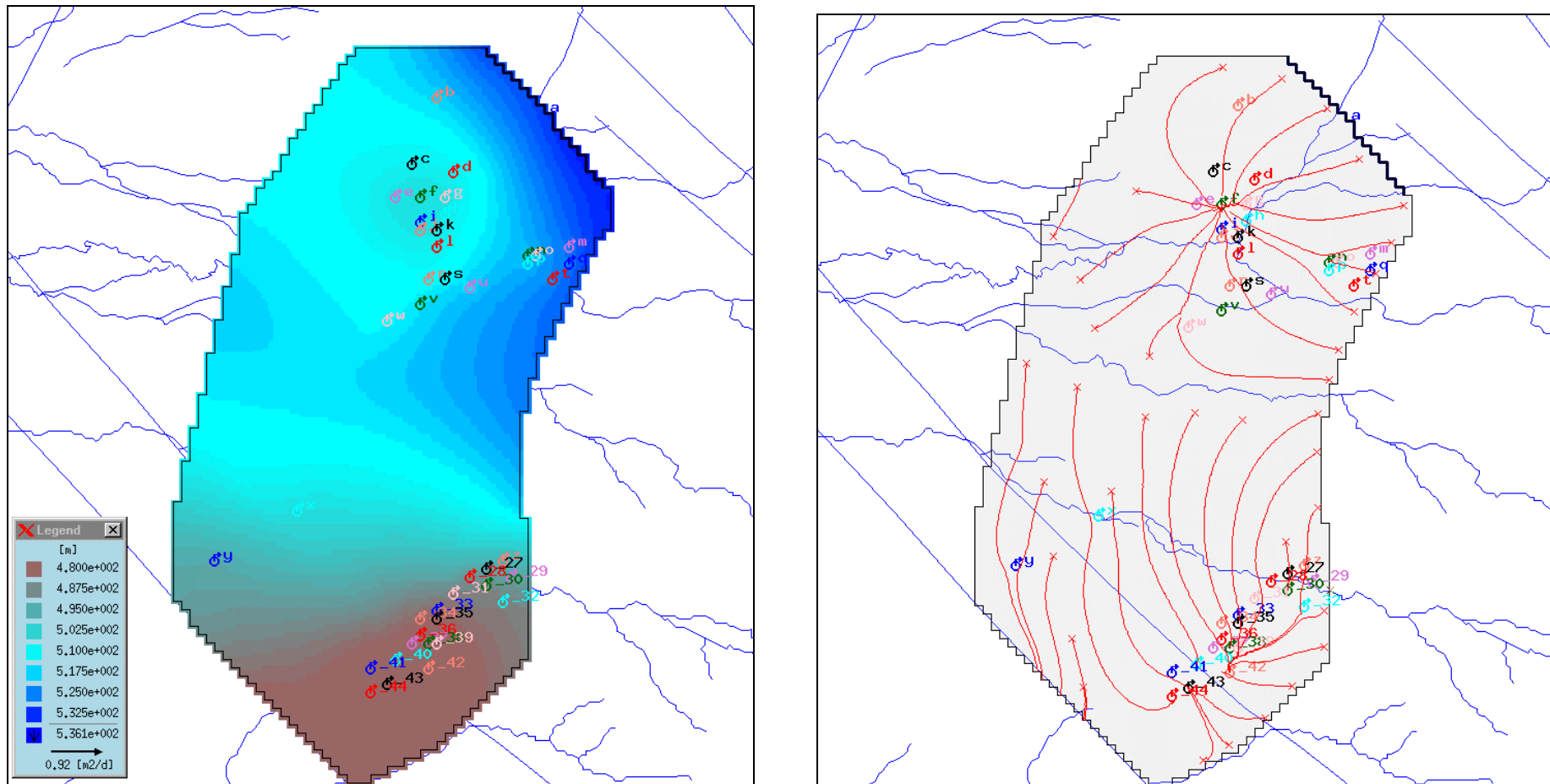


Fig. 6.8: Simulated transient groundwater flow in 1999.

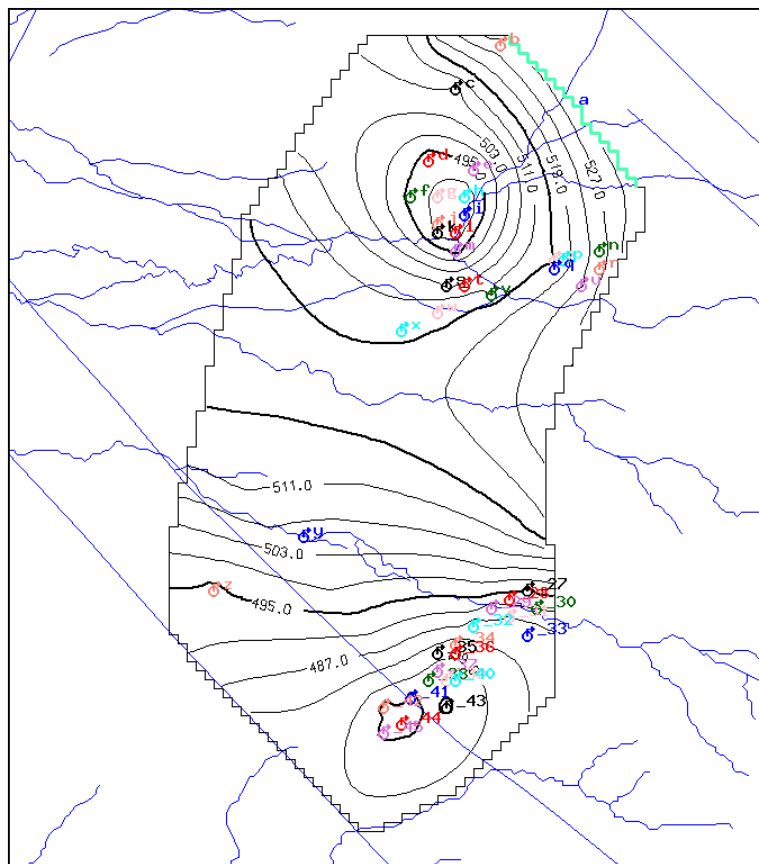
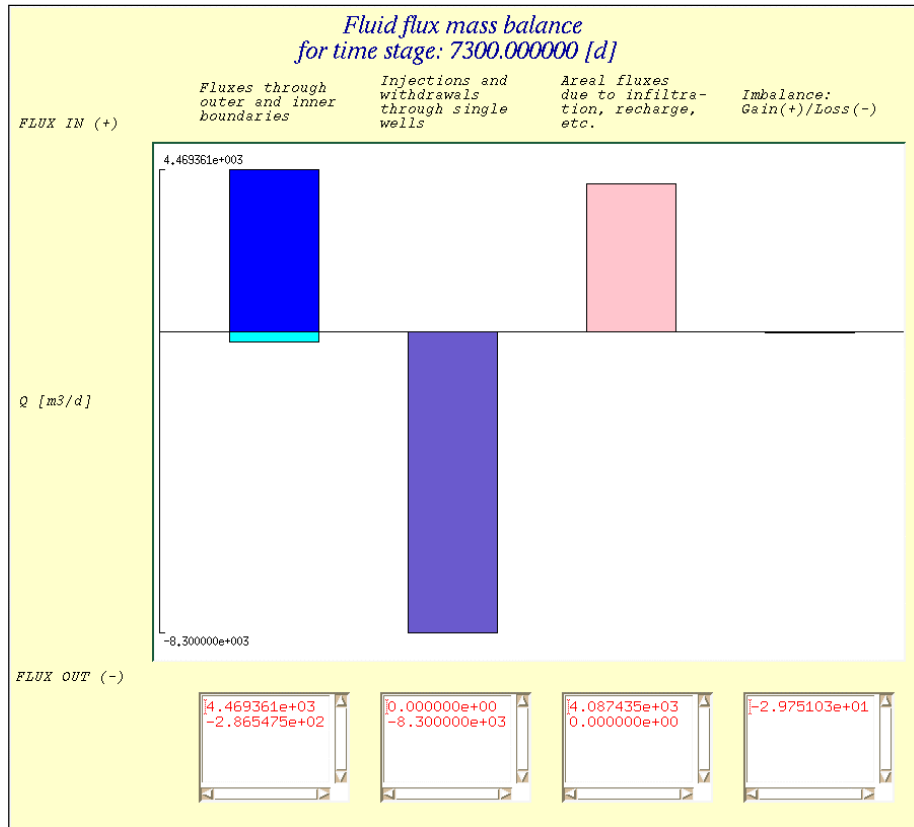


Fig. 6.9: pumping additional 3000 m³/d from 10 existing Azaza wells cause 19m drop (level 496m) in the middle.

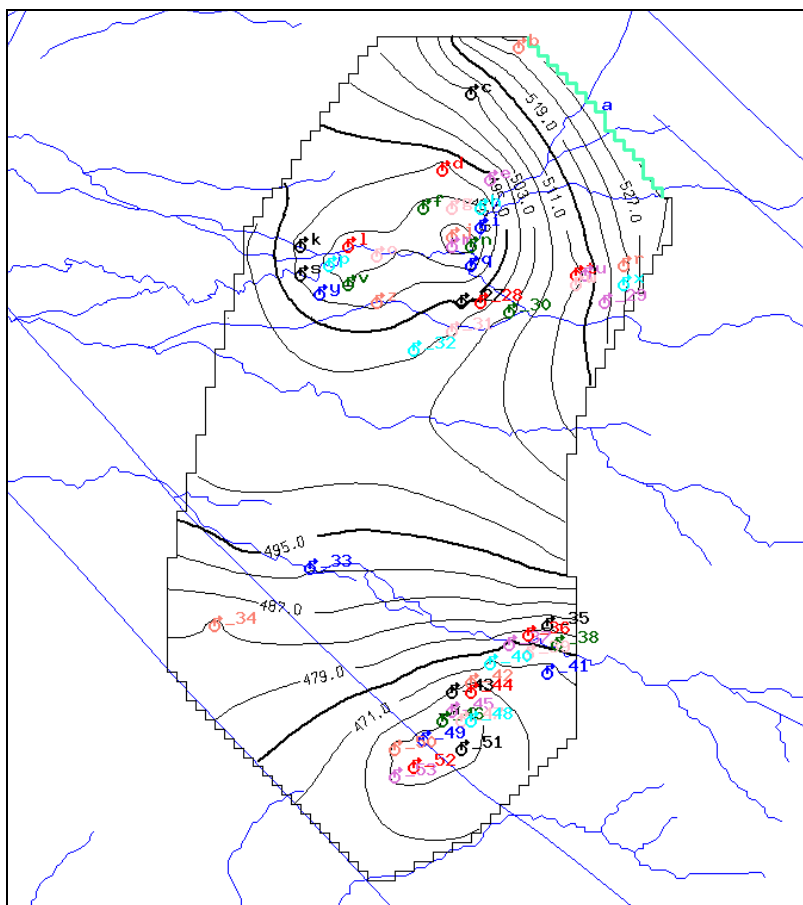
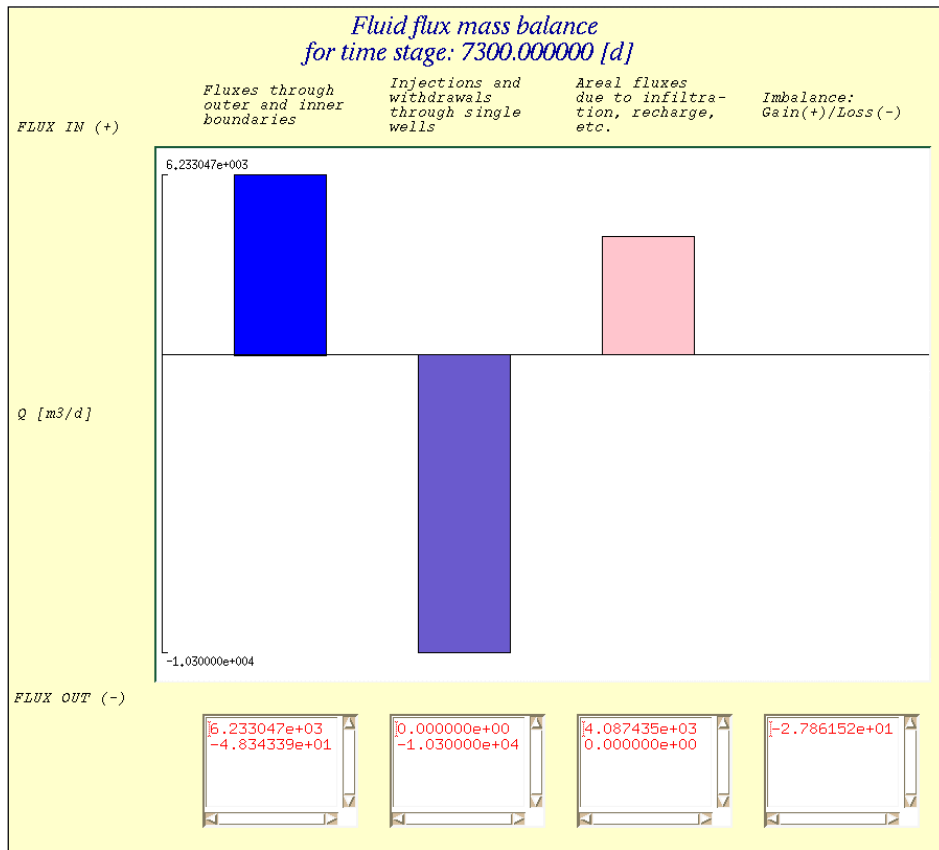


Fig 6.10: simulation results after 20 years with additional development of 5000 m³/d.

6.7. Sensitivity analysis

Several runs are performed to allow for the sensitivity (interval) analysis of calibrated model parameters that are not supported by any measurements. The tested parameters included the vertical leakage and the storativity. Within the prescribed model accuracy, a possible range of the vertical leakage is found between 3385 and 4730 m³/d. The range of storativity lied between 0.001 and 0.004. The above ranges are estimated allowing for a root mean square error of up to ± 6.30 and a water budget error of up to 10%.

6.8. Conclusion

The numerical modeling of the groundwater flow allowed for the calibration of the main hydrogeologic parameters, and hence led to improved representation of the head distribution and the subsequent flow pattern. In the scope of groundwater management, the numerical simulation of the west Gedaref main aquifer helped to assess possible consequences of different development scenarios.

The results from the various scenario runs demonstrate that at the present extraction rate, the inflows balances the out flows in the model area. In the next 20 years the decline in water levels is estimated at 13 m maximum under similar leakage rate and boundary conditions. Raising the production rate from the established well fields by doubling the abstraction (6000 m³/d) from Azaza wellfield, the levels will decline to 19.0 m in the center of the wellfiled. However, the aquifer remains under confined conditions (no dewatering occurs), within the safe reserves.

Expanding Azaza wellfiled to the west is found to be the most feasible new development in the main modeled aquifer within the assumed safe reserves (above 480m NN). An additional pumpage of 2000 m³/d is the maximum safe yield for the new western development.

At the eastern part of the model area, new developments would probably lead to excessive decline in water levels both in the Azaza and Abu-Naga areas below the aquifer top (480 to 460 m NN). However, it is expected that considerable amounts could be delivered from the upper and lower layers.

A total of 12000 m³/d is considered as a safe yield from existing and recommended development in the middle aquifer horizon. An additional amount of 6000 m³/d is expected from upper and lower horizons as indicated by the seasonal rise in water levels and by well yield analysis.

An informal sensitivity exercise has confirmed the reliability of the model estimates within the specified criteria. However, the calibration criteria was based on scarce data and hydrological judgment.

7. Discussion of the results

Some discussion was partly combined with the results in several chapters according to the subject considered. Here the results of the modeling process will be discussed

Modeling of the Gedaref hydrogeologic system lead to the identification of the flow parameters, as well as the prediction of future development consequences. In the Gedaref case, identified parameters included the hydraulic properties T and S, the boundary fluxes, the areal recharge or vertical leakage entering or leaving the aquifer through boundary aquitards.

The flow model was calibrated against three targets. These targets include steady state head data, steady state water budget, and transient head data.

To assess the calibration, and the underlying assumptions associated with the conceptual models, two principal points has to be emphasized, namely:

- 1- A model cannot be more accurate than the data used to build it. Thus, the first step is to analyze the certainty range and the available data limitations. This step will enable the evaluation of the inverse modeling effort.
- 2- Without adopting specific objective criteria one (the modeler or the decision maker) is never satisfied with whatever modeling effort.

Based on the above points, the problem was not the "flow" portion of the model, but rather, advances in the conceptualization, calibration, error diagnosis and uncertainty evaluation processes.

The main evaluation criteria were the scatterplot, the RMS error and the water budget. The scatterplot was used to eliminate the bias of the simulated head. The targeted RMS error criterion was evaluated using the range of error expected in the measured data. The theoretical head variance provided a tolerable error range of $\pm 6.30 m$. This value is largely affected by the well design. Ignoring head values at boreholes tapping upper aquifer layer, the error range should lie between ± 0.80 to $\pm 3.25 m$. Considering only the RMS error criteria several calibrations were possible. A water budget target within $\pm 10\%$ coefficient of variation was helpful in identifying the best calibration among a set of possible calibration. Compared to some regional models (e.g. CHRISTENSEN et al. 1998, YEH and MOCK, 1995, ANDERSON and WOSSNER, 1992, AGNESE, et al. 1999, ABRAHAM and SPRINGER, 1992) the above considered measures of fit is typical.

The flow in the area is controlled by a multi-layer aquifer system. The aquifer system (a sequence of aquifers with intervening confining layers) is simulated with a quasi-three dimensional model whereby a leakage term is used to simulate the vertical exchange between the layers. The effort to model regional flow in a heterogeneous porous fractured sandstone has highlighted the need to consider all possible models of heterogeneity applied both for porous and fracture simulation. Several assumptions are considered in this study to describe the real horizontal transmissivity distribution based on the available data in the main aquifer layer. Both deterministic discrete sub-units as well as stochastic continuous T fields are tested.

Zoned heterogeneity (or homogenous sub-units) was applied for the Gedaref case, as it is suitable to the limited data. However, it is found that pure deterministic description of the aquifer heterogeneity does not seem efficient in the case of poorly configured data samples. The study has shown the important role of geostatistic in the estimation/interpolation of different inputs of the flow model. Besides, geostatistical parameterization has guided the zonation method, and provided the estimation variance as a measure of the parameter prior estimates.

To describe continuous heterogeneous transmissivity field in the Gedaref aquifer, two variogram models were considered. The first model is a nested variogram model, which assumes that the geologic media is composed of homogeneous zones at different scales. The second model is based on Neuman's universal scale model assuming fractal behavior. Although both the fractal or the nested hierarchical model are physically justifiable for describing regional transmissivity structures, the choice of the appropriate model was judged by the end results of the estimation method (Kriging or conditional simulation). Finally, the inverse solution of the flow model allowed for additional conditioning of the flow parameters to the targeted state variables, the head and the water budget.

From the inverse modeling results, it is found that the model of homogenous sub-units gives better results in terms of the specified criteria. This demonstrates that the small-scale heterogeneity has no significant effect on regional flow pattern. However, it must be emphasized that, even with the data and software restrictions, the continuous models of heterogeneity have produced comparable results to the zonation counterpart. Full use of the continuous heterogeneity models is expected to produce better results, and greatly reduce the

time and the effort required by the deterministic zonal adjustment. It would also enable the certainty evaluation of the identified parameter.

The aquifer reserves in the study area are very limited. However, the annual replenishment is considerable. An estimated amount of about $6.5 \times 10^3 \text{ m}^3 / \text{d}$ ($2.4 \times 10^6 \text{ m}^3 / \text{y}$) reaches the middle horizon under steady conditions from direct vertical seepage beside the indirect recharge through the boundary basalt. This amount represents only 12% of the potential recharge ($19.8 \times 10^6 \text{ m}^3 / \text{y}$) estimated by SKAP (1992) through exposed basalt and sandstone. This result suggest that considerable amount is probably received by other aquifer parts/horizons.

Hydraulic parameters identified by the calibrated flow model include an average T range between $2.0 - 20.0 \times 10^{-4} \text{ m}^2 / \text{s}$ and an average storage coefficient of 0.002. The yield of the transient model reached more than $10 \times 10^3 \text{ m}^3 / \text{d}$ under confined conditions causing 21 m lowering of water levels in the center of the Azaza wellfield. This result were obtained ignoring possible upward leakage from the lower sandstone, and assuming that the boundary conditions remain constant during the next 20 years. To avoid excessive lowering of the piezometric level, planned variation in the amount and location of the pumping over time is needed.

Compared to previous studies in other parts of the Gedaref basin, the aquifer properties in the model area lie within the range reported for T and S by SULIEMAN (1986), SALAMA (1976), RWC (1979), VAN ENK (1984) and EL SEED (1987). Compared to the Nubian sandstone aquifers in other parts of the Sudan, the west Gedaref aquifer showed low transmissive and storage properties as well as low yield. In a study by IFAD (1987), the lowest values encountered in the Nubian aquifer in Khartoum and Gezira areas for T are between 100-1000 m^2 / d , and the specific capacity lies between 450-1100 $\text{m}^3 / \text{d} / \text{m}$. Although the yield estimated by the model apply only to the middle sandstone layer (40 m thickness), the yield of the whole aquifer system will not exceed the double of the model yield.

To the end of this discussion, some shortcomings are discussed for future studies in the area. In the present study the results are governed by the adopted concepts and methods of analysis. The 2D-model representation of the west Gedaref hydrogeology was a necessary simplification of reality. However, dealing with a heterogeneous porous fractured sandstone,

strong spatial anisotropy is expected to dominate. Such complicated aquifer system would require advanced modeling based on 3D information and mapping, which is only possible with further investigations. Interaction between aquifer layers needs proper account of the spatial variability of the vertical hydraulic conductivity which, require proper pumping tests. Monitoring of seasonal variation in groundwater levels should pay attention to nearby pumping, and should continue throughout the year to allow adequate recharge estimation.

8. General conclusion

The focus of the present study was to determine the nature of the groundwater occurrence in the Nubian sandstone aquifers west of the Gedaref city to enable proper planning and management of available resources. Towards this purpose, the study objectives was set to carryout the difficult task of characterizing the hydrogeological system based on very limited data, a common problem connected to the costly hydrogeological data collection in Sudan. In this respect, the process of analyzing and predicting groundwater flow in the area was based on a series of decisions of a conceptual and qualitative nature. For the quantification of the aquifer properties and the subsequent prediction of its behavior, the study relied mainly on the use of models as the most feasible approach. Both geostatistical models and deterministic flow models are used to describe and simulate the real flow system in the Gedaref sandstone aquifer.

Although simple in principle, unlike other methods, modeling of hydrogeological systems requires critical and time-consuming processes, fitting variogram models and calibration of parameters. Parameterization of aquifer properties with geostatistical methods proved to be more efficient in terms of the time they require and the accuracy of results. Zonal parameterization has lead to more accurate results compared to geostatistics in case of limited data. However, it can be concluded that for regional flow simulation aimed at aquifer management conditional stochastic simulation would do a better job, as it provides a complete assessment of the reliability of its results.

The study of the west Gedaref sandstone basin showed the existence of a heterogeneous aquifer system modified with complex tectonic structures. The thickness of the Nubian formation in west Gedaref area ranges from less than 100 to 273 m. The sandstone thickness represents a about 30 to 70% of the formation thickness, with its maximum at the Azaza-Abu Naga area. Correlating the subsurface geology and the hydrogeological data in the west Gedaref basin, it was shown that local and sub-regional flow systems dominate the area. Three hydraulically connected aquifer subsystems are identified. The most productive one covers the area of the Azaza and Abu-Naga wellfields (200 km²), which was the subject of detailed analysis. The Azaza-Abu Naga aquifer (50-120 m thick) is multi-layer aquifer system. It consists of three sandstone layers separated by mudstone or clayey aquitards. The aquifer

system is mainly developed at its middle horizon, which is characterized by a transmissivity range of $2.0 - 20.0 \times 10^{-4} m^2/s$, a moderate yield ($16.25 m^3/h$ on average) and good water quality ($TDS_{avg} = 660 mg/l$). The lowest layer possesses comparable transmissive properties as the middle one, but with lower quality water (up to $TDS \cong 1300 mg/l$). The upper most layer is the less productive aquifer horizon due to its limited storage capacity. However it receives considerable recharge from rain water during the rainy season, and therefore is a major source of recharge to the middle aquifer through leakage at fractures zones and where thin or relatively permeable confining bed. The aquifer reserves in the study area are very limited. However, annual replenishment from vertical seepage (around $4 \times 10^3 m^3/d$) beside the boundary flux from the basalt aquifer make up the major resources of the Azaza-Abu Naga aquifer system.

Model estimates helped to identify the flow parameters, and the development scenarios that may be pursued in the Azaza Abu Naga area. Furthermore, model uncertainty assessment suggest building a groundwater monitoring system to fill the data gaps in some promising areas, and to confirm the modeling results in those areas. The transient flow model lead to a maximum safe yield of $10 \times 10^3 m^3/d$ (around 18% of the estimated potential recharge) from the Azaza Abu Naga middle aquifer. This amount is partly drawn from vertical leakage ($4.1 \times 10^3 m^3$, about 1.3% of the rainfall in the model area), and partly from boundary inflows. Additional development should be carefully planned to avoid exhausting the limited aquifer reserves.

As a first comprehensive study in the area, it is expected to guide planning and management of future project. By providing a detailed account of the hydrogeologic situation, the study has stimulated several investigations in the area. It is recommended that future investigations should concentrate on collecting more data on the area of Al-Laya wadi system south of the Azaza. Geophysical investigations is needed to explore tectonic and structural controls affecting the groundwater flow. Drilling of observation wells in separate aquifer horizons is very important for accurate characterization. Pumping tests should be planned in the area of the wellfields with consideration of filter position and nearby transient effects. Abstraction rate should be measured separately for each well.

With regard to the management problem, the results of the study suggest the use of groundwater storage conjunctively with surface water from local and imported sources. Previous studies have revealed the considerable potential for recharge from seasonal surface water resources. Therefore, Future studies should concentrate on methods to enhance the recharge from surface water sources based on proper hydrological and structural information.

9. References

- ADLER, P. M., 1991,
Fractal porous media, in BEAR and CORAPCIOGLU, Transport processes in porous media, p. 723-743. Kluwer Academic Publishers, the Netherlands.
- AHMED, S. and G. De MARSILY, 1988,
Co-kriging estimates of transmissivities using jointly water level data. In ARMSTRONG, *Quantitative geology and geostatistics*, volume 2, p. 615-628. Kluwer Academic Publishers, Dordrecht.
- AHMED, SHAKEEL, and G. DE MARSILY, September 1987,
Comparison of Geostatistical Methods for estimating transmissivity using data on transmissivity and specific capacity; *Water Resour. Res.*, vol.23, no. 9, p. 1717-1737.
- ALMOND et al., 1984,
Alkaline Basalt volcanism in north eastern Sudan, a comparison of Bayoda and Gedaref areas, *Jour. of African earth Sci.*, Vol. 2, No. 33, p. 233-245.
- ANDERSON, MARY, 1997,
Characterization of geological heterogeneity. In Subsurface flow and transport by DAGAN and NEUMAN, *International hydrology series*, UNESCO. Cambridge university press. p. 23-43.
- ANDERSON, M.P., 1991,
Comment on "Universal scaling hydraulic conductivities and dispersivities in geologic media" by S.P. NEUMAN, *Water resources research*, 27(6), p. 1381-1382.
- ANDERSON, M. P. and WILLIAM W. WOESSNER, 1992,
Applied groundwater modeling, Simulation of flow and advective transport. Academic Press Inc.
- APPELO, C. A. J. and D. POSTMA, 1994,
Geochemistry, groundwater and pollution; A. A. Balkema/ Rotterdam/ Brookfield.
- BEAR, JACOB, 1972,
Dynamics of Fluids in Porous Media; (Environmental Science Series), Elsevier, New York. 764 p.
- BEAR, JACOB, 1979,
Hydraulics of groundwater. McGraw-Hill Inc., New York. 569 p.
- BEAR, JACOB and YAVUZ CORAPCIOGLU, 1991, Proceedings of the NATO Advanced Study Institute on: Transport Processes in Porous Media, 9-18 July, 1989. *Series.E: Applied Sciences – Vol. 202*.
- BUSSERT, ROBERT, 1998,
Die Entwicklung interakratonaler Becken im Nordsudan; Berliner Geowissenschaftliche Abhandlung, Reihe A: Geologie und Paläontologie. FU. TU TFH. Berlin.

- CHIALVO, J., 1975,
Contribution a la geologic du confluent Atbara Setit; Unpublished thesis, University of Grenoble, France.
- CHILES, J.-P. and PIERRE DELFINER, 1999,
Geostatistics, modelling Spatial Uncertainty. New York, Willy. 695 p.
- CHRISTENSEN, S. and RICHARD L. COOLEY, September 1999,
Evaluation of prediction intervals for expressing uncertainties in groundwater flow model predictions. *Water Resou. Res.* Vol. 35, No. 9, p. 2627-2639.
- CHRISTENSEN S., K. R. ASMUSSEN and K. MOLLER, 1998,
Prediction of regional ground water flow to streams. *Ground Water*, Vol. 36, No. 2, p.351-359.
- CHRISTENSEN, S. and RICHARD L. COOLEY, September 1996,
Simultaneous confidence intervals for steady-state leaky aquifer groundwater flow model. In KOVAR & HEIDE,: *Calibration and reliability in groundwater modeling*.
- CLIFTON, PETER M. and S. P., NEUMAN, 1982,
Effects of Kriging and inverse modeling on conditional simulation of the Avra valley aquifer in southern Arizona. *Water resources research*, 18(4), p. 1215-1234.
- CONNORTON, B.J., 1985,
Does the regional groundwater-flow equation model vertical flow?
J. Hydrol. 79: p. 279-299.
- CUSHMAN, J.H., 1991,
Dynamics of Fluids in Hierarchical Porous Media. Academic press Inc., Harcourt Brace Jovanovich publishers.
- DAFALLA, MOHAMMED E. Y., 1993,
Gravity survey in Gedaref-Azaza area, Eastern Sudan; Geological research authority of Sudan (GRAS).
- DAGAN, GEDEON, 1997,
Stochastic modeling of Flow and transport: the broad perspective; In subsurface flow and transport: a stochastic approach, *International Hydrology Series*.
- DAVIS, JOHN C., 1986,
Statistics and data analysis in Geology. John Willy, New York, 646 p.
- D'AGNESE, F. A., C. C. FAUNDT, M. C. HILL and A. K. TURNER, 1999,
Death valley regional groundwater model calibration using optimal parameter estimation methods and geoscientific information systems, *Advances in Water Resources* vol. 22, No. 8, p. 777-790.
- DE CESARE, L. and POSA, D., 1995,
A simulation technique of a non-Gaussian spatial process, *Computational statistics & data analysis* 20, p. 543-555.

- DELHOMME, J. P., April 1979,
Spatial Variability and uncertainty in groundwater flow parameters: A geostatistical Approach; *Water Resou. Res.* Vol. 15, no. 2, p. 269-280.
- DE MARSILY, GHISLAIN, 1986,
Quantitative Hydrogeology - Groundwater Hydrology for Engineers. Academic Press, INC.
- DEUTSCH, CLAYTON V. and ANDRE G. JOURNAL, 1998,
GSLIB, Geostatistical Software Library and user's guide. Oxford university press, New York. 369 p.
- DIERSCH, HANS-JÖRG G., May 1998,
Finite element subsurface flow system (FEFLOW), Reference manual.
- DIERSCH, HANS-JÖRG G., May 1998,
Finite element subsurface flow system (FEFLOW), Getting started.
- DOHERTY, JOHN, 1994,
PEST, Model-independent parameter estimation. User's Manual.
- DOMENICO, P. A. and F. W. SCHWARTZ, 1997,
Physical and Chemical Hydrogeology, second edition. John Wiley & Sons, Inc. 506 p.
- ELSEED, ELNAZEER G., 1987,
Water resources evaluation of Gedaref basin (East central Sudan), Ph.D. thesis, University of Khartoum. 252 p.
- FETTER, C. W., 1994,
Applied hydrogeology. Third edition, Prentice Hall, Englewood Cliffs, NJ 07632.
- FRANSSEN, H-J. H., J. J. GOMEZ-HERNANDEZ, J. E. CAPILLA and A. SAHUQUILLO, 1999,
Joint simulation of transmissivity and storativity fields conditional to steady-state and transient hydraulic head data. *Advances in Water Resources* 23, p. 1-13
- FREEZE, R. A. and J. A. CHERRY, 1979,
Groundwater. Prentice Hall, Inc., Englewood Cliffs, N.J.
- GELHAR, LYNN W., August 1993,
Stochastic subsurface hydrology from theory to applications, *Water resources res.*, Vol. 22, No. 9, p. 135S-145S.
- GIBB, SIR ALEXANDER AND PARTNERS, 1987,
Groundwater assessment in Sudan.
- GIDDO, I. M., 1986,
Unpublished M.Sc. thesis, University of Khartoum, Sudan.
- GOMEZ, J. JAIME and STEVEN M. GORELICK, March 1989,
Effective groundwater model parameter values: Influence of spatial variability of hydraulic conductivity, Leakage and recharge. *Water Resou. Res.*, vol. 25, No. 3, p. 405-419.

- GOOVAERTS, PIERRE, 1997,
Geostatistics for Natural resources evaluation. Applied geostatistics series, Oxford university press, Inc. 481 p.
- GRAS, 1993,
Vertical electrical sounding in the Azaza area, Gedaref, unpublished report.
- HILL, MARY C., 1998,
Methods and guidelines for effective model calibration; *U.S. Geological Survey, Water-resources investigations report 98-4005.*
- HOFFMAN, JOE D., 1992,
Numerical Methods for Engineers and scientists. McGraw-Hill, New York.
- HÖLTING, BERNWARD, 1996,
Hydrogeologie: Einführung in die allgemeine und angewandte Hydrogeologie. 3. Auflage, Ferdinand Enke Verlag, Stuttgart. 396 p.
- HUSSEIN, M. T. and E. G. ADAM, April 1995,
Water quality of the Gedaref basin, Sudan, *Hydrological Sciences*, 40, 2, p. 205-216.
- HUSSEIN, M. T., K. E. IBRAHIM and E. G. ADAM, 1994,
Comparison of hydrogeological and electrical properties of a consolidated sandstone aquifer, *Arab Gulf J. Scient. Res.*, 12(2), p. 211-229.
- HUSSEIN, T., A. G. MULA and H. SCHNEIDER, 1989,
Geological and seismic investigation with regard to shallow groundwater exploration in Eastern Sudan republic, *Journal of African Earth Sciences*, vol. 8, No. 1, p. 75-78.
- IBRAHIM, K. E., M. T. HUSSEIN and I. M. GIDDO, May 1992,
Application of combined geophysical and hydrogeological techniques to groundwater exploration: a case study of Showak-Wad Elhelew area, Eastern Sudan, *Journal of African Earth Sciences*, Vol. 15, No. 1, p. 1-10.
- IBRAHIM, K. E., M. T. HUSSEIN and N. G. ADAM, 1994,
Application of combined geophysical and hydrogeological techniques to groundwater, *JKAU: Earth Sci.*, Vol. 7, p. 27-39.
- IFAD, 1987,
Development and utilization of the Nubian sandstone aquifer in the Sudan.
- JOURNAL, A. G. and HUIJBREGTS, CH. J., 1978,
Mining Geostatistics. Centre de Geostatistique Fontainebleau, France. Academic press.
- KECKLER, DOUG, 1995,
Surfer for Windows, User Guide. Contouring and 3D Surface Mapping. Golden Software, Inc.
- KEIDSER, ALLAN and DAN ROSBJERG, September 1991,
A comparison of four inverse Approaches to groundwater flow and transport parameter identification; *Water Resour. Res.*, Vol. 27, No. 9, p. 2219-2232.

- KHALAFALLA, O. M. and M. A. OSMAN, December 1986,
Gedaref Water supply intake siltation problem. International conference on Water resources needs and planning in drought prone areas, Khartoum. p. 315-322.
- KINZELBACH, W., S. VASSOLO and G.-M. LI, 1996,
Determination of capture zones of wells by Monte Carlo simulation; in KOVAR and DER HEIJDE, *Calibration and Reliability in groundwater modeling*, IAHS Publication No. 237.
- KRUSEMAN, G. P. and N. A. DE RIDDER, 1991,
Analysis and Evaluation of Pumping Test Data, ILRI publication 47. International Inst. for land reclamation and improvement, Wageningen.
- LONG, JANE C. S., et al, 1997,
Component characterization: an approach to fracture hydrogeology. In DAGAN and NEUMAN, *Subsurface flow and transport*, p. 179-195. *International hydrology series*, UNESCO. Cambridge university press.
- MCDONALD, M. G. and ARLEN W. HARBAUGH, 1988,
A modular three-dimensional finite-difference groundwater flow model, *USGS survey Open-file Report* 83-875.
- MEUNIER, M., G. COLLO and P. BOUISSET, May 1985,
Onshore Soudan, Block G, Geological field survey, Total Soudan.
- MIZELL, S A., A. L. GUTJAHR, and L. W. GELHAR, 1982,
Stochastic analysis of spatial variability in two-dimensional steady groundwater flow assuming stationary and non-stationary heads.
Water Resour. Res., 18(4), p. 1053-1067.
- MULA, A. G. and OMER M. K., 1983,
A geophysical survey in Gedaref area. Unpublished Report, University of Khartoum.
- MYERS, JEFFREY C., 1997,
Geostatistical error management; Quantifying uncertainty for environmental sampling and mapping.
- MYERS, D. E., 1989,
To be or not to be...Stationarity? That is the question, *Mathematical Geology*, Vol. 21, No. 3, p. 347-362..
- NEUMAN, S.P., 1997,
Stochastic Approach to subsurface flow and transport: a view to the future. In DAGAN and NEUMAN, *Subsurface flow and transport*, p. 231-241. *International hydrology series*, UNESCO. Cambridge university press.
- NEUMAN, S. P., 1994,
Generalized scaling of permeabilities: validation and effect of support scale. *Geophysical Research letter*, 21(5), p. 349-352.

- NEUMAN, S. P., August 1990,
Universal scaling of Hydraulic conductivities and dispersivities in Geologic media, *Water resources research*, Vol. 26, No. 8, p. 1749-1758.
- NEUMAN, S.P., 1991,
Reply to comment by M. P. Anderson. *Water resources research*, 27(6), p. 1749-1758.
- NEUMAN, SHALOM P., 1984,
Role of Geostatistics in subsurface hydrology. In VERLY et al, Geostatistics for Natural resources characterization, part 2. *NATO ASI series*. Series C; 122. p. 787-816. Reidel, Dordrecht.
- OTHMAN, M. A., 1996,
Flood mitigation of Abu-Farga Khor, Gedaref area, first part. Unpublished report, university of Khartoum.
- PANNATIER, YVAN, 1998,
VARIOWIN, software for spatial data analysis. Springer Verlag.
- ROEHRICH, THOMAS, 1996,
Hydro Tec for Windows, version 4.
- ROBERTSON RESEARCH, 1988;
Geological map of Sudan, scale 1:1000 000.
- RUSHTON, K. R., 1991,
Groundwater modeling – A critical review, in BEAR and CORAPCIOGLU: Transport processes in porous media, *NATO ASI series*.
- RUSHTON, K. R., 1979,
Seepage and groundwater flow.
- RUXTON, B. P., 1956,
An account of the geology of the Sennar and Gedaref area, University of Khartoum.
- RWC / TNO, 1979,
Groundwater Investigation, a cooperation project implemented by the Rural Water Corporation, Khartoum and the TNO, Delft.
- SAGHAYRON, EL-ZEIN et al., 1996,
Gedaref Water, part one: Assessment of the current situation and future demands. Unpublished report, Ministry of Engineering affairs, The Gedaref state.
- SALEEM, HASHIM A., December 1998,
The current situation of the rural water supply in Gedaref, unpublished paper presented for the workshop on the water supply problems in the Gedaref.
- SCHAFMEISTER, M.-T., 1999,
Geostatistik für die hydrogeologische Praxis. Springer Verlag, Berlin, Heidelberg, New York, 172 p.

- SCHAFMEISTER, M. and G. De MARSILY, 1993,
Regionalization of some hydrogeological processes and parameters by means of geostatistical methods – current status and future requirements. In DIMITRAKOPOULOS, *Quantitative Geology and geostatistics*, vol. 6., p. 383-392.
- SINGHAL, B. B. S. and R. P. GUPTA, 1999,
Applied hydrogeology of fractured rocks. Kluwer Academic Publishers, Dordrecht / Boston / London. 400 p.
- SKAP, 1992,
South Kassala Agricultural development project. Landuse survey report, volume II. Ministry of Agriculture, natural and animal resources, Sudan.
- SUDANESE GENERAL PETROLIUM, 1984,
Gravity map of the Gedaref Basin.
- SULIEMAN, YOUSIF, May 1968,
The Hydrogeology of part of eastern Sudan (Gedaref District), Geological survey department, Bulletin No. 16.
- SUN, NE-ZHENG, 1994,
Inverse problems in groundwater modeling. Theory and applications of transport in porous media, volume 6. Kluwer academic publishers.
- TOTAL SOUDAN, 1985;
Geological field survey; Gravity study, Block G.
- TWISS, ROBERT J. and ELDRIDGE M. MOORES, 1992,
Structural Geology. W. H. Freeman and company, New York. 532 p.
- VAN ENK, D. C., 1979,
Water resources of the Gedaref area, A summary of the results of investigations in 1977-1978, Institute of applied geoscience, report no. IS 84-O4.
- WHEATCRAFT, W. S. , et al., 1991,
Fluid flow and solute transport in fractal heterogeneous porous Media,
In CUSHMAN, J., Dynamics of fluids in hierarchical porous media.
- WANG, HERBERT F. and M. P. ANDERSON, 1995,
Introduction to groundwater modeling, finite difference and finite element methods. Academic Press, San Diego, California. 237 p.
- WHITEMAN, A. J., 1971,
The geology of the Sudan Republic, Clarendon press Oxford.
- WIPKI, MARIO, 1995,
Eigenschaften, Verbreitung und Entstehung von Kaolinlagerstätten im Nordsudan,
Wissenschaftliche Schriftenreihe Geologie und Bergbau, Band 2.

YEH, WILLIAM W-G. February 1986,
Review of parameter identification procedures in groundwater hydrology: The inverse problem. *Water Resou. Res.* Vol. 22, No. 2, p. 95-108.

YEH, T.-C. JIM and PETER A. MOCK, May-June 1995
A structured Approach for calibrating steady-state groundwater flow models. *Groundwater*, Vol. 34, No. 3, p.444-450.

No.	Site Name	Long.	Lat.	X	Y	Z	Depth	SWL	DWL	Yield	Basalt	Remarks
1	Wad Shaboot	35.45	14.23	764579.56	1574164.25		138.70	88.40				
2	Wad Kabo	35.50	14.25	769265.31	1576150.00	597.27	135.90	107.31	114.04	175.2	67.0	D36L3A710113
3	Karadis-old2	35.33	14.23	750939.44	1573860.50	595.33	137.20				0.0	D36L2D630625
4	karadis-old1	35.33	14.23	750935.06	1573672.88	595.33	178.31	79.00	84.60	57.6	0.0	D36L2B731204
5	Karadis-new_WB	35.33	14.22	750912.13	1572977.75	594.67	138.00	47.80			0.0	D36L2B880303
6	Wad Alnayir	35.54	14.21	774047.56	1572420.63	602.00	259.70	105.00			0.0	
7	Sufi Albashir	35.89	14.19	811512.50	1570764.75	520.00	79.60				0.0	
8	Umm Khanger-D1	35.28	14.18	745737.50	1568443.88	575.83	143.90	69.18	80.31	129.6	0.0	D36L2B690328
9	Umm Khanger-D2	35.28	14.18	745483.56	1568349.38	575.22					0.0	D36L2B610420
10	Dar Alzeein	35.62	14.17	782531.38	1567624.50	582.73	263.70	91.50			141.7	
11	Umm Shoraba	35.17	14.17	733694.63	1566971.63	544.52	199.40	64.98			0.0	
12	Rawashda	35.56	14.16	776569.06	1566820.50	597.33	240.80	84.52			0.0	
13	Hagokat	35.41	14.16	760427.81	1566402.00	636.67	253.90	102.11			128.0	D36L2B680224
14	Aza-Madrassa-J	35.31	14.15	748945.88	1565548.38	576.32	190.50	67.37	74.53	163.2	0.0	D36L2B880229
15	Aza-Madrassa(1)	35.31	14.15	748777.13	1565346.88	577.50	184.40	36.58			0.0	D36L3A701101
16	umm-Guid	35.42	14.13	761237.19	1563642.88	640.00	211.50	92.96			93.0	D36L2B710121
17	Aza Airport	35.30	14.13	748358.31	1563328.88	577.69	193.85	58.95	67.37	127.2	0.0	D36L1B700131
18	Aza(DW2)	35.30	14.13	748336.38	1562898.75	578.57					0.0	
19	Aza(DW1)	35.30	14.13	748273.13	1562842.75	578.57					0.0	
20	Aza1	35.31	14.12	749043.69	1562357.75	579.17	194.40	63.48	88.01	545.3	0.0	D36L2B920101
21	Aza5	35.29	14.12	746887.56	1561930.50	572.50	72.50				?	
22	Aza6	35.30	14.12	748399.13	1561654.13	575.83	158.50	43.20	75.64	628.3	?	D36L2B920413
23	Umm Sinebra	35.35	14.11	753130.50	1561131.88	590.00	285.00	82.00			155.4	D36L2B700426
24	Kilo6	35.17	14.11	734436.94	1560407.63	528.72	156.36	51.99			0.0	D36L2B720211
25	Kilo6	35.17	14.10	734413.31	1560054.00	528.48	186.00				0.0	D36L2B690511
26	Aza4	35.29	14.10	746821.63	1559726.13	566.00	173.70	48.28	68.52	628.3	?	D36L2B920310
27	Wad Bazil	35.61	14.09	781332.31	1559400.00	584.50	199.10	93.00				
28	Idd EITin	35.38	14.09	757412.81	1559022.25	615.00	340.16				233.0	D36L2B680520
29	Aza3	35.28	14.09	746483.88	1559021.13	563.00	176.80	57.40	93.52	392.6	?	D36L2B920227
30	Umm Shagara	35.48	14.09	767261.38	1558848.25	637.69	131.1 / 260	20.00			131.0	
31	Alagool	35.52	14.09	772455.06	1558719.00	616.36	190.50	114.20	130.05	216.0	57.9	
32	Hilat Hassan	35.55	14.08	775400.88	1558320.25	600.00	196.60	53.40			51.8	

No.	Site Name	Long.	Lat.	X	Y	Z	Depth	SWL	DWL	Yield	Basalt	Remarks
33	Rufaa	35.44	14.08	762885.75	1558033.25	636.67	65.40	94.20				
34	Aza2	35.28	14.08	746051.88	1557951.00	557.50	191.60	46.98	56.52	628.3	0.0	D36L2B920201
35	Aza7	35.29	14.08	747241.81	1557488.75	560.00	188.40	49.43	61.79	554.4	0.0	
36	UmmGulja	35.28	14.07	746344.19	1556951.00	557.78	152.40	48.90			0.0	D36L2B901209
37	Aza8	35.29	14.07	747068.19	1556906.00	557.14	171.00	48.89	71.73	471.4	0.0	D36L2B920514
38	Al Hissanat	35.48	14.07	767432.88	1556789.88	637.78	167.10	25.80			167.1	
39	Umm Gulga	35.27	14.07	745493.44	1556786.00	553.00		46.10	54.80		0.0	D36L2B570625
40	Aza9	35.29	14.07	746982.50	1556382.75	556.67	175.30	47.08	65.00	538.6	0.0	D36L2B920523
41	Aza13	35.28	14.07	746461.88	1556267.00	555.00	161.50	44.90	65.81	538.6	0.0	D36L2B920706
42	Aza12	35.28	14.07	746374.81	1555998.25	554.50	167.60	46.28	67.97	628.3	0.0	D36L2B920627
43	Aza10	35.29	14.07	746743.63	1555943.25	553.91	186.20	45.25	57.01	377.0	0.0	D36L2B920610
44	shimeliyab	35.49	14.06	768677.06	1555480.75	629.00	140.00				140.0	
45	J.Twawa	35.35	14.06	753624.25	1555429.63	657.00	216 / 189					
46	Twawa-Uni	35.32	14.06	750822.56	1555374.50	570.00	146.31	32.70	69.58	654.5	50.3	D36L2B701112
47	Aza11	35.29	14.06	746779.44	1555369.13	556.00	167.70	45.80	68.99	538.6	0.0	D36L2B920623
48	Tawawa	35.32	14.06	750699.38	1555328.00	570.00	216.00	38.70			62.8	
49	shimeliyab	35.48	14.06	767450.00	1555160.25	637.78	331.50	120.00			140.0	
50	Twawa-Shahid	35.32	14.06	750811.94	1554916.25	570.00	237.00	18.39				D36L2B930523
51	Twawa-MB	35.31	14.06	749446.69	1554905.88	563.08	147.20	21.80			0.0	
52	UmmHigliga	35.29	14.05	747701.31	1554750.50	557.69	44.20				0.0	
53	Aza15	35.29	14.05	746989.00	1554497.88	555.83	143.30	29.31	54.90	428.4	0.0	D36L2B920801
54	Aza14	35.28	14.05	746548.81	1554419.38	554.71	128.00	19.34	42.13	654.5	0.0	D36L2B920725
55	Twawa-A/Dug	35.32	14.05	750283.06	1554400.63	568.13	185.93	53.89				
56	Aza16	35.30	14.05	747796.19	1554253.38	558.75	134.10	29.96	57.07	628.3	0.0	D36L2B921018
57	Sharafa	35.51	14.05	770644.38	1553994.75	620.91	194.00	123.70			93.6	
58	Chinese	35.28	14.05	746378.31	1553732.25	554.21		22.93			0.0	
59	Mohamed Elsir	35.27	14.04	745233.19	1553275.38	551.58	102.13	38.35			0.0	
60	Gedaref-RWC	35.37	14.03	755714.81	1551749.25	594.44	204.00	43.50			?	D36L2B900113
61	Umm Shigera	35.48	14.02	767816.75	1551689.38	632.22	137 / 345.3	30.60			279.0	
62	Gedaref	35.35	14.01	753541.69	1550005.25	582.00						D36L2B680522
63	Umm Sonta	35.78	14.00	799818.25	1549677.13	554.55	105.20				0.0	
64	Donky Elnus	35.35	14.01	753377.81	1549521.00	580.00		37.14				
65	Wad Wadida	35.32	14.01	750220.44	1549419.13	570.00	205.13	54.00		101.3	163.0	D36L2B711229

No.	Site Name	Long.	Lat.	X	Y	Z	Depth	SWL	DWL	Yield	Basalt	Remarks
66	Abayo	35.39	14.00	757818.56	1548819.13	616.00	250.50	37.80			156.0	
67	Terria-old	35.25	13.99	742540.69	1547577.25	557.14	180.00	45.64	65.00	293.8	0.0	D36L2B881029
68	Gibesha	35.45	13.98	764200.63	1546946.25	650.00	154.00					
69	Naga1	35.30	13.98	748766.19	1546198.25	577.50	115.82	53.00			18.6	D36H5D680403
70	Terria-new	35.22	13.98	740112.19	1545989.38	555.00	150.00	56.80	72.54	345.6	0.0	D36L2B881029
71	Naga2	35.30	13.97	748207.31	1545894.50	575.00					43.3	
72	Naga3	35.30	13.97	747853.00	1545620.50	574.17	199.60	58.99	92.78	392.6	42.7	
73	Naga6	35.31	13.97	748985.88	1545511.88	577.27	243.00	82.42	110.61	392.6		
74	naga4	35.30	13.97	748404.88	1545352.38	577.08	228.00	60.49	83.06	327.1	50.6	
75	Naga7	35.29	13.97	747254.31	1545042.50	572.61		69.52				
76	Naga12	35.29	13.97	747254.88	1545024.38	572.61	153.92	69.52	99.08	523.7	27.4	D36H5D830329
77	Naga5	35.30	13.97	748849.81	1544962.75	577.69	227.10	60.07	85.86	523.7	56.4	D36H5D910303
78	Naga8	35.29	13.96	746838.06	1544682.13	572.38	135.00	67.36	88.16	448.8		
79	Ghreigana-WB	35.35	13.96	754329.88	1544678.50	597.00	169.20	65.70	87.81	523.7		D36H5D930401
80	Ghreigana-Jap.	35.37	13.96	755594.75	1544595.75	605.00	336.80	102.94	110.28	252.0	99.1	
81	Naga9B	35.28	13.96	746390.31	1544370.38	573.43	246.00	68.15	75.58	628.3	0.0	D36H5D910517
82	Naga13B	35.28	13.96	746721.56	1544281.38	572.73	153.31	69.58	76.26	523.7	24.4	D36H5D910227
83	Gaboob	35.74	13.95	796520.94	1543948.63	558.70	130.80	42.70				
84	Naga22	35.28	13.96	746377.25	1543850.75	573.85	153.31	74.34			24.4	D36H5D910524
85	Naga10	35.28	13.96	746119.81	1543784.13	573.33	196.60	67.92	75.55	523.7	25.6	
86	Naga23	35.28	13.96	746551.75	1543781.63	574.10	153.31	76.37			19.8	
87	Naga14	35.28	13.95	746764.00	1543629.88	571.94	156.97	74.00	81.55	628.3	28.0	
88	Naga11	35.27	13.95	745650.44	1543226.25	570.97	116.00	60.36	79.35	392.6	0.0	
89	Umm Shugerat	35.22	13.95	739327.94	1543169.13	551.30		63.63			0.0	
90	Naga17	35.27	13.95	744797.31	1542990.00	568.57	275.00	57.41	84.97	523.7	0.0	D36H5D870419
91	Naga15	35.28	13.95	746674.75	1542928.13	572.31	161.54	76.92	81.55	130.8	27.4	
92	Naga16	35.27	13.94	745342.56	1542528.13	568.67	161.54	48.24	100.37	392.6	16.8	
93	Naga18	35.27	13.94	744902.75	1542271.75	565.00	296.00	81.89	102.77	392.6		
94	AsSarraf-old	35.36	13.93	755028.00	1541183.50	612.31	277.67	77.10	86.67	432.0	61.0	D36H5D691102
95	AsSarraf	35.36	13.93	755091.63	1540833.50	613.85	255.00	73.50	78.90	432.0	70.0	D36H5D700531
96	Kanz	35.42	13.93	761653.94	1540740.38	637.00	174.90	60.00			135.0	
97	Suffara	35.28	13.92	746535.31	1540227.25	565.00	209.70	50.24			29.0	D36H5D690425
98	Huri-old	35.23	13.92	740399.56	1539938.75	545.00	131.00	83.82			0.0	

No.	Site Name	Long.	Lat.	X	Y	Z	Depth	SWL	DWL	Yield	Basalt	Remarks
99	Domat	35.09	13.92	725415.25	1539874.50	524.93	52.60					
100	Huri-Jap.	35.23	13.92	740482.19	1539825.63	544.55	100.00	76.20	80.85	57.6	0.0	D36H5C690516
101	Huri-new	35.22	13.91	739867.50	1539069.75	540.91	105.20	69.00			0.0	D36H5D871226
102	Jana Barra	35.29	13.91	746975.19	1538826.50	562.86	117.35	26.48	39.11	673.3	36.6	D36H5B930427
103	Tamergu	35.83	13.90	806106.50	1538678.50	569.09	115.80	60.00			0.0	
104	Wad Kabarus	35.36	13.91	754935.63	1538396.75	625.00	243.00	62.26	73.77	331.2		
105	Wad Kabarus	35.36	13.90	754998.31	1538108.38	610.91	211.84	65.63	78.57	230.4	88.4	D36H5D690505
106	Kagara	35.41	13.90	759912.81	1537462.75	620.00	196.60	69.50	82.63	362.9	64.0	D36H5D721205
107	Abulraif	35.28	13.90	746697.13	1537443.38	563.33	274.32	44.59	74.87	303.3	45.7	D36H5D710103
108	Kamadeib-Jap.	35.23	13.89	740652.13	1536420.75	539.57	237.50	48.28	90.47	286.3	0.0	D36H5C650623
109	Domat	35.09	13.89	725688.13	1536157.25	516.43	54.90	30.80				
110	Assar	35.42	13.88	761036.25	1535675.25	630.91	147.83	83.28	98.28	314.2	97.5	D36H5D900903
111	Kamadeib	35.22	13.88	740091.63	1535665.38	538.33					0.0	D36H5C881214
112	Wad-ElSanosi	35.41	13.88	759986.50	1535538.63	618.89						
113	Shasheyina	35.59	13.87	779375.81	1535145.63	626.67	473.40	120.00			399.0	
114	Kumur	35.42	13.87	761120.94	1534093.50	630.00	314.00	68.30			120.0	
115	Shaykhan	35.70	13.86	791257.50	1533954.50	587.50	143.30	51.80			0.0	
116	Wad Daif-old	35.38	13.86	756843.44	1533225.63	592.22	141.73	42.63	61.58	360.0	33.5	D36H5B710102
117	Saseib	35.27	13.85	745404.63	1531903.13	547.27	271.88	35.54	47.14	370.5	0.0	D36H5C680605
118	Saseib	35.27	13.84	745348.06	1531521.38	546.67	106.68				0.0	1970-italian
119	Genan	35.46	13.84	765501.75	1531431.38	653.33	256.10	93.90	115.46	218.9	165.0	
120	Kassab-old	35.42	13.84	761591.50	1531284.00	618.57	152.40	67.50	88.36	293.8	114.0	D36H5D901002
121	Wad Abu Asal	35.53	13.83	773601.50	1530009.88	632.22	310.90	158.50			310.9	
122	Cumshiita	35.43	13.82	762436.44	1528787.38	635.00	189.00	86.80			135.0	
123	Wad el Halangi	35.43	13.80	762389.88	1527217.88	613.00	253.00	67.42	92.00	218.9		
124	Umm Sawaney	35.67	13.79	788432.13	1525926.75	602.86	135.50	48.50			0.0	
125	Wad Yousif	35.94	13.76	817391.44	1522573.38	570.00	192.90	39.60			0.0	
126	Shoab	35.87	13.75	809947.44	1521499.38	612.50	160.00	99.10			0.0	
127	Mahal	35.44	13.73	764283.50	1518505.38	588.89	118.00	28.27	62.35	144.0	0.0	
128	Qureisha_R	35.93	13.72	816902.69	1518291.75	590.00	149.40	33.50			0.0	
129	Qureisha	35.92	13.72	815549.69	1518244.63	591.67	237.00	51.40	84.60	432.0	0.0	
130	Zreiqa AlHila	35.49	13.72	768856.88	1518121.63	620.00	232.00	48.25	74.91	362.9	0.0	
131	Qala Salamat	35.81	13.72	804365.31	1518081.00	635.38	178.60	86.90			45.7	

No.	Site Name	Long.	Lat.	X	Y	Z	Depth	SWL	DWL	Yield	Basalt	Remarks
132	Tagali	35.49	13.69	768772.75	1514584.63	589.23	155.40	28.50	-	-	0.0	
133	Zreiqa AIDonki	35.52	13.69	772080.88	1514495.75	590.00	92.00	38.20	66.80	174.8	0.0	
134	Saboni	35.55	13.66	775448.50	1511640.50	596.00	186.00	27.30	-	-	0.0	
135	Hamra	35.58	13.64	779232.38	1509281.88	587.31	254.50	53.40	-	-	54.0	
136	Samina	35.71	13.62	793087.69	1507464.63	652.50	335.30	16.50	-	-	300.0	
137	Kakoum	35.94	13.62	817608.75	1507134.13	620.67	264.60	69.00	-	-	-	
138	Wad AlShagora	35.73	13.57	794990.56	1501365.75	613.85	201.00	12.50	-	-	270.3	
139	Tawarit	35.63	13.55	784631.69	1499437.63	595.71	213.00	22.90	36.45	293.8	0.0	
140	Doka	35.76	13.53	799102.75	1496921.63	646.67	200.00	14.90	-	-	590.0	
141	Khor Bakeit	35.58	13.52	779558.38	1495539.50	559.00	146.00	56.40	-	-	0.0	
142	Alsufi Elazraq	35.36	14.05	754701.00	1554106.25	-	-	-	-	-	-	
143	Umm Gulga_L	35.28	14.08	745608.06	1557030.00	-	-	-	-	-	-	
144	Twawa_HB	35.31	14.06	749559.38	1555039.13	-	158.50	46.10	54.80	654.6	-	
145	Twawa_OB	35.32	14.06	749976.25	1555350.63	-	147.22	28.74	47.09	621.9	-	
146	Wad Elsaid	35.51	14.05	770752.00	1554948.38	-	-	113.10	-	-	-	
147	Wad Ali	35.36	14.09	754750.19	1558226.88	-	-	-	-	-	-	
148	Rashid	35.64	13.52	785268.06	1496060.75	-	175.00	14.63	42.77	360.0	-	
Explanation of column lables:												
	Long. :	Longitude										
	Lat. :	Latitude										
	X:	Easting (UTM coordindtes)										
	Y:	Northing (UTM)										
	Z:	Ground level in m above mean sea level										
	Depth:	Borehole depth										
	SWL:	Static water level										
	DWL:	Dynamic water level										
	Yield:	Well yield										
	Basalt:	Basalt thickness										

Table 4.6: Results of water samples analysis.

INDEX	Site	Lithology	Water Depth	pH	Cond.	TDS	Na	Mg	Ca	F	Cl	SO4	NO3	NO2	HCO3	Water Type
1	Aza16	N	29.96	7.1	1290	1007	175.0	53.5	44.0	1.3	92.2	59.3	0.440		610.0	Na-Mg-HCO ₃
2	Aza15	N	29.31		1022											
3	Aza14	N	19.34	8.1	1081	725	240.0	65.6	20.0	0.6	127.6	28.6	0.530		451.4	Na-Mg-HCO ₃ -Cl
4	Aza13	N	44.90	7.8	1380	1012	0.0	58.3	64.0	0.6	109.8	65.8	0.000		366.0	Mg-Na-HCO ₃ -Cl
5	Aza12	N	46.28	7.9	1769	1167	292.0	68.0	20.0	1.5	180.7	166.2	0.198		634.4	Na-Mg-HCO ₃ -Cl
6	Aza8	N	48.89	7.8	1307	1007	227.0	68.0	52.0	0.6	113.4	80.2	0.130		414.9	Na-Mg-HCO ₃ -Cl
7	Aza2	N	46.98		1610											
8	Chinese	N	22.93	8.5	975	759	119.0	43.7	48.0	0.4	77.9	190.0	0.132		292.8	Na-Mg-Ca-HCO ₃ -Cl
9	Mohamed Elsir	N	38.35	8.0	841	599	131.0	36.5	20.0	2.0	56.7	122.6	0.165		329.4	Na-Mg-HCO ₃ -SO ₄
10	Twawa-MB	N	21.80	8.1	1102	839	83.0	60.7	60.0	2.0	92.2	83.9	0.198		427.0	Mg-Na-Ca-HCO ₃ -Cl
11	Twawa-Dug	B/N	53.89	7.9	1820	1291	126.0	85.1	92.0	0.6	194.9	18.9	0.396		134.2	Mg-Na-Ca-Cl
12	Twawa-Sh.	B/N	18.39	7.9	1016	737	9.0	53.5	68.0	0.6	88.6	70.8	0.825	0.05	244.0	Mg-Ca-HCO ₃ -Cl
13	Azaza Airport	N	58.95	7.3	944	745	8.0	64.6	80.0	2.5	75.9	4.1	0.198		451.4	Mg-Ca-HCO ₃ -Cl
14	Azaza-M	N	36.58	0.0	970	691	14.0	57.8	52.0	2.5	61.5	20.6	0.165		341.6	Mg-Ca-HCO ₃ -Cl
15	Karadis	N	47.80	7.8	497	352	5.0	29.4	52.0	0.6	26.9	14.8	0.132		134.2	Ca-Mg-HCO ₃
16	Umm Khanger	N	69.18	7.0	1256											
17	Kilo6	N	61.00	7.7	1312	918										
18	Kagara	B/N	69.50	7.8	495	391	21.0	17.1	41.8	0.5	24.8	2.5	0.132		219.6	Ca-Mg-Na-HCO ₃
19	Assar	B/N	81.44	8.3	1032	743	90.0	36.7	18.4	4.5	45.4	2.5	0.132		378.2	Na-Mg-HCO ₃
20	Kassab	B/N	67.50	7.5	582	461	43.0	36.3	57.6	0.4	80.9	18.4	0.165	0.02	305.0	Mg-Ca-Na-HCO ₃ -Cl
21	Wad Daif	B/N	42.63	7.8	828	650	5.0	70.1	26.4	0.4	16.3	15.6	0.165		366.0	Mg-HCO ₃
22	Wad Kabarus	B/N	62.20	6.5	1152											
23	AsSarra	B/N	73.50	7.3	1393											
24	AsSarra-old	B/N	77.10	7.5	1013	753	104.0	23.0	67.2	2.5	45.4	17.3	0.000		475.8	Na-Ca-HCO ₃
25	Ghreigana	B/N	65.70	7.4	1215	1243	172.0	4.9	68.0	3.5	51.1	17.2	1.760		597.8	Na-Ca-HCO ₃
26	Jana Barra	B/N	26.48	7.5	636	387	94.0	18.1	44.0	0.5	28.4	91.3	0.000		305.0	Na-Ca-HCO ₃ -SO ₄
27	Terria-new	N	56.58	7.3	976											
28	Terria-old	N	45.64	6.9	692											
29	Naga12	B/N	69.52		831											
30	Naga17	N	57.41		1008											
31	Umm Shugerat	N	63.63	8.1	1030	784	56.0	54.9	68.0	4.0	86.6	138.0	2.200		317.2	Mg-Ca-Na-HCO ₃ -SO ₄
32	Huri-old	N	83.82	7.3	1165	709	13.0	38.2	56.0	0.7	78.1	14.6	2.000		244.0	Mg-Ca-HCO ₃ -Cl
33	Huri-new	N/B	69.00		896											
34	Kamadeib	N	48.28	7.2	714	561	18.0	46.1	46.4	2.5	72.4	12.8	0.000		280.6	Mg-Ca-HCO ₃ -Cl
35	Saseib	N	35.54	7.5	500	499	88.0	14.7	44.8	0.5	26.9	127.0	0.000		237.0	Na-Ca-HCO ₃ -SO ₄